

FLUIDIC PLATFORMS FOR HIGH-THROUGHPUT PROTEIN SYNTHESIS AND  
THEIR APPLICATIONS IN DRUG SCREENING

By

RUBA KHNOUF

A DISSERTATION PRESENTED TO THE GRADUATE SCHOOL  
OF THE UNIVERSITY OF FLORIDA IN PARTIAL FULFILLMENT  
OF THE REQUIREMENTS FOR THE DEGREE OF  
DOCTOR OF PHILOSOPHY

UNIVERSITY OF FLORIDA

2010

© 2010 Ruba Khnouf

To my Parents

## ACKNOWLEDGMENTS

I would first like to thank Dr. Z. Hugh Fan for his support, advice, and for giving me the independence to try whatever ideas I had on my own. I am very grateful to Dr. Shouguang Jin for taking a lot of his time to discuss my project, to give me ideas, and to explain with a lot of patience the details of molecular biology techniques.

I would like to thank Dr. Richard Dickinson and Dr. William Ogle for taking the time to serve on my committee, I would also like to thank Dr. David Beebe and Dr. Matthew Coleman for their collaboration and for allowing me to use technologies developed in their labs. Thanks also go to Dr. Phillip Laipis, Dr. Nancy Denslow, and Dr. Daniel Purich for their advice and feedback.

I would like to express my gratitude to present and past members of the Microfluidics lab, especially Dr. Champak Das, Dr. Zheng Xia, Dr. Hong Chen, Jackie Viren, Karthik Pitchaimani, Dr. Ke Liu, Kiri Hamaker, and Rahul Kamath. And of course thanks go to undergraduate students, Corey Walker, Austin Gispanski, and especially Daniel Olivero and Benjamin Chapman for helping me with device design and fabrication and for putting up with me in general. I also owe thanks to the Jin lab members especially Candace Bichsel, Dennis Neeld, and Harald Messer for all their help, advice, and encouragement.

I would like to thank my friends in the United States and Jordan. I also thank my family both in Jordan and the US, I never realized how useful it is to have a large family until I found tons of support and encouragement from them. I would especially like to thank my aunt Marni, and her husband Basel for all their confidence in me through both my undergraduate and graduate time away from home. I would like to thank my younger brother and sister, Nassif and Majd, for becoming such wonderful people and great

friends. Finally, thanks would not be enough for my parents, Mrs. Suhair Nasser and Dr. Elias Khnouf, for the one thing I am grateful for the most is being their daughter.

# TABLE OF CONTENTS

	<u>page</u>
ACKNOWLEDGMENTS.....	4
LIST OF TABLES.....	9
LIST OF FIGURES.....	10
ABSTRACT.....	13
CHAPTER	
1 INTRODUCTION.....	15
1.1 Protein Production and Purification.....	16
1.1.1 Cell-Free Protein Synthesis (CFPS).....	17
1.1.1.1 Continuous exchange cell-free (CECF) protein synthesis.....	20
1.1.1.2 Advantages of CECF.....	21
1.1.1.3 CECF formats.....	22
1.1.2 Protein Purification.....	23
1.1.3 High Throughput Protein Synthesis (HTPS).....	24
1.2 MicroFluidics.....	25
1.3 Miniaturization and Biotechnology.....	27
1.4 Applications of Microfluidics and BioMEMS.....	28
1.5 Drug Screening and High-Throughput Screening.....	29
1.5.1 Optical Detection for Drug Screening.....	30
1.5.2 Enzyme Fingerprinting and Screening.....	31
1.5.3 Membrane Proteins.....	32
1.5.3.1 Nanolipoproteins (NLP).....	32
1.5.3.2 Membrane protein expression in cell-free systems and its advantages.....	33
1.5.4 Antibiotic Resistance.....	34
1.5.5 B-Lactamase.....	35
1.5.6 Protein Synthesis Inhibitors (PSI).....	36
1.6 Motivation and Objectives.....	37
2 USE OF PASSIVE PUMPING FOR CELL-FREE PROTEIN SYNTHESIS IN A MICROFLUIDIC DEVICE.....	50
2.1 Introduction.....	50
2.2 Materials and Methods.....	51
2.2.1 Materials.....	51
2.2.2 Device Fabrication.....	51
2.2.3 Protein Expression.....	52
2.2.4 Luciferase Detection.....	52
2.2.5 Applying Passive Pumping to Cell-Free Protein Expression.....	53

2.3	Results and Discussion .....	55
2.3.1	Protein Expression in Device .....	55
2.3.2	Amount of Nutrient Solution .....	56
2.3.3	Feeding Frequency of Nutrient Solution and Its Delivery Rate .....	57
2.3.4	Amount of Reaction Mix .....	59
2.4	Conclusion .....	59
3	DESIGN, OPTIMIZATION, AND FABRICATION OF A DEVICE FOR MINIATURIZED CONTINUOUS EXCHANGE CELL-FREE PROTEIN SYNTHESIS.....	66
3.1	Introduction .....	66
3.2	Materials.....	67
3.3	Methods.....	67
3.3.1	Prototype Device Fabrication .....	67
3.3.2	Protein Expression.....	68
3.3.3	Luciferase Detection .....	68
3.3.4	Membranes .....	69
3.3.5	Reaction Mix and Feeding Solution Volume Ratio .....	69
3.3.6	Exchange Surface Area of Membrane.....	70
3.3.7	96 Well-Plate Design .....	71
3.3.8	PDMS Thickness .....	72
3.3.9	Device Fabrication .....	72
3.3.10	Device Tests .....	72
3.3.10.1	The dispensing test.....	73
3.3.10.2	Luminescence measurement .....	73
3.3.11	Protein Purification.....	73
3.4	Results .....	74
3.4.1	Membrane Effect .....	74
3.4.2	Reaction Mix and Feeding Solution Ratio.....	75
3.4.3	Membrane Surface Area .....	76
3.4.4	PDMS for Microstamping.....	76
3.4.5	Device Fabrication and Testing.....	77
3.4.6	Protein Purification.....	78
3.5	Conclusion .....	78
4	HIGH THROUGHPUT PROTEIN SYNTHESIS AND DETECTION .....	92
4.1	Introduction .....	92
4.2	Materials and Methods .....	93
4.2.1	Plasmid Construction and Expression .....	93
4.2.2	Protein Expression.....	98
4.2.3	Detection of Glucuronidase (GUS) .....	100
4.2.4	B-Galactosidase (LacZ) Detection .....	101
4.2.5	Alkaline Phosphatase (AP) Detection .....	101
4.2.6	B-Lactamase (B-Lac) Detection .....	102
4.3	Results .....	102

4.3.1	Luciferase Expression Yield .....	102
4.3.2	Protein Expression Levels .....	103
4.3.3	Co-Expression .....	105
4.4	Conclusion .....	105
5	MEMBRANE PROTEIN EXPRESSION & DRUG SCREENING .....	120
5.1	Introduction .....	120
5.1.1	Clavulanate Acid .....	121
5.1.2	Sulbactam .....	121
5.1.3	Tazobactam .....	122
5.2	Materials and Methods .....	123
5.2.1	Membrane Protein Expression .....	123
5.2.1.1	Vesicle and retinal preparation .....	123
5.2.1.2	Protein expression.....	124
5.2.1.3	SDS PAGE and Western blotting .....	124
5.2.2	B-Lactamase Inhibition Assays .....	126
5.2.3	Protein Synthesis Inhibitor Target Selection and Design .....	127
5.3	Results and Discussion .....	128
5.3.1	Miniaturization of the Membrane Protein Expression Assay.....	128
5.3.2	Membrane Proteins' Solubility .....	129
5.3.3	B-Lactamase Inhibitor Detection as an Example for Drug Screening	130
5.3.4	PSI Target Screening .....	131
5.4	Conclusion .....	132
6	CONCLUSION .....	144
6.1	Assessment.....	144
6.2	Future Work .....	145
6.2.1	Evaporation Control .....	145
6.2.2	In Situ Protein Purification .....	146
6.2.3	Automated Dispensing and Mixing .....	147
6.2.4	Universal Detection Method .....	148
	LIST OF REFERENCES .....	149
	BIOGRAPHICAL SKETCH.....	157

## LIST OF TABLES

<u>Table</u>		<u>page</u>
1-1	Comparison between traditional and high throughput screening .....	46
1-2	Common modes of interface (noise) with high throughput assays .....	46
3-1	List of membranes tested for cell free protein synthesis .....	79
3-2	Thickness of each membrane measured .....	80
3-3	Surface area of membranes and their corresponding bottom well depth .....	80
3-4	Results for GFP purification .....	91
4-1	Comparison in protein synthesis yield between device and conventional microplate. ....	115
4-2	Values comparing protein synthesis yield indicated by the signal from each assay when all proteins are coexpressed in the same reaction .....	119
5-1	Table of sequences to synthesize the PSI targets used.....	142

## LIST OF FIGURES

<u>Figure</u>	<u>page</u>
1-1 Schematic for traditional cell-based protein expression .....	39
1-2 Schematic of continuous exchange cell-free protein synthesis (CECF) .....	40
1-3 Bilayer CECF in a multiter plate.....	40
1-4 Silicon chip design for CECF protein synthesis .....	41
1-5 CECF design in which the expression mix is entrapped in a lipid micelle .....	42
1-6 The structure of nickel-nitrilotriacetic acid and its binding to His tags.....	43
1-7 Applications for high-throughput (HT) protein expression and purification .....	44
1-8 Radii of curvature for two axes normal to each other that describe a curved surface. ....	45
1-9 Model of passive pumping device and its parameters .....	45
1-10 Model of Nanolipoprotein (NLP) where a disk forms when the lipoprotein binds to the edge of a liposome and stabilizes the discoid structure .....	47
1-11 Schematic for cell-free protein synthesis of bacteriorhodopsin and nanolipoproteins in the presence of liposomes and retinal.....	48
1-12 Mechanism of hydrolyzing $\beta$ -lactam ring by classes A and B $\beta$ -lactamases .....	49
2-1 Picture of device and outline of the reaction in the channels .....	61
2-2 Comparison in luciferase expression yield between a microcentrifuge tube and the passive pumping device .....	62
2-3 Effect of the amount of the nutrient solution added in intervals of time on protein expression yield .....	62
2-4 Effects of the amount of the nutrient solution added at once on protein expression yield.....	63
2-5 Effect of feeding frequency and pumping rate on protein synthesis yield.....	64
2-6 Effect of the amount of the expression solution on protein production .....	65
3-1 Original device used for optimization experiments .....	79

3-2	Locations of wells and footprint in standard 384 well-plate defined by the Society of Biomolecular Screening.....	81
3-3	Design of top plate .....	82
3-4	Bottom part design .....	83
3-5	Effect of different membranes on protein expression yield in CECF devices .....	84
3-6	Effect of using different amounts of feeding solution on protein synthesis yield. The same amount of reaction mix was used in the CECF device.....	85
3-7	Effect of the surface area of the membrane on protein expression yield.....	86
3-8	Effect of spinning parameters on PDMS thickness.....	87
3-9	Model and picture of 96-well fluidic device.....	88
3-10	Comparison of protein synthesis yield between regular 384 well-plate and fluidic device .....	89
3-11	Comparison in luminescence signal between the device and a commercial 384 well-plate .....	89
3-12	Difference in luminescence signal between a reaction mix with luciferase expressed and reaction mix with no DNA when the signal is read from a device. ....	90
3-13	Gel of GUS purification results .....	90
4-1	Screening for restriction sites in GFP and GUS vectors.....	107
4-2	Vector maps for plasmids used for PCR and protein expression.....	108
4-3	Screening for colony containing correct $\beta$ -lactamase gene.....	109
4-4	Screening for colonies containing correct alkaline phosphatase gene .....	109
4-5	Agarose gel of all plasmids run.....	110
4-6	GUS enzyme kinetics with its substrate 4-methylumbelliferyl $\beta$ -D-glucuronide (4-MUG).....	111
4-7	Enzyme kinetics of $\beta$ -Galactosidase with its substrate Fluorescein mono- $\beta$ -D-Galactopyranoside (FMGal).....	111
4-8	$\beta$ -lactamase detection using m-[[[(Phenylacetyl)glycyl]oxy]benzoic acid which was added to the reaction product of $\beta$ -lactamase .....	112

4-9	Luciferase expression over time .....	113
4-10	Comparison between protein expression yield for each of the six proteins .....	114
4-11	Expression of 6 different proteins in a conventional microplate and the detection of each of them with assays specific for each protein expressed .....	116
4-12	Expression of 6 different proteins in the fluidic device and the detection of each of them with assays specific for each of the proteins .....	117
4-13	Detection of different protein levels when all are expressed in the same reaction both in the 96- well device and a regular 96- well plate.....	118
5-1	Structure of antibiotics and inhibitors with $\beta$ -lactam ring .....	133
5-2	Mechanism of Sulbactam inhibition of $\beta$ -lactamase.....	133
5-3	The change in color of DMPC solution after sonication.....	134
5-4	Cefotaxime structure.....	134
5-5	Ricin , hygromycin B, and sparsomycin targets .....	135
5-6	Comparison between coexpressin bacteriorhodopsin and apolipoprotein in batch format and in CECF format in 96- well device .....	135
5-7	Pictures of microcentrifuge tubes containing centrifuged aliquots from 96-well device with protein synthesis reaction mix with different plasmids added at the beginning of the reaction .....	136
5-8	Protein gel and Western blot of membrane protein samples .....	137
5-9	Kinetics of $\beta$ -lactamase in the presence of different concentrations of the inhibitor tazobactam.....	138
5-10	Kinetics of $\beta$ -lactamase in the presence of different concentrations of the inhibitor clavulanate acid.....	139
5-11	Calibration curves for three different $\beta$ -lactamase inhibitors .....	140
5-12	Structure of protein synthesis inhibitor targets and aptamers used .....	141
5-13	The effect of different RNA aptamers on ricin inhibition .....	142
5-14	The effect of hygromycin B target on the level of protein synthesized, represented by the luminescence signal.....	143
5-15	The effect of sparsomycin inhibition by sparsomycin target and hygromycin B target as a negative control.....	143

Abstract of Dissertation Presented to the Graduate School  
of the University of Florida in Partial Fulfillment of the  
Requirements for the Degree of Doctor of Philosophy

FLUIDIC PLATFORMS FOR HIGH-THROUGHPUT PROTEIN SYNTHESIS AND  
THEIR APPLICATIONS IN DRUG SCREENING

By

Ruba Khnouf

May 2010

Chair: Z. Hugh Fan  
Major: Biomedical Engineering

Protein expression and purification are a limiting step in many areas of research including structural biology, drug screening, and protein function and interaction studies. Conventional protein expression techniques are laborious and time consuming. In order to overcome these obstacles scientists have developed multiple formats and approaches for cell-free protein synthesis, however, in spite of these developments conventional methods are still prevalent mainly because of their higher protein synthesis yield and lower cost. To address these two challenges microfluidics based platforms were tested and developed to enhance protein synthesis yield, miniaturize the reaction volume, lower reagent consumption and cost, and allow high throughput screening. Two microfluidic devices were tested and conditions were optimized to both miniaturize cell-free protein synthesis and to enhance its yield. In the first device the passive pumping mechanism was utilized to provide cell-free protein synthesis reactions with nutrients and energy for yield enhancement. Different parameters were investigated to optimize expression yield and reagent consumption. In the second device, miniaturization of continuous exchange cell-free protein synthesis was optimized; nutrients and energy components were supplied to the reaction through a semipermeable membrane. The

device was also designed to be compatible with commercial detection and dispensing systems.

High throughput protein synthesis was demonstrated by expressing multiple proteins that can be optically detected. The versatility of the device was shown by expressing both soluble and insoluble membrane proteins that are functional and can be further used in assays such as drug screening. Potential applications of the platforms in drug screening were also demonstrated by searching for  $\beta$ -lactamase inhibitors, important components of modern antibiotics. Drug screening was further demonstrated by utilizing cell-free protein synthesis for detecting protein synthesis inhibitors and their molecular targets. Results show the versatility of the device and the potential of using fluidic platforms for the advancement of protein expression and drug screening.

## CHAPTER 1 INTRODUCTION

After the completion of the human genome project in 2003, scientists turned to face the next obstacle; understanding what these genes code for, what is the importance and function of the corresponding proteins, and diseases that may result from a specific DNA sequence. Many tools have been developed and utilized for DNA sequencing. Traditional methods such as the Sanger methods, which depended on the use of dideoxynucleotide triphosphates to terminate DNA amplification prematurely during (Polymerase Chain Reaction) PCR, became very popular and its concept was developed into different formats. Such adaptations included using dye tags, fluorescently tagged terminators, and radiolabeling. However, with the cost and effort required for using these methods in whole genome sequencing the need for high throughput DNA sequencing increased drastically. To overcome these obstacles, some of these methods required the utilization of technologies outside of traditional biological and even chemical techniques. Technologies such as photolithography and other microfabrication tools borrowed from the field of MEMS (Micro-Electro-Mechanical Systems) were used to achieve high throughput DNA sequencing using DNA microarrays.

The obvious contribution of MEMS and miniaturization to DNA sequencing raised expectations to applying these techniques to overcome the challenges to decipher and understand the human proteome. Especially that understanding the proteomic content of cells would give a much better understanding of the biology of all species than that provided by genomic information. Unfortunately, reaching this understanding is much more elusive. For example, the genomic content of all cells from one species is the

same at all time, but the protein content, whether it is the protein identity or its concentration, differ from cell to cell and from time to time in each cell. Post translational modification, alternative splicing, and protein degradation make predicting the protein content of the cell very difficult.

In addition to such biological processes adding complexities to protein studies, practical challenges are also present. Proteins are much more difficult to handle because of their functional dependence on their 3 dimensional (3D) configuration which is sensitive to many environmental factors including mechanical stress and temperature change. However, the bottleneck for most proteomic studies ranging from protein identification to protein-protein interactions is producing sufficient quantities of a desired protein.

The discovery of Taq polymerase, a thermostable DNA polymerase, in the 1960s revolutionized genomic research by using this enzyme in PCR to amplify DNA. Unfortunately, no similar technique has been found to amplify proteins, making protein expression an obstacle in many research applications. For example, in spite the difficulties that structural biologists face in X-Ray crystallography ranging from finding optimum crystallization conditions to deciphering the complex information provided by X-ray, obtaining sufficient amounts of protein remains the major hurdle in discovering the structures of many proteins.

## **1.1 Protein Production and Purification**

Protein expression involves the process by which DNA is transcribed into mRNA, which in its turn is translated into a polypeptide chain, making a protein. The process is highly regulated depending on the species, cell, and physiological conditions. This process is used by scientists to produce proteins for different types of studies such as

understanding protein structure and function. This technique is also used in industry, for example for insulin production for diabetes patients.

Cell-based systems have been traditionally used to obtain proteins for different purposes. Different systems have been used, the most common ones are bacterial systems especially those based on Escherichia Coli (E Coli) cells. Other eukaryotic systems are also used especially yeast systems such as Pichia pastoris and S. cerevisiae.<sup>1</sup> Many protocols have been developed for protein production and purification and there is no universal technique or method that would result in optimum yield for all proteins.<sup>2</sup> However, general steps are followed in most cell-based protein expression systems.

Constructing a DNA vector containing the gene that codes for the desired protein is usually the first step in protein production. This step includes amplifying the target insert gene, purifying it, amplifying a vector that has been optimized for the RNA polymerase in the cell system used, and adding appropriate promoters to optimize yield.<sup>3</sup> The vector is then cloned into bacteria and the vector construct is verified. After verification the vector is transformed into the desired cell-system usually through chemical poration or electroporation, the transformed cells are then grown. Usually a smaller culture is grown for screening and after the cells reach an appropriate density they are harvested, lysed, and the proteins produced are analyzed to verify the production of the correct protein usually via SDS-PAGE.<sup>4-5</sup> A general flow chart of the protocol is outlined in figure (1-1).<sup>6</sup>

### **1.1.1 Cell-Free Protein Synthesis (CFPS)**

In order to overcome the laborious task of protein production, scientists attempted cell-free protein synthesis beginning in the 1960s.<sup>7-8</sup> The principle behind the methods

lies in the fact that the presence of a whole cell is not necessary for protein synthesis as long as the components needed for it such as protein synthesis machinery, enzymes, amino acids, and energy components are present.<sup>9</sup> Two main configurations were developed for CFPS. The traditional configuration, called the uncoupled system, only involves the translation phase of gene expression where mRNA is added to the components required for translation and it is translated into a polypeptide. The other configuration, called the coupled transcription/translation CFPS systems, includes both the transcription and translation phase of protein synthesis in the reaction. Recombinant cDNA is added to the reaction and is first transcribed into mRNA by RNA polymerase before it is translated in its turn to protein. Uncoupled systems were initially favorable because of the different optimum conditions for transcription and translation such as ion concentration which would ideally lead to higher protein synthesis yield. However, the difficulty of handling RNA because of its structural instability and the abundance of nucleases makes using the uncoupled system very difficult, which caused for optimizing coupled systems to make up for their shortcomings.

Many advantages have been reported about cell-free protein synthesis. In addition to its ease of use and application, CFPS is faster, allows for the expression of proteins that are toxic to cells, and can be adapted into many formats including its adaptation for high throughput protein synthesis<sup>7</sup> and screening.<sup>10</sup> In spite of all the mentioned advantages, cellular-based methods remain the prime techniques for protein synthesis because of the drawbacks that CFPS still possess. The first is the absence of post translational modification such as glycosylation, phosphorylation, and formation of disulfide bonds. Another drawback was the short lifetime of the reaction which lasted for

less than an hour, resulting in low protein synthesis yield.<sup>11</sup> This is believed to be a result of fast energy depletion and the accumulation of inhibitory byproducts especially phosphates which inhibit protein synthesis when complexing with magnesium ( $Mg^{+2}$ ) and then inhibit ribosomes as a result.<sup>12</sup>

Traditionally, CFPS has been achieved by providing cell-extracts that contain the components necessary for protein synthesis. The first system was developed from E Coli extracts in the 1960s.<sup>7</sup> This system was improved by Zubay et al. to reduce the amount of background peptide produced by eliminating endogenous DNA and RNA through subjecting the cell-extract to endonucleases before adding template DNA or RNA.<sup>8</sup> The same paper was also the first to explain the use of the coupled transcription/translation system explained earlier.

In addition to E Coli extract, wheat germ extract became popular for the expression of eukaryotic based proteins. These systems were also optimized to increase protein synthesis yield by removing inhibitory agents such as the suicide system, which increased protein synthesis yield significantly.<sup>13</sup> Rabbit reticulocyte extract has become the most used mammalian system for CFPS, especially after demonstrating the ease of removing endogenous mRNA.<sup>14</sup> Cancer cells were also used as a source of extract for CFPS, but rabbit reticulocyte remains the most popular mammalian system.<sup>15</sup> Most recently Shimizu et al. developed a cell-free protein synthesis system that consists of 100 different components for protein synthesis. Most of the components were expressed as recombinant proteins such as elongation and initiation factors, only ribosomes were purified from E Coli cells and the separate components were mixed together. The system was developed to result in higher protein

synthesis yield because it did not contain the inhibitory factors that cell-lysates might have such as endogenous DNA and RNA.

Another approach for maintaining protein synthesis for longer periods of time is to replenish the system with the energy that would allow the reaction to last for a longer period of time, hence enhancing protein synthesis yield. This was done either by adding energy regenerating systems for example using creatine phosphate<sup>16</sup> and fructose 1,6- biphosphate<sup>12</sup> or by mechanically adding the energy components and amino acid to the reaction. This was first accomplished by Spirin et al. when they developed the continuous-flow cell-free (CFCF) protein synthesis where energy components are pumped into the reaction and the inhibitory products are pumped out.<sup>11</sup> Kim et al. developed a simpler configurations where the addition of energy and removal of by-products takes place through a semipermeable membrane in a passive format<sup>17</sup> called the continuous exchange cell-free (CECF) protein synthesis system.<sup>18-20</sup>

Recently, applying post-translational modification to CFPS has proven more successful by taking advantage of the open nature of CFPS and adding components required for post-translational modification. For example glycosylation in a cell-free system was successfully achieved by adding microsomal fractions to the cell-free protein synthesis reaction. As a result of this progress, CFPS has become more attractive as an option for protein production.<sup>21</sup>

#### **1.1.1.1 Continuous exchange cell-free (CECF) protein synthesis**

The CECF protein synthesis format is based on separating high molecular weight protein synthesis components from low molecular weight nutrients and energy components with a semi-permeable membrane (Figure 1-2).<sup>11</sup> The high molecular weight components include cell lysate extracts, enzymes such as the different tRNA

synthetase, and both types of nuclear acids. This mixture is usually referred to as the reaction mix or protein synthesis mix. The low molecular weight solution includes deoxyribonucleic triphosphates (dNTPs), amino acids, energy components usually in the form of adenosine or guanine triphosphates, ATP or GTP. This solution is referred to as the feeding mix or solution. After the reaction is triggered by the addition of DNA the difference in concentration of both nutrients and inhibitory byproducts causes both components to move across the membrane through simple diffusion. The continuous supply of nutrients and energy and removal of byproducts, which are diluted in the feeding solution, allows the reaction to last for longer periods of time allowing greater amounts of proteins to be synthesized.<sup>22</sup>

In conventional and most reported CECF systems, the ratio between the amount of reaction mix and feeding solution has been given different values in literature ranging from 1:10 to 1:50.<sup>23</sup> The optimum usually depends on the type of cell extract and the setup used. In addition, the range of molecular weight cut off for the dialysis membrane used to separate the reaction mix from the feeding solution also varies from 10,000 to 50,000 daltons, and the size of the reaction is usually in the range between 0.5 - 1 ml of reaction mix.

#### **1.1.1.2 Advantages of CECF**

CECF has been shown to improve protein synthesis over the batch format, which is the reaction mix on its own. It has been shown that the amounts of protein synthesized in CECF are comparable to conventional cellular formats, with concentrations up to mg per ml. The yield was also multiple times greater than the batch system. CECF is also simpler to set up than the initial attempt of continuous flow cell-free (CFCF) protein synthesis. CFCF depends on continuously pumping amino

acids and energy components into a chamber containing the reaction mix and at the same time pumping out the byproducts.

CFCF's setup is more complex since it requires additional tubing and two pumps to manipulate fluid flow. CFCF has resulted in maintaining protein synthesis reaction for a longer period of time than the regular batch system. However, the rate of protein expression in CFCF is much lower than the regular batch system,<sup>24</sup> which reduces the amount of protein synthesized per unit time.<sup>15</sup> As a result the total amount of protein synthesized is reduced and is even sometimes less than the amount produced in a batch system with the same volume of reaction mix.<sup>25</sup>

CECF has the same initial protein synthesis rate as the batch system, which in turn is faster than the protein synthesis rate of CFCF. At the same time CECF lasts for much longer periods of time than does the batch system, sometimes lasting up to weeks.<sup>10</sup> CECF is able to produce protein amounts in a few days similar to what conventional cellular systems usually produce in months, making it a very convenient and efficient method to obtain proteins for applications varying from drug screening, to function and structure analysis.

### **1.1.1.3 CECF formats**

CECF has been described as complicated and difficult to apply despite its simplicity in comparison to other formats such as CFCF protein synthesis. Many formats and setups for CECF protein synthesis have been developed driven by a desire to simplify the system, increase protein synthesis yield, or both.

Sawasaki et al. developed a CECF protein synthesis system that separated the protein synthesis components from the small molecule nutrients components by a phase when forming a bilayer of the two mixtures.<sup>26</sup> In these experiments 50  $\mu$ l of

feeding substrate was overlaid onto 10  $\mu$ l of protein synthesis reaction components. This system resulted in a protein synthesis yield ten times greater than the batch system(Figure 1-3).<sup>26</sup>

Hahn et al also miniaturized CECF protein synthesis by designing and building a microreactor in polydimethylsiloxane (PDMS) and using a 6000 - 8000 dalton cutoff regenerated cellulose membrane.<sup>19</sup> Two different designs were tested; one with the membrane separating the reaction solution and the feeding solution lying horizontally and the other with the membrane installed vertically (Figure 1-4). In both designs, 5 - 9  $\mu$ l of reaction solution was used with 49  $\mu$ l feeding solution. The vertical configuration proved more successful because it prevented the accumulation of salts on the membrane hence enhancing exchange through it. The microreactor resulted in doubling protein synthesis yield compared to the batch format.<sup>19</sup>

Another format for CECF protein synthesis was attempted by Noireaux et al., who used protein synthesis components for the construction of an artificial cell.<sup>27</sup> This was done by encapsulating an e coli cell-free protein synthesis system with a phospholipid vesicle. The vesicle and its contents were immersed into a feeding solution which continuously supplied the protein synthesis components with nutrients via diffusion through the phospholipid bilayer (Figure 1-5). Results showed that the expression of Green Fluorescent Protein (GFP) in the vesicle was 3 times than that of the batch format.<sup>27</sup>

### **1.1.2 Protein Purification**

Protein purification is essential for many areas of proteomics research including structural and functional studies, protein/protein, and protein/substrate interactions. Because of the importance of protein purification many approaches have been

developed to achieve this goal. These methods range from different types of chromatography such as size exclusion chromatography and affinity chromatography to ultracentrifugation techniques such as sucrose gradient ultracentrifugation.

Metal affinity chromatography has been one of the most efficient and frequently used protein purification techniques. It is based on the phenomena that histidine and cysteine side chains have high affinity to metal ions such as  $Zn^{2+}$ ,  $Ni^{2+}$ ,  $Co^{2+}$ ,  $Cu^{2+}$ , and  $Mn^{2+}$ .<sup>28</sup> In order to take advantage of this phenomenon different protein tags have been developed especially when specific expression systems are used. These tags are dependent on the protein expressed and are usually a part of recombinant DNA to express the protein with the tag.

The most common tag for protein purification is the histidine tag also known as the 6xHIS tag, which is a series of the amino acid histidine added to the C-terminus or N-terminus of a protein. This tag takes advantage of histidine's high affinity to the metal Nickel or the metal Cobalt.<sup>29-30</sup> Many technologies have been developed to take advantage of this property such as Ni purification columns, nickel-nitrilotriacetic acid (Ni-NTA) coated magnetic beads, and Ni coated microplates for protein purification. The chemical basis for this bond is the binding between  $Ni^{2+}$  and nitrogen in the imidazole ring in histidine when it is in an ionic form (Figure1-6). The bond can be abolished by protonating the nitrogen. In practice, lowering the pH of the solution or adding imidazole which would compete with the histidine and break the bond is used.<sup>28</sup>

### **1.1.3 High Throughput Protein Synthesis (HTPS)**

High throughput protein synthesis's goal is producing multiple proteins simultaneously. This can be used in two broad experimental categories. The first is screening for optimal protein synthesis conditions or gene constructs before large scale

protein synthesis is implemented. The second is for direct use in other high throughput screening applications such as drug and enzyme screening. Figure 1-7 shows the areas in which HTPS can be applied.<sup>31</sup>

One of the advantages of CFPS is its adaptability to different formats, one of which is high throughput formats. Different proteins can be synthesized simultaneously by simply changing the DNA vector for each reaction. CFPS has been argued as favorable for high throughput protein synthesis.<sup>32</sup> Cell-free HTPS has also been used for the construction of in situ protein arrays.<sup>33-34</sup> In these arrays a protein is synthesized on a plate that either has DNA immobilized on the surface or the protein itself has a tag that attaches to a corresponding conjugate that is on the surface.<sup>33</sup>

## **1.2 MicroFluidics**

Microfluidics is a field that has been defined by Whitesides as “the science and technology systems that process and manipulate small ( $10^{-9}$ – $10^{-18}$  liters) amounts of fluids, using channels with dimensions of tens to hundreds of micrometers”.<sup>35</sup> The main components of microfluidic systems include microchannels, pumps, valves, and mixers.<sup>35</sup> Since pumps are part of this dissertation, a brief discussion is included below.

Pumps are one of the important components for fluid manipulation. Many methods have been developed for manipulating fluids in microchannels. Each method has its own advantages and disadvantages.<sup>36</sup>

Electroosmotic pumps take advantage of the high surface area to volume ratio in microchannels where electroosmotic flow (EOF) results from a formation of a positive charge layer at the interface of liquid and channel material. Applying an electric field would cause the cations to move towards the cathode and the rest of the fluid moves

with it.<sup>37</sup> Electroosmotic pumps have been especially effective in DNA electrophoretic separation,<sup>38-39</sup> and protein separation.<sup>40</sup>

Pressure based pumps cause fluid to flow due to an application of pressure, or a pressure difference. The most widely used pressure pumps are syringe pumps. Syringe pumps have been used to study mixing,<sup>41</sup> electrochemical sensing,<sup>42</sup> and immunoassays.<sup>43</sup>

Both electroosmotic pumps and pressure based pumps needed external or additional parts to cause fluid flow. Because of the nature of microfluidics and the preference for simplicity, a need for simpler pumps arose. Such pumps include gravity dependent pumps or hydrostatic pumps. Hydrostatic pumps depend on the difference in water level in the microchannel, causing liquid to flow from the higher level to the lower level.

Passive pumping is a simple liquid pumping method that is utilized in microfluidic applications for manipulating small amounts of liquid.<sup>44</sup> The method primarily depends on the forces resulting from the surface tension of small liquid droplets. Based on the Young-Laplace equation the pressure within a droplet at an air-liquid interface  $P$  is equal to  $\gamma(1/R_1 + 1/R_2)$ , where  $\gamma$  is the surface free energy which is a material property of a liquid,  $R_1$  and  $R_2$  are the radii of curvature perpendicular to one another that are sufficient for the description of a curvature (Figure 1-8). In the case of a spherical surface the equation reduces to  $P = 2\gamma/R$ , where  $R$  is the radius of the sphere (Figure 1-9).<sup>45-46</sup>

Based on the previous equation there is an inverse relationship between the radius of the drop and the force created by the pressure at the air-liquid interface,

meaning that the internal pressure is greater for smaller drops. The passive pumping method takes advantage of this fact by creating a pressure difference between two different sized drops on the ends of a tube, the pressure difference is a result of the difference in radii between the two drops causing fluid to flow from the higher pressure point at the location of the smaller drop is to the lower pressure the location of the larger drop.<sup>44</sup>

Such pumps are not as pulsatile as syringe pumps, they also do not need a “world-to-chip” interface.<sup>47</sup> These pumps have been used in cell sorting<sup>48</sup> and immunoassays.<sup>47</sup>

### **1.3 Miniaturization and Biotechnology**

Biological processes in general, and specifically molecular biology processes take place in the cellular and subcellular level. This level is in the order of a few micrometers, since the average diameter of a cell is ~10  $\mu\text{m}$ . The minute scale at which central biological processes take place has always been a great challenge. The inability to visualize most of the components, and the extreme difficulty in manipulating single components, have caused molecular biologists to search for solutions outside the traditional techniques used in their fields. This, in combination with the increased need for higher quality medical care, biofluid assays, and cell and tissue diagnostics, have been the driving force for the emerging of new fields such as microfluidics and BioMEMS.<sup>49</sup>

BioMEMS or biomedical microelectromechanical systems has emerged from the MEMS field with the aim of biological and medical applications. It takes advantage of fabrication technologies developed initially for the fabrication of semiconductor device technologies such as integrated circuits. The development of BioMEMS has lead to a

departure from traditional MEMS techniques and materials. For example, silicon has been the most popular material for MEMS but more and more BioMEMS applications are being done in polymers and hydrogels.

Miniaturization of any biomedical system can result in many advantages including a decrease in reaction time and reagent cost, which is a direct result of the decrease in reagents and materials volumes used.<sup>50</sup> Miniaturization also increases the sensitivity of the system by reducing the sensor to element scale,<sup>50</sup> which allows the observation of phenomena and mechanisms that cannot be detected in large scale studies.<sup>51</sup> Another obvious advantage to miniaturization would be portability of the system. In addition, high throughput format and integrating multiple processes in one system become possible.<sup>52</sup>

Chemically and physically speaking, miniaturization allows for increased efficiency in the reactions. The larger surface to volume ratio results in increasing the efficiency of exothermic reactions, low mass-transfer distance would increase reaction efficiency and result in higher selectivity, and ultimately resulting in more precise kinetics.<sup>53</sup>

#### **1.4 Applications of Microfluidics and BioMEMS**

Microfluidics research and applications have grown exponentially in the past few years. However, the academic world remains the main producer and consumer of microfluidic devices in spite of the success of some commercial devices. Examples of microfluidic devices with biological applications include the triage cardiac panel device, a commercial device developed for point of care cardiac protein detection and measurement.<sup>54</sup> Another microfluidic device that demonstrates the promise of microfluidics in biomedicine, is the protein crystallization device that is used to define optimum conditions for protein crystallization.<sup>55-56</sup>

## 1.5 Drug Screening and High-Throughput Screening

Drug screening is a part of the drug discovery process, which initially searches and identifies entities against a specific target or a specific function.<sup>51, 57-58</sup> Drug screening involves evaluating the biological role of the compounds being considered as drug candidates.<sup>59</sup> High throughput screening (HTS) has become an integral part of drug screening especially in cases where the structure of the target is unknown.

Traditionally, each target was studied in a 1 ml reaction in a separate tube. This has limited laboratory capabilities to 20-50 tests a week.<sup>60</sup> Such difficulties resulted in the conception of the idea of high throughput screening, which allows the study of a large number of molecules simultaneously, in a miniaturized in vitro format. In addition to cutting down screening time dramatically, miniaturization results in a decrease in reagent volume and cost. HTS also allows for the study of a much larger library increasing the probability of finding the correct target (Table 1-1).

The most widely used high throughput (HT) formats in both industry and research are 96 and 384 well-plates. The use of these plates has increased with the commercialization of automated measurement systems and highly sensitive detectors. Microplate readers, robotic dispensers, and plate stackers enabled HTS to be faster, easier, and robust, which is important for a field that requires a high degree of statistical certainty such as drug screening.

The development of the sophisticated, sensitive, and accurate detection systems came hand in hand with the development of easily detectable assays. This is crucial for HTS since there is no point in conducting highly dense experiments without having a technique to measure the outcome of these reactions quickly and accurately. For example, traditional DNA and protein detection techniques such as molecular weight

based separation would be very challenging to run on 384 samples. Such difficulties led to the development of optically detectable techniques that mostly depend on fluorescence and luminescence.<sup>59</sup>

### **1.5.1 Optical Detection for Drug Screening**

With the discovery of new enzymes and the evolution of the field of enzyme engineering, new enzymatic assays are being developed to adapt to high-throughput screening methods that make enzyme catalyzed transformations visible. The most common methods depend on optical detection through a change of fluorescence or absorbance signals.<sup>61</sup> The advantage of using such enzymatic assays lies not only in the ease of activity detection, but also in the intrinsic property of signal magnification. Once the enzyme catalyzes one molecule it moves on to catalyze others, causing a high turnover and amplifying the signal.<sup>62</sup>

Fluorescence is the emission of a light signal at a specific wavelength after the emitting substance absorbs a light at a different wavelength. The absorbed light has a higher energy and a shorter wavelength. After it is absorbed light loses some of its energy and the wavelength becomes longer changing the color when it is emitted.

The most widely used enzyme fluorogenic substrates are umbelliferone and fluorescein. Umbelliferone is a fluorogenic phenol which is highly fluorescent when it is catalyzed from its esters and ethers. The emission of blue fluorescence increases 20 fold at a pH above 6.5.<sup>63</sup> Another fluorogenic substrate is fluorescein or fluorescein isothiocyanate (FITC), which emits a bright green fluorescent signal after it is cleaved from the attached substrate.

Chromogenic substrates contain chromophores which change the color of the assay upon enzymatic activity. This change in color can either be detected visually or using a spectrophotometer.<sup>64</sup>

Chemiluminescent substrates are substrates that release energy in the form of light upon oxidization. Their oxidization is catalyzed by an enzyme. The presence of the enzyme is confirmed using an optical transducer -often a photomultiplier- which detects the light signal emitting from the reaction.

In spite of the convenience that these high throughput assays presents, these assays carry some probability for error which stems from various sources of interference. For example, autofluorescence is an interference source specific for fluorescent assays. Table 1-2 summarizes types of interference and their causes related to the optical assays described above.

### **1.5.2 Enzyme Fingerprinting and Screening**

As mentioned above, substrates are used to verify the activity of the protein and to confirm its correct conformation. An important application of these substrates is their utilization as probes in assays called activity based protein profiling (ABPP).<sup>65</sup>

This technique also called enzyme fingerprinting<sup>61</sup> tests the affinity and the enzymatic potency of a protein on different substrates. Not only is this technique important for discovering the function of newly discovered genes and their corresponding proteins, but it is also necessary for new enzyme engineering techniques. Such techniques are essential for drug discovery applications, disease prevention and treatment, and understanding protein function and efficiency.

Enzyme fingerprinting enables the differentiation between proteins, their function, and their efficiency based on the different catalytic effect they have on a range of

different probed substrates. This would have an effect on accelerating protein function assignment, and also have a major role in discovering and optimizing pharmaceutical targets.

### **1.5.3 Membrane Proteins**

Membrane proteins are an important class of proteins whose structure is the least discovered and understood. Although the first protein crystal structure was discovered in the late 19th century<sup>66</sup> the first three dimensional structure of a membrane protein was only deciphered in the year 2000, and only a few membrane proteins' structures have been found since then.<sup>67</sup> The importance of understanding membrane proteins and their structure stems from their multiple functions and necessity for many cellular processes. Their functions include; transportation of molecules ranging from ions to large molecules (such as proteins), cell-cell communications through either chemical signal or through electric current transportation, and for cell-cell anchorage and cell-extracellular matrix anchorage.

Membrane proteins constitute 20% to 30% of all proteins. Their pivotal role in molecular and cellular processes has made them the main target for pharmaceutical drugs. Their role in disease precedes any other type of protein. For example since voltage gated and ion gated channels are primarily membrane proteins, any defect in these proteins will cause both neurological problems such as epilepsy and cardiac problems (e.g. arrhythmias).<sup>68 69-70</sup>

#### **1.5.3.1 Nanolipoproteins (NLP)**

Apolipoproteins are a class of naturally occurring amphipathic  $\alpha$ -helical proteins found in plasma. These proteins self-assemble when phospholipids are present in and form discoidal particles called nanodiscs.<sup>71</sup> These nanodiscs are believed to form as

follows; upon dissolving phospholipids liposomes which are spherical closed bilayers with an aqueous interior are formed. Apolipoproteins associate with the edge of the liposome stabilizing the liposome in a disk like form (Figure 1-10).<sup>72</sup> These nanodiscs have been measured to have an average height of 5 nm with a standard deviation of 0.5nm, and a diameter ranging from 10 to 60 nm. Factors that define the dimensions of the nanodiscs are the type of lipid used and the specific apolipoprotein holding the structure.<sup>73</sup> The advantage of inserting membrane proteins into nanodiscs/NLP lies in the fact that this increases the solubility of the membrane protein, which makes it easier to study. Although it has been shown that membrane proteins can be easily expressed with liposomes and are completely functional when being inserted in liposomes, their structures are insoluble and very unstable. In addition, when a membrane protein is inserted into a liposome only one of its sides that is exposed to the environment outside of the liposome can be studied while the other side is inaccessible because it is exposed to the liposome's aqueous core.

#### **1.5.3.2 Membrane protein expression in cell-free systems and its advantages**

Incorporating membrane proteins in nanolipoproteins was first attempted by separately expressing the NLP and then incorporating it with the lipid micelles. Afterwards, the membrane protein is added to the nanodiscs and associates with them.<sup>74</sup>

Recently, the open nature of cell-free protein synthesis systems has been used to express membrane proteins in nanodiscs, assembled nanodiscs were added to a cell-free protein synthesis reaction mix, and the synthesized membrane protein embedded itself in the nanodisc as it was expressed.<sup>75</sup> More recently, both apolipoprotein and

bacteriorhodopsin were co-expressed in a cell-free system in the presence of liposomes and retinal cofactor and both the nanodisk structure and the nanodisk-bacteriorhodopsin assembly were formed.<sup>73</sup> This technique simplifies the process and reduces the time and labor required to express membrane proteins (Figure 1-11).

The advantage of expressing membrane proteins in a cell-free protein system exceeds the usual advantages of this system such as parallel expression and miniaturization. When using cell-based membrane protein expression, overexpression of the proteins is required. This forces the membrane to break with the proteins embedded in it. However, this complex method has many drawbacks including protein aggregation, misfolding, cell-toxicity, and low yield. These drawbacks make the cell-free approach very attractive for membrane protein expression.<sup>75-76</sup> Other specific advantages include the ability to directly add cofactors necessary for the reaction, and eliminate the need for a translocation or transportation system for the membrane protein expressed.<sup>77-78</sup> The ease of use of commercial cell-free protein synthesis systems led to membrane protein expression in different cell-free formats, such as expressing membrane proteins without additives making a precipitate that was later added to detergents or membranes,<sup>79</sup> expression in the presence of a detergent, and in the presence of membrane fragments or liposomes.<sup>80-81</sup>

#### **1.5.4 Antibiotic Resistance**

Since their discovery in the 19th century, antibiotics have played a very important role in human survival and improving the quality of life. However, their extensive use and misuse has led to bacteria evolving antibiotic resistance, which is making antibiotic use ineffective and in some cases useless.

Bacteria has evolved multiple mechanisms to resist antibiotics. One of two main mechanisms is antibiotic inactivation through enzymatic modifications. A prominent example is the evolution of  $\beta$ -lactamase enzymes that inactivate many classes of antibiotics including penicillins.<sup>82</sup> The second common antibiotic resistance mechanism is decreasing the accumulation of antibiotics in the cells, which is accomplished either by changing the permeability of the cellular membrane, or by using pumps to pump out antibiotics from the cells.<sup>83</sup> Cellular pumps are membrane proteins, usually ATP-driven pumps that are bound to the cellular membrane, which ascertains the critical role of membrane proteins discussed earlier.

### **1.5.5 B-Lactamase**

B-Lactam antibiotics are antibiotics whose structure contains a 4 sided  $\beta$ -lactam ring. These antibiotics constitute 50% of antibiotic consumption around the world. They are heavily used, which is the main reason that bacteria have developed resistance mechanisms against them.<sup>84</sup>

There are more than 190 types of  $\beta$ -lactamases. The most common types belong to class A and class C  $\beta$ -lactamases, which include many chromosomally encoded  $\beta$ -lactamases and plasmid encoded ones. For example the  $\beta$ -lactamase encoded in the PUC 18 plasmid has the type TEM-1  $\beta$  lactamase which belongs to class C.<sup>85</sup> This type is the most common plasmid-mediated  $\beta$ -lactamase since it consists of 72% of these enzymes,<sup>86</sup> and is responsible for 80% of the resistance to the popular antibiotic amoxicillin.<sup>87</sup> The mode of action of this type of enzyme is illustrated in figure (1-12). In summary, the  $\beta$ -lactam ring binds non-covalently to the active site of the enzyme. A serine residue in the active site is covalently acylated to the active  $\beta$ -lactam ring which

ruptures the ring. Finally, the acylated enzyme is hydrolyzed resulting in the release of the inactive drug and the liberation of the enzyme.<sup>84</sup>

In order to overcome the resistance to antibiotics caused by  $\beta$ -lactamase, antibiotics are being given to patients in combination with  $\beta$ -lactamase inhibitors to inactivate the enzyme and prevent it from hydrolyzing the antibiotics.

The first antibiotic/ $\beta$ -lactamase inhibitor combination to be approved for pharmaceutical use is the combination of amoxicillin antibiotic with the inhibitor Clavulanate Acid. Another common combination antibiotic is Sultamicillin which is an equimolar mixture of ampicillin and Sulbactam.<sup>88</sup>

### **1.5.6 Protein Synthesis Inhibitors (PSI)**

Protein synthesis inhibitors (PSI) are a group of substances that negatively affect the process of protein synthesis either by completely stopping the process, slowing it down, or causing errors in it. Most PSIs function during the translational phase of protein synthesis, and most of this category are considered ribosomal inhibiting proteins (RIP) which bind to different part of the ribosome—usually ribosomal RNA (rRNA)-and prevent different stages of mRNA translation into a polypeptide chain. However, a few PSIs function in the transcriptional phase of protein synthesis such as Rifampicin, which binds to the beta-subunit of RNA polymerase in prokaryotes and inhibits DNA transcription into mRNA.<sup>89</sup>

Other PSIs bind to other protein synthesis molecules. For example diphtheria toxin acts on eukaryotic elongation factor 2 (eEF2) by binding to it and deactivating it. This is done by ADP-ribosylating the diphthamide, which is a post translationally modified histidine amino acid. ADP-ribosylation renders eEF2 dysfunctional, inhibiting the translational stage of protein synthesis.<sup>90-91</sup>

Some PSIs specificity for prokaryotic systems allows them to be used as antibiotics. The definition of an antibiotic is a compound that kills or inhibits the growth of bacteria.<sup>92</sup> Prokaryotic PSIs achieve that by inhibiting the protein synthesis process and as a result inhibit growth and cause cell-death. Only prokaryotic PSIs are used as antibiotics because other PSIs-eukaryotic and universal- not only effect bacteria but also affect the cells of the host organism such as humans. In some cases – with very potent eukaryotic and universal PSIs- being subjected to these compounds can lead to poisoning complications that can be as severe as death. Some eukaryotic PSIs such as Ricin and Diphtheria toxin are very hazardous to humans and are listed as bioterrorism agents.

## **1.6 Motivation and Objectives**

This research aims to improve cell-free protein synthesis through the utilization of microfluidic and BioMEMS platforms. It also aims to adapt these platforms for high throughput protein synthesis and screening, and adjust these platforms for other applications such as drug screening.

Chapter 2 discusses the use of a passive pumping device developed by Beebe et al. for miniaturizing cell-free protein synthesis and enhancing its yield. The chapter discusses the pumping mechanism and the effect of different parameters on protein synthesis yield.

Chapter 3 describes the optimization process for miniaturizing continuous exchange cell-free protein synthesis. The development of a fluidic device that has multiple miniaturized CECF protein synthesis units is also described. The dimensions and materials are based on the optimized features, and the device is also designed to be compatible with commercial measurement systems. The chapter describes the

fabrication process, and testing of the device for improving protein synthesis yield and compatibility with detection and dispensing system. Finally, the chapter describes the utilization of Ni-coated magnetic beads for protein purification.

The goal of chapter 4 is to demonstrate the ability of the device described in chapter three in high-throughput protein synthesis and enzyme screening. In the chapter, six proteins which are either optically detectable or have an optically detectable enzymatic assay are synthesized and detected simultaneously. The chapter describes the utilization of enzymatic assays developed for cellular systems in detecting enzymes synthesized in a cell-free format. Protein synthesis yield between the fluidic device and a conventional microplate is compared, and the possibility of co-expressing proteins in a cell-free format is discussed.

Chapter 5 further shows the versatility of the device by utilizing it in a number of applications related to drug screening. The device is used to synthesize both soluble and insoluble membrane proteins. The ability to use the protein synthesized in the device for drug screening directly is shown by studying the inhibition of  $\beta$ -lactamase by multiple compounds used in antibiotics. The use of the device and assays for screening targets of anti-tumor drug candidates is presented.

Finally, the work is summarized in chapter six and future work and directions are discussed.

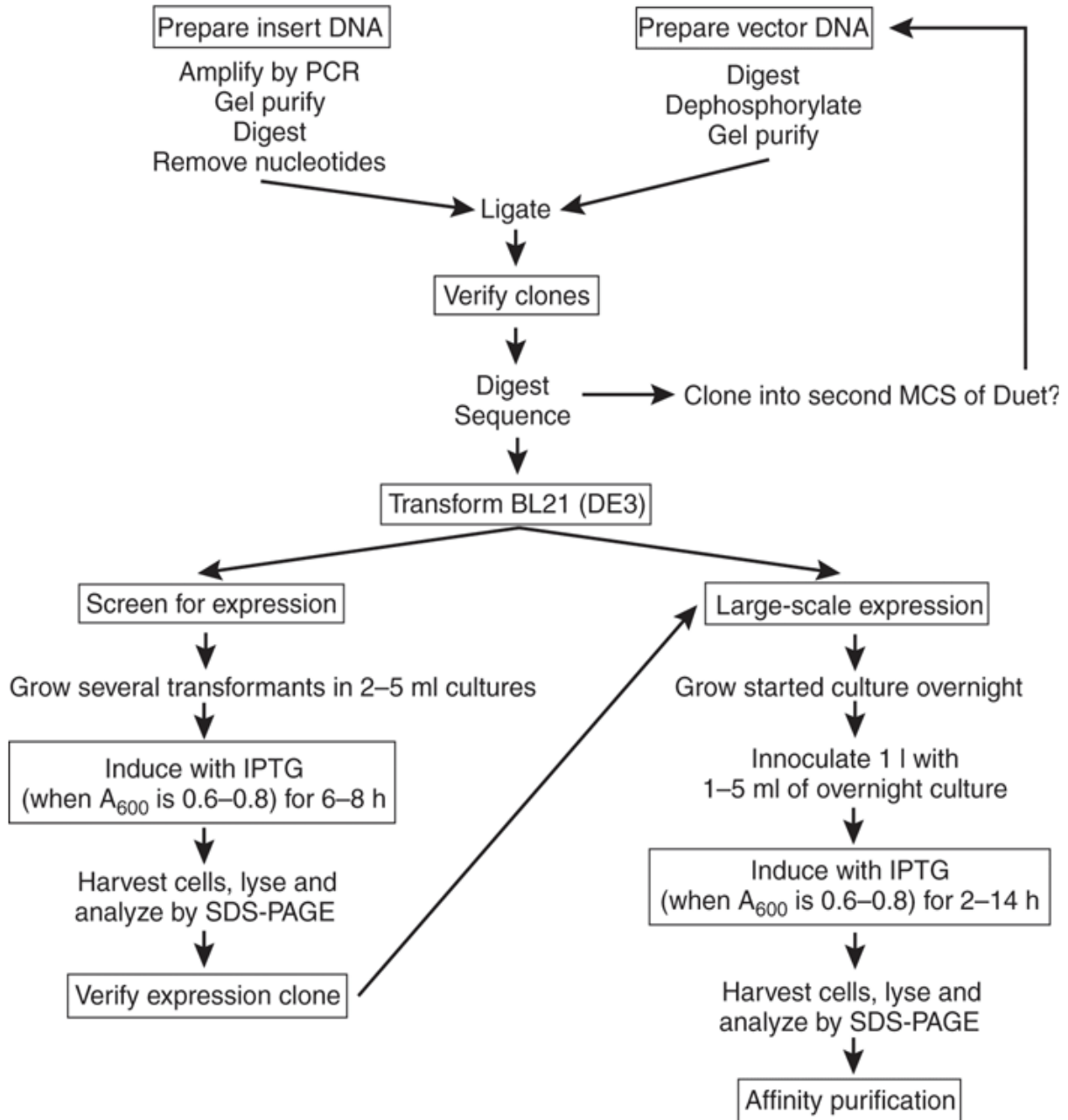


Figure 1-1. Schematic for traditional cell-based protein expression. [Reprinted by permission from Macmillan Publishers Ltd: [Nature Methods] (N. H. Tolia and L. Joshua-Tor, *Nat. Methods*, 2006, 3, 55-64.), copyright (2006)]

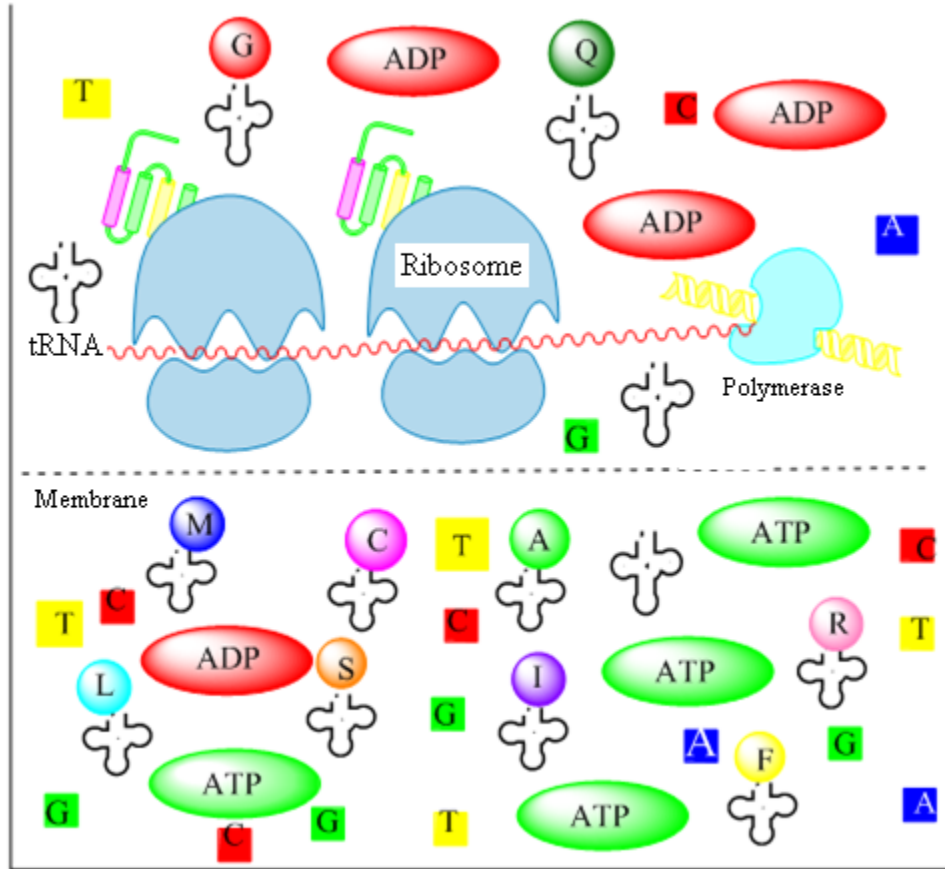


Figure 1-2. Schematic of continuous exchange cell-free protein synthesis (CECF). Circles with letters represent amino acids, squares with letters represent nucleotides. (organelles are not drawn to scale)

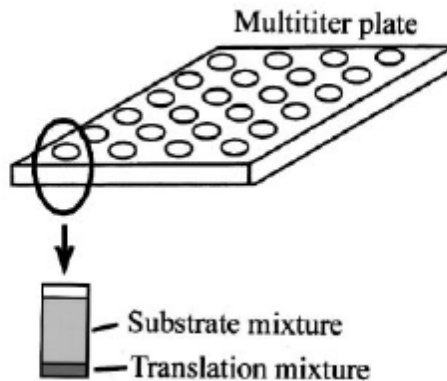


Figure 1-3. Bilayer CECF in a multiter plate. [Reprinted from FEBS Letters, 514, T. Sawasaki, Y. Hasegawa, M. Tsuchimochi, N. Kamura, T. Ogasawara, T. Kuroita and Y. Endo, A bilayer cell-free proteinsynthesis system for high throughput screening of gene products, 102-105, Copyright (2002), with permission from Elsevier.]

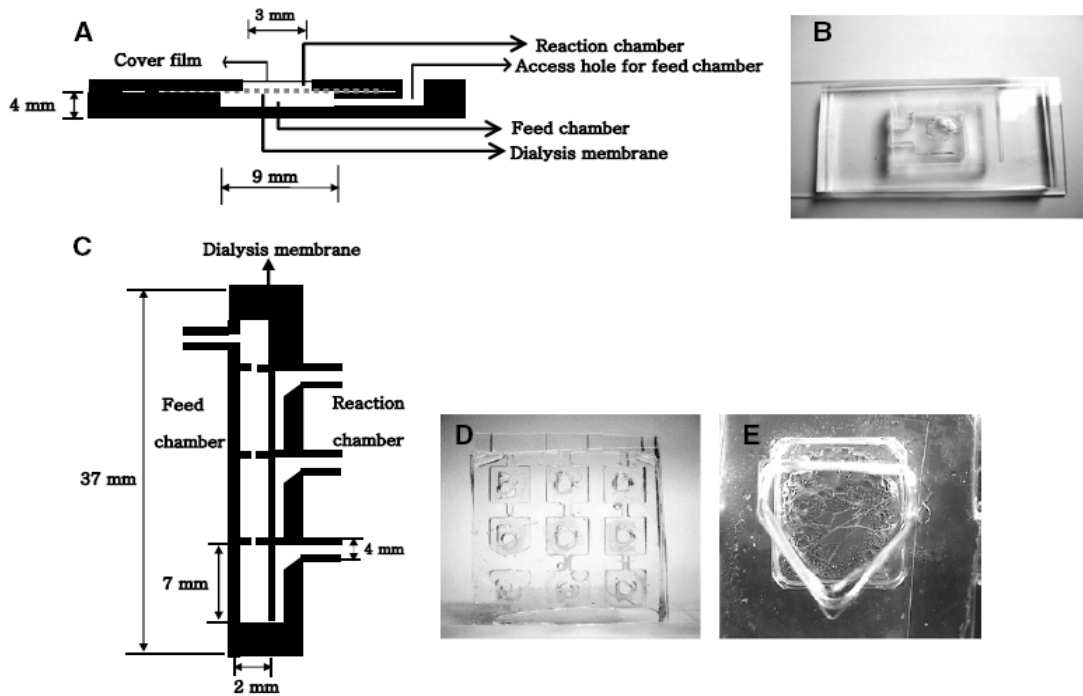


Figure 1-4. Silicon chip design for CECF protein synthesis. A) Schematic of the first design with a horizontally lying membrane. B) First design Silicon chip. C) Perpendicularly placed membrane design with three reactors. D) perpendicular design chip E) single reactor from perpendicular design. [Reprinted from Analytical Biochemistry, 365, G. H. Hahn, A. Asthana, D. M. Kim and D. P. Kim, A continuous-exchange cell free protein synthesis system fabricated on a chip, 280-282, Copyright (2007), with permission from Elsevier ]

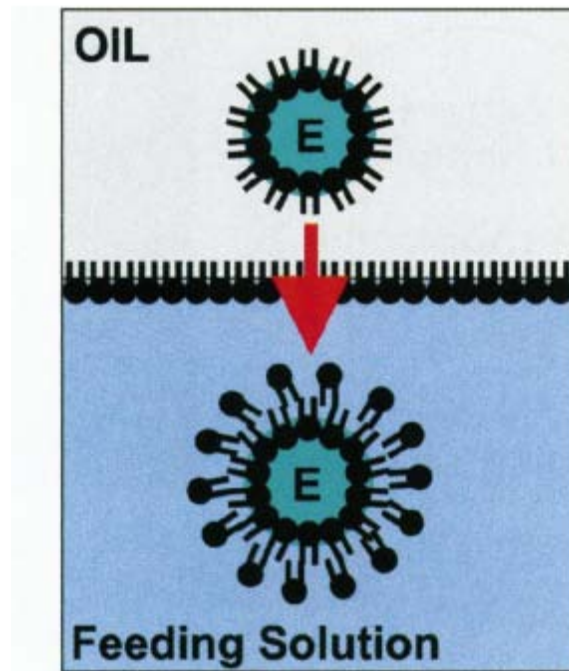


Figure 1-5. CECF design in which the expression mix is entrapped in a lipid micelle that is incubated in the feeding solution. Exchange takes place through the lipid membrane to simulate a living cell.<sup>27</sup>

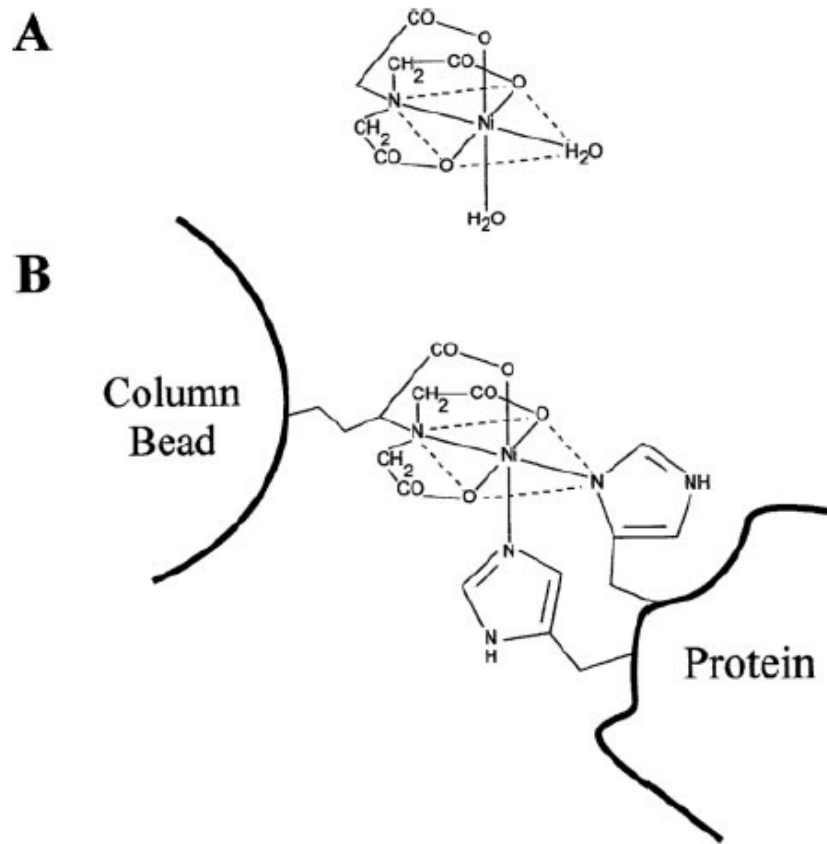


Figure 1-6. The structure of nickel-nitrilotriacetic acid and its binding to His tags. A) nickel- nitrilotriacetic acid (Ni-NTA). B) Ni-NTA column or bead binding to a his-tagged protein. [Reprinted from Journal of Structural Biology, 127, J. F. Hainfeld, W. Liu, C. M. R. Halsey, P. Freimuth and R. D. Powell, Ni-NTA-Gold Clusters Target His-Tagged Proteins, 185-198, Copyright (1999), with permission from Elsevier]

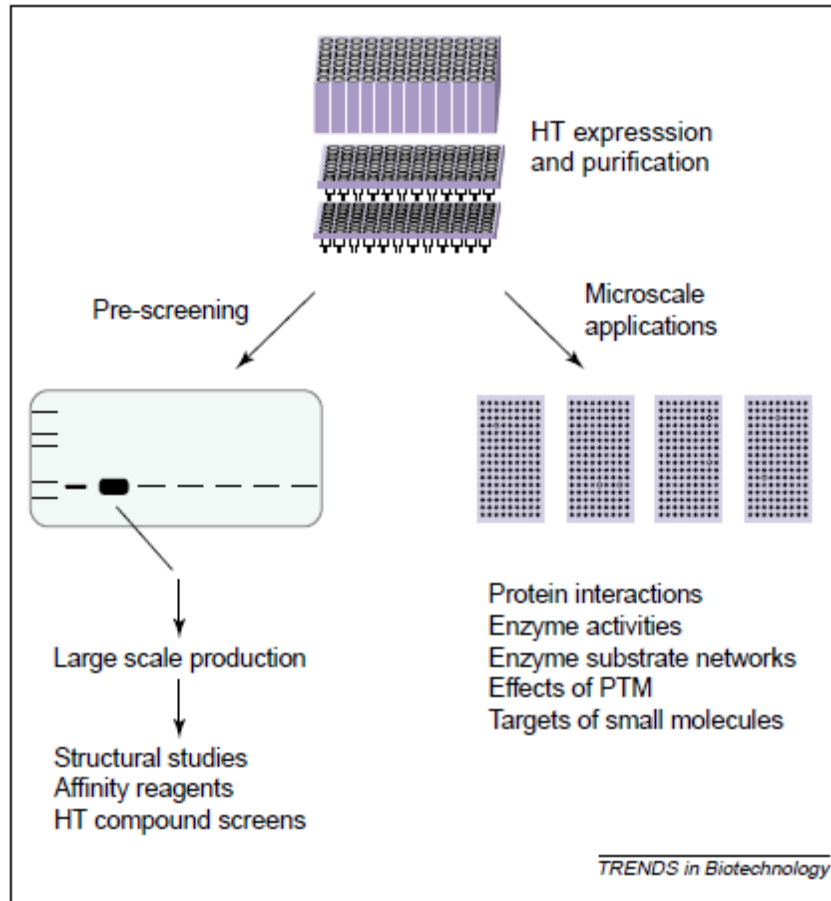


Figure 1-7. Applications for high-throughput (HT) protein expression and purification. For applications that require large amounts of purified proteins (mg) HT methods for protein isolation can be used to efficiently screen many different constructs (orthologues, tags etc.) to identify those that produce a high yield of soluble protein. For microscale applications HT protein purification provides the front end to produce proteins for various applications that require limited amount of protein per sample. [Reprinted from Trends in Biotechnology, 21, P. Braun and J. LaBaer, High throughput protein production for functional proteomics, 383-388, Copyright (2003), with permission from Elsevier]

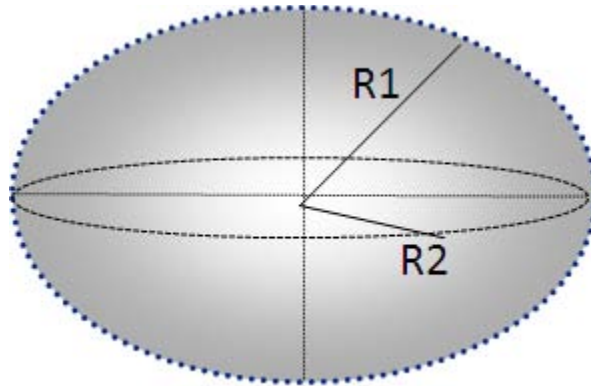


Figure 1-8. Radii of curvature for two axes normal to each other that describe a curved surface.

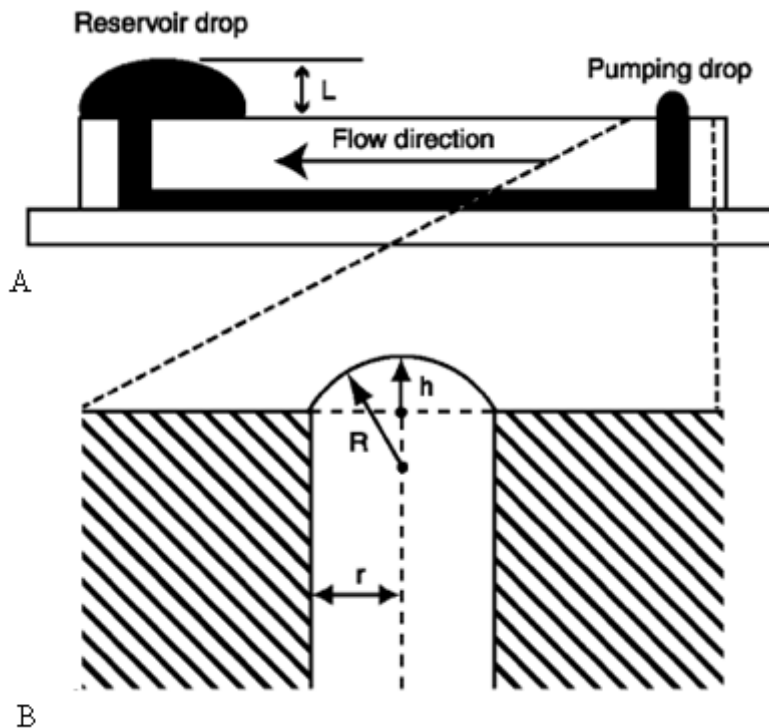


Figure 1-9. Model of passive pumping device and its parameters. A) Side view of a microchannel. A reservoir port (outlet) with a large drop and pumping port (inlet) with a smaller drop are required for fluid flow. B) A drop of volume  $V$  will form a spherical cap of radius  $R$  on a port of radius  $r$ . The cap will rise above the surface of the device a distance  $h$ . If the drop volume is less than that for a hemisphere of radius  $r$ , then the drop radius,  $R$ , will be larger than  $h$ . [G. M. Walker and D. J. Beebe, A Passive Pumping Method for Microfluidic Devices, *Lab on Chip*, 2002, 2, 131- 134. Reproduced by permission of The Royal Society of Chemistry]

Table 1-1. Comparison between traditional and high throughput screening<sup>60</sup>

Traditional screening	High throughput screening
Single tube	Array format 96-well
Large assay volume ~ 1 ml	Small assay volume 50- 100 $\mu$ l
Compound used ~ 5-10 mg	Compound used ~ 1 $\mu$ g
Mechanical action 1:1	Mechanical action 1:96
Dry compounds- custom solution	Compound file in solution- DMSO
Assay slow and laborious	Assay fast and efficient (~1 min/step/96-well plate)
Screen 20-50 compounds/week/lab	Screen 1000- 10000 compounds/week/ lab
Limited number and diversity screened	Unlimited number and diversity screened

Table 1-2. Common modes of interface (noise) with high throughput assays<sup>59</sup>

Assay type	Interference	Cause
Fluorescence, luminescence	Innerfilter effect	Compound absorption of excitation or emission light from tracer
Fluorescence	Autofluorescence	Assay component emission of light in range of assay signal
Fluorescence, luminescence, colorimetric	Light scattering	Compound or assay component insolubility
Enzyme Inhibition	Non-specific loss of signal	Aggregation of enzyme by compound
Fluorescence	Loss of signal	Photobleaching

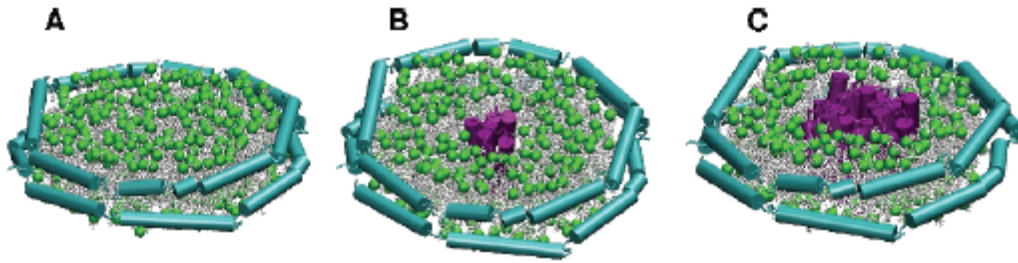


Figure 1-10. Model of Nanolipoprotein (NLP) where a disk forms when the lipoprotein binds to the edge of a liposome and stabilizes the discoid structure. A) Model of a Nanolipoprotein particle (NLP) with a lipid bilayer in the middle and apolipoproteins encircling the hydrophobic portion of the lipids. B) NLP modeled with a bacteriorhodopsin monomer inserted in the hydrophobic lipid core C) NLP modeled with a bacteriorhodopsin trimer inserted in the hydrophobic lipid core

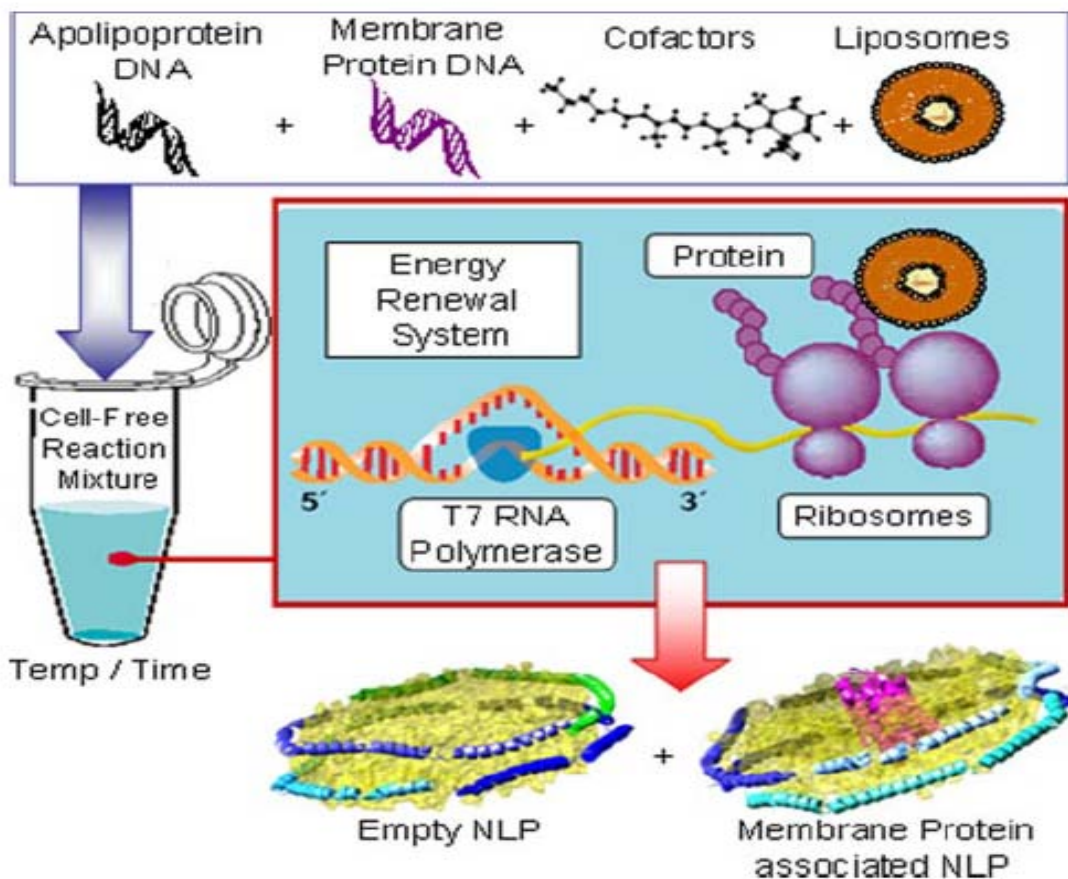


Figure 1-11. Schematic for cell-free protein synthesis of bacteriorhodopsin and nanolipoproteins in the presence of liposomes and retinal to form soluble, correctly folded bacteriorhodopsin in a nanodisc.[ Reprinted with permission from F. Katzen, J. E. Fletcher, J. P. Yang, D. Kang, T. C. Peterson, J. A. Cappuccio, C. D. Blanchette, T. Sulchek, B. A. Chromy, P. D. Hoeplich, M. A. Coleman and W. Kudlicki, Insertion of Membrane Proteins into Discoidal Membranes Using a Cell-Free Protein Expression Approach, *J. Proteome Res.*, 2008, 7, 3535-3542. Copyright 2008 American Chemical Society]

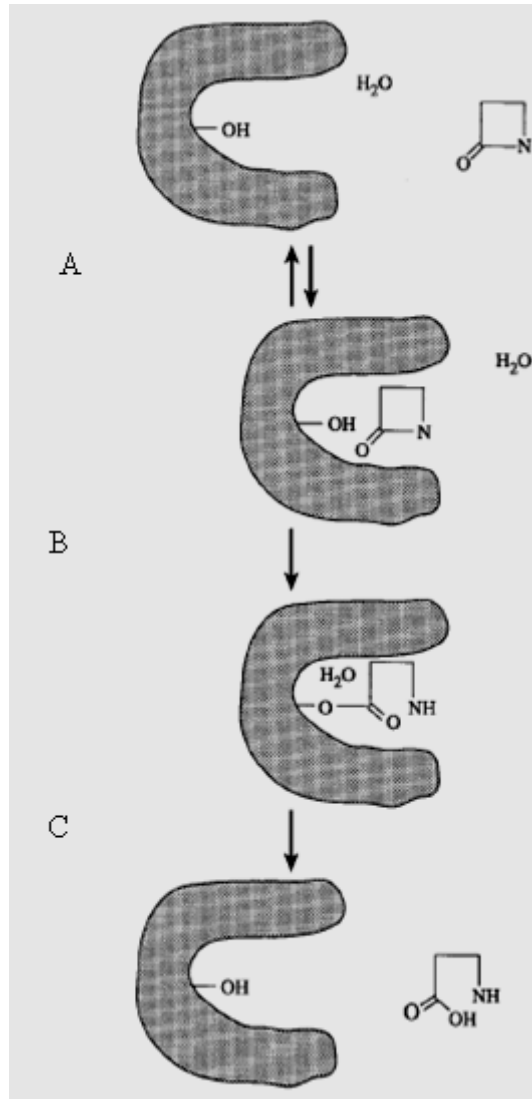


Figure 1-12. Mechanism of hydrolyzing  $\beta$ -lactam ring by classes A and B  $\beta$ -lactamases. A) Binding of  $\beta$ -lactamase to  $\beta$ -lactam ring B) Hydrolysis of  $\beta$ -lactam ring C) Release of  $\beta$ -lactam ring. [Clinical Microbiology Reviews, 1988, 1, 109-123, reproduced with permission from American Society for Microbiology]

## CHAPTER 2 USE OF PASSIVE PUMPING FOR CELL-FREE PROTEIN SYNTHESIS IN A MICROFLUIDIC DEVICE\*

### 2.1 Introduction

With the completion of the human genome project and other projects to decipher the genomes of different species, the need to match the genes discovered to their corresponding proteins and to understand the structure and functions of these proteins has increased exponentially over the past decade. In contrast to DNA, protein synthesis, purification, and detection are much more complex. In the absence of a protein amplification technique similar to PCR, methods for protein synthesis and purification are arduous, costly, and time consuming.

Cell-free protein synthesis (CFPS) has become an attractive alternative to traditional cellular platforms because of its ease of applicability, time efficiency, and miniaturization and high throughput possibilities.<sup>93</sup> However, cell-free systems have a few drawbacks that prevented them from replacing traditional protein synthesis approaches, these shortcomings include high sensitivity to ribonucleases and other protein synthesis inhibitors, and more importantly low protein synthesis yield.<sup>77</sup>

Microfluidics and BioMEMS have been suggested as methods to miniaturize, automate, and enhance CFPS. Many formats and devices have been developed for these purposes including chips, microreactors, and droplets.<sup>19, 94</sup>

In this chapter, I introduce the utilization of a passive micropump designed by Walker and Beebe<sup>44</sup> for cell-free protein synthesis. The pumping mechanism is used to deliver nutrients and energy sources to the reaction solution containing the protein synthesis machinery. The chapter will also discuss optimizing different pumping

\* A part of this chapter has been published: R. Khnouf, D. J. Beebe, Z. H. Fan, "Cell-Free Protein Expression in a Microchannel Array with Passive Pumping," *Lab on Chip*, 9, 2009, 56-61.

parameters to maximize protein expression yield such as amount of nutrients pumped, pumping frequency, and other variables.

## **2.2 Materials and Methods**

### **2.2.1 Materials**

RTS 100 Wheat Germ kit was purchased from Roche (Manheim, Germany). T7 luciferase control DNA vector, luciferase assay reagent, and DNase/ RNase free water were all purchased from Promega (Madison, WI).

### **2.2.2 Device Fabrication**

The microfluidic device contains 192 open ended channels in which passive pumping, described in chapter 1, can be applied. Each channel has a well at each of its ends, the distance between the centers of the two wells is 4.5 mm which matches the standards of a 384 well plate according to the standards set by the Society of Biomolecular Screening (SBS)(Figure 2-1).

The microchannels were machined using a CNC (Computer Numerical Controlled) machine in acrylic to make a master device. Using the master a soft elasmomer tool was cast with resin pellets of polystyrene (PS 168 N, Frantschath Rothrist AG). This was achieved by placing the pellets in the master and subjecting them to different pressure values and temperatures to thermally form the pellet. The formed polystyrene was rinsed with a 20% solution of dichloromethane for 1 minute and afterwards rinsed with methanol, the structure was then place on a Nunc OmniTray. In order to cause another solvent-assisted bonding the thermoformed polystyrene was subjected to another pressure/ temperature cycle. The complete fabrication process was done by Edge Embossing LLC (Medford, Ma, USA).

### **2.2.3 Protein Expression**

The contents of the RTS 100 wheat germ kit were reconstituted with a provided reconstitution buffer from their lyophilized state based on the manufacturer's recommendations. Afterwards the protein expression solution and the feeding solution were prepared. The protein expression solution was prepared by mixing the following components: 15  $\mu$ l wheat germ cell lysate, 15  $\mu$ l reaction mix, 4  $\mu$ l amino acids, 1  $\mu$ l methionine, and 2  $\mu$ g T7 luciferase control DNA vector in 15  $\mu$ l total volume. The feeding solution was prepared as follows: 900  $\mu$ l feeding mix, 80  $\mu$ l amino acids, and 20  $\mu$ l methionine. The negative control was prepared by making the same protein expression solution however 15  $\mu$ l of nuclease free water was added instead of nuclease free water containing DNA.

### **2.2.4 Luciferase Detection**

Luciferase was detected by using its enzymatic assay in which luciferase catalyzes the reaction in which luciferin is oxidized into oxyluciferin releasing energy in the form of light. The presence of luciferase is detected by detecting the luminescence resulting from its catalyzing this reaction, and the amount of light or signal detected is proportional to the amount of luciferase used and in these experiments it is related to the amount of luciferase synthesized in the cell-free protein expression system.

The assay used started by aliquoting 5  $\mu$ l of protein expression mix which is supposed to contain synthesized luciferase into a 384-well Berthold microplate. The microplate is inserted in a Mithras microplate reader which is programmed to inject 35  $\mu$ l of luciferase assay reagent, shake the microplate for 2 seconds, and finally read and average the luminescence signal over 10 seconds. In order to ascertain the detection of

a signal a negative control consisting of protein expression mix with no plasmid added was also measured as described to differentiate it from the positive control.

### **2.2.5 Applying Passive Pumping to Cell-Free Protein Expression**

Before applying cell-free protein synthesis components to any of the channels, each channel was rinsed before use. Rinsing was done using nuclease-free water, water was pumped and withdrawn from the channel using a pipette. The reason for rinsing the channel was for increasing the hydrophilicity of the surface which influenced the pumping mechanism in the channel.

In order to compare protein synthesis yield between the device and a regular microcentrifuge tube, 6  $\mu$ l of protein expression mix was pipetted into the channel from the inlet and 4  $\mu$ l feeding solution were added to the outlet every 10 minutes until a total of 12  $\mu$ l feeding solution were pipetted. The feeding solution's amount pipetted each time had to be less than the total amount of protein expression mix to maintain a pressure difference between the inlet and the outlet and allow the pumping mechanism to take place. The same amount of protein expression mix (6  $\mu$ l) was aliquoted into a centrifuge tube and incubated for the same amount of time that the reaction took place in the device (30 minutes). Each experiment was repeated four times to obtain an average.

The effect of the volume of feeding solution added was studied by adding different amounts of feeding solution (1, 2, 3, and 4  $\mu$ l) at 10 minute intervals for an hour. The solution was added to the same amount of protein expression solution in all cases namely, 6  $\mu$ l.

We also compared the effect of adding different amounts of feeding solution at a steady flow rate continuously and not at intervals as described above. The feeding

solution was delivered to the inlet of the channel using a syringe pump (Ultra Micropump II) from Precision World Instruments, Sarasota, Fl. The syringe pump was used to deliver fixed amounts of feeding solution which would form small drops that would be pumped in the channel with its passive pumping mechanism. The pressure provided from the syringe pump does not provide any driving force to move the feeding solution to the protein expression mix through the channel.

The feeding frequency's effect was analyzed by pumping the same amount of feeding solution (24  $\mu$ l) over the same total period of time however the amount of feeding solution and the amount of times it was pumped differed. The feeding frequencies used were 0.0067 Hz (once every 2.5 minutes), 0.0033 Hz (once every 5 minutes), and 0.0017 (once every 10 minutes). The nutrient amounts were 1  $\mu$ l, 2  $\mu$ l, and 4  $\mu$ l, respectively. The total amount of feeding solution pumped in all three cases was 24  $\mu$ l pumped over an hour.

Using the syringe pump and the setup described above the effect of steadily delivering the same amount of feeding solution at different rates. A total of 12  $\mu$ l feeding solution was pumped through the passive pumping device after being delivered to the inlet port, the amount of protein expression mix forming the outlet drop is 6  $\mu$ l. The rates at which the syringe pump delivered the feeding solution to the inlet port were 33 nl/s, 100 nl/s , 200 nl/s, and 1000 nl/s.

Finally, the effect of amount of protein expression mix was investigated by pumping the same amount of feeding solution to different amounts of protein expression mix. 12  $\mu$ l of feeding solution were delivered to the inlet port using the syringe pump at a rate of 1000nl/s. The protein expression mix amounts used were 5, 6, 7, and 8  $\mu$ l.

## 2.3 Results and Discussion

The aim of using the passive pumping device for protein expression was to use the device's mechanism as a conduit to deliver the feeding solution to the protein synthesis mix. In addition, the format of the device allows for 196 reactions to take place simultaneously allowing high throughput experimentation for protein synthesis and for studying different experimental conditions.

### 2.3.1 Protein Expression in Device

The goal of using the device is delivering the feeding solution and its contents to the protein synthesis machinery in the protein expression mix. The passive pumping mechanism described above is used by filling the channel and forming a relatively larger drop from the protein expression mix at the outlet of the pump (the side where a larger drop is formed) with protein synthesis reaction mix. The feeding solution is pumped to the outlet from the inlet by forming a small drop (has to be smaller than the drop formed at the outlet). Comparing the difference in luminescence signal –amount of protein produced- between having 6  $\mu\text{l}$  of reaction mix without adding any feeding solution and adding 4  $\mu\text{l}$  of feeding solution at the inlet every 10 minutes over 30 minutes (total of 12  $\mu\text{l}$ ) to 6  $\mu\text{l}$  protein synthesis reaction mix in the device. The luminescence measurement was done by measuring luminescence of 5  $\mu\text{l}$  of alloquoted mix and feeding solution at the outlet as described in the methods section above. The result for each condition is the average of four readings, and the error bars are one standard deviation.

Results in figure 2-2 clearly shows that the addition of feeding solution increases the amount of protein produced, where the amount produced in the device was 4.9 times greater than the tube.

### 2.3.2 Amount of Nutrient Solution

In order to study the effect of the amount of feeding solution on protein expression yield two approaches were used. The first was pumping different amounts of feeding solution through pipetting at the inlet over time. Four different amounts were tested (1, 2, 3, and 4  $\mu\text{l}$ ) these amounts were pipetted into the inlet every 10 minutes over an hour for a total of (6, 12, 18, and 24  $\mu\text{l}$ ) respectively. For example, the experiment with the least amount of feeding solution started by pipetting 1  $\mu\text{l}$  into the inlet, waiting 10 minutes then pipetting another 1  $\mu\text{l}$  of feeding solution into the inlet and waiting. This was repeated for an hour and the same was applied for the different amounts. As expected the more feeding solution pipetted the greater the protein synthesis yield as shown in figure 2-3. However the relationship was not linear and had an exponential trend to it, a phenomenon that can be used to magnify protein synthesis.

A second approach to study the effect of the amount of feeding solution added through the passive pump is delivering small amounts of feeding solution through a syringe pump to the inlet. The syringe pump's function was not providing the force to pump the liquid through the channel but rather to deliver the liquid to the inlet drop. The feeding solution was pumped through the channel to the outlet through the passive pumping mechanism because of the difference in surface tension between the drops on the two sides of the channel as described earlier. The same amounts used above (4, 8, 12, 16, 20, and 24  $\mu\text{l}$ ) and were pumped at a flow rate of 1000 nl/s. Although a trend similar to the one observed earlier was expected the results proved differently. Although the amount of protein produced increased when the amounts in the lower range were added however the trend changed and the amount of protein produced decreased when adding a greater amount of feeding solution. The results are shown in figure 2-4 (a).

Another experiment was carried out to ascertain the described trend and to attempt to explain it. The amounts of feeding solution added to the expression mix in the experiment described previously (4, 8, 12, 16, 20, and 24  $\mu\text{l}$ ) were added to the same amount (6  $\mu\text{l}$ ) of protein expression mix in a microcentrifuge tube. The exact trend observed when using the device to deliver the feeding solution was observed again in this experiment where there was an optimum value of feeding solution added that caused the maximum amount of protein to be synthesized after which the amount of protein produced starts declining as shown in figure 2-4 (b).

The trend in these studies can be explained by the increased dilution which reduces the optimum concentrations of protein synthesis machinery and necessary ions. This reduced concentration could result in reducing protein synthesis rate and yield.

Another possible explanation is related to the optimum concentrations of the necessary ions such as  $\text{Mg}^{+2}$ . In the case of  $\text{Mg}^{+2}$  the concentrations required for transcription are much higher than  $\text{Mg}^{+2}$  concentration required for translation. By diluting the optimized concentrations of  $\text{Mg}^{+2}$  the process of transcription would be negatively affected and hence the mRNA available for translation would be reduced, as a result the amount of protein produced would decrease.<sup>18</sup> When the feeding solution was added over an hour the concentrations were not altered as quickly and the reaction was driven towards product which would explain the discrepancy between adding the feeding solution directly and adding it over time.

### **2.3.3 Feeding Frequency of Nutrient Solution and Its Delivery Rate**

Since the amount of nutrient solution has an effect on protein expression yield, the effect of feeding frequency (i.e., the number of the nutrient solution per unit time) on

protein expression was studied. In all experiments, the total amounts of the nutrient solution added to each reaction mix were the same over the same period of time. However the amount added each time and the time interval between feedings were different. Figure 2-5 (a) shows the protein expression yield as a function of the feeding frequency. The studied feeding frequencies are 0.0067 Hz (once every 2.5 minutes), 0.0033 Hz (once every 5 minutes), and 0.0017 (once every 10 minutes). The nutrient amounts are 1  $\mu$ l, 2  $\mu$ l, and 4  $\mu$ l, respectively. As a result, the total amount of the nutrient solution added was 24  $\mu$ l in one hour for all three cases. The results in Figure 2-6 (a) suggest that protein expression yield is higher at a higher feeding frequency while there is no significant difference between low frequency feedings.

The increase in expression yield at a higher feeding frequency is probably a result of increased mixing when the nutrient solution is frequently supplied.<sup>46</sup> In order to maintain the total volume while increasing the pumping frequency, the volume of feeding solution pumped each time decreases with the increase of frequency. A smaller volume at the inlet port leads to a smaller inlet drop radius, which increases the pressure at this port increasing the pumping velocity of the feeding solution and enhancing mixing. More mixing is known to improve the reaction kinetics and increase cell-free protein expression yield.<sup>95-96</sup>

To confirm the effect of the feeding frequency, we also investigated using the syringe pump as the feeding approach. The delivery rates of the nutrient solution ranged from 33 nL/s to 1000 nL/s, and the delivery time varied to maintain that the total nutrient solution pumped was 12  $\mu$ L. Protein expression reactions were allowed for 30 minutes after the initiation of delivery. Figure 2-5 (b) shows the protein expression yield

as a function of the delivery rate. The result indicates that protein production yield increased initially with the delivery rate of the nutrient solution. Similarly, the observation can be explained by the increase in mixing at a higher delivery rate.

#### **2.3.4 Amount of Reaction Mix**

Since one of the goals of this research is to achieve the maximum protein production with the least amount of reagents and cost, we studied the effects of the amount of the expression solution on protein production. Different amounts of expression solution were placed in the outlets while the same amount of the nutrient solution was used in the inlets. The nutrient solution (12  $\mu\text{L}$ ) was added using a syringe pump with a delivery rate of 1000 nL/s. Figure 2-6 shows the protein expression yield as a function of the amount of the expression solution. The results indicate that there is no significant difference among experiments when different amounts of expression solution were used, at least within the range of the experimental conditions used. The results are significant since we can use a smaller amount of the expression reagents for protein production as long as enough amount of the nutrient solution is used.

Comparison of the results from figure 2-6 with the results in figures 2-2 indicates that the amount of the nutrient solution has a greater effect on the protein production than the amount of expression solution. This finding is in agreement with incorporation of microfluidic channels for supplying nutrients, as well as in agreement with the reports using continuous flow or CECF configurations.<sup>10-11</sup>

## **2.4 Conclusion**

Production of luciferase using a cell-free expression system was demonstrated in a microchannel array device. The mechanism of passive pumping which takes advantage of surface tension to pump fluid was used to pump nutrient solution

containing small molecular entities necessary to maintain protein synthesis such as amino acids, nucleotides, and ATP to the reaction mix containing protein synthesis machinery. Factors that maximize protein synthesis were analyzed where the amount of nutrient solution, high pumping frequency, and high delivery rates increased the amount of protein synthesized. The device and the setup can be used for high throughput protein synthesis, screening, and drug screening.

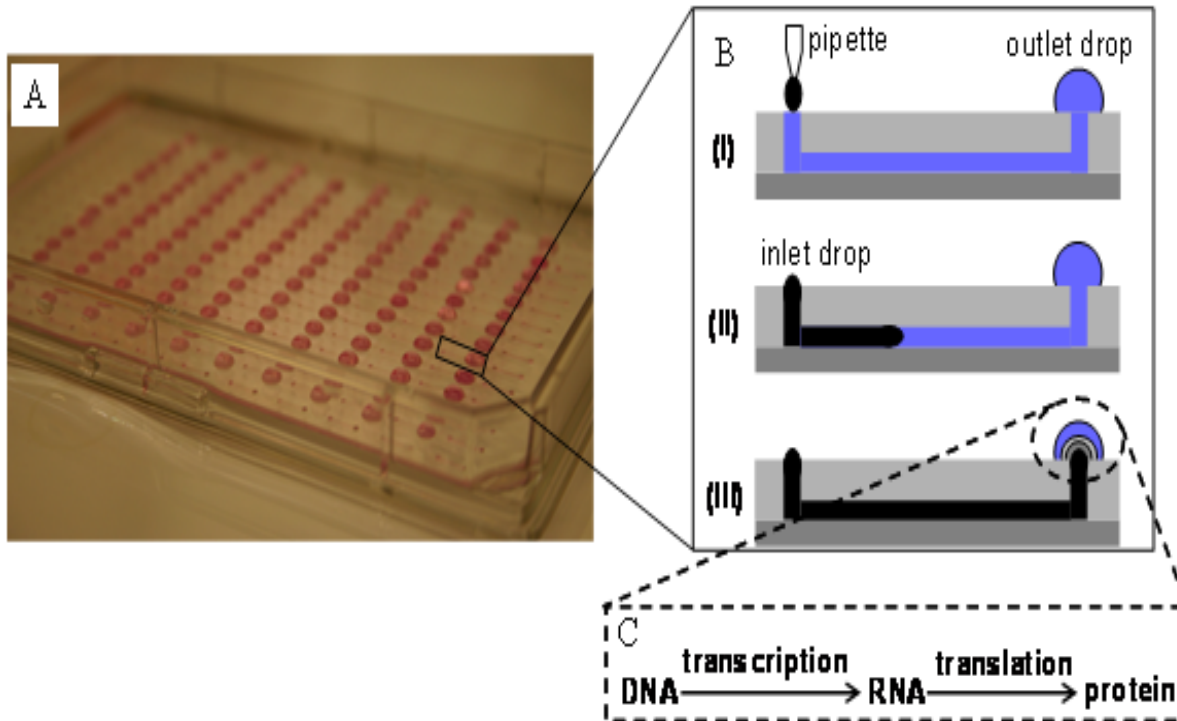


Figure 2-1. Picture of device and outline of the reaction in the channels. A) Picture of the device used in this work. The device consisted of 192 channels and 384 wells. Each pair of two adjacent wells was connected by one channel. B) For each channel, a larger droplet was placed in the outlet, followed by a smaller droplet in the inlet. The difference in the surface tension between two different sized droplets generated a pumping pressure, producing a flow in the channel from the inlet to the outlet. C) Protein expression in the droplet at the outlet consisted of DNA transcription and protein translation.

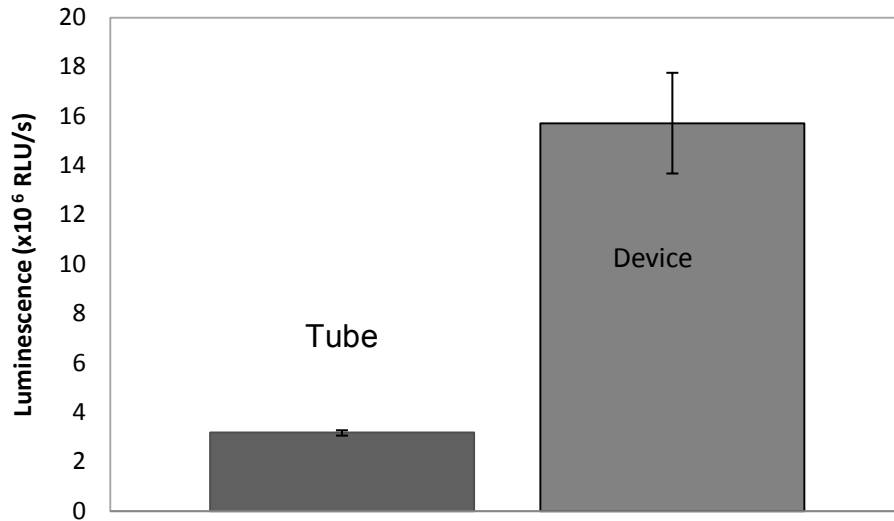


Figure 2-2. Comparison in luciferase expression yield between a microcentrifuge tube and the passive pumping device. The yield is represented by the luminescence signal of the luciferase assay while the error bars indicate the standard deviation of signals from four repeat experiments in different channels.

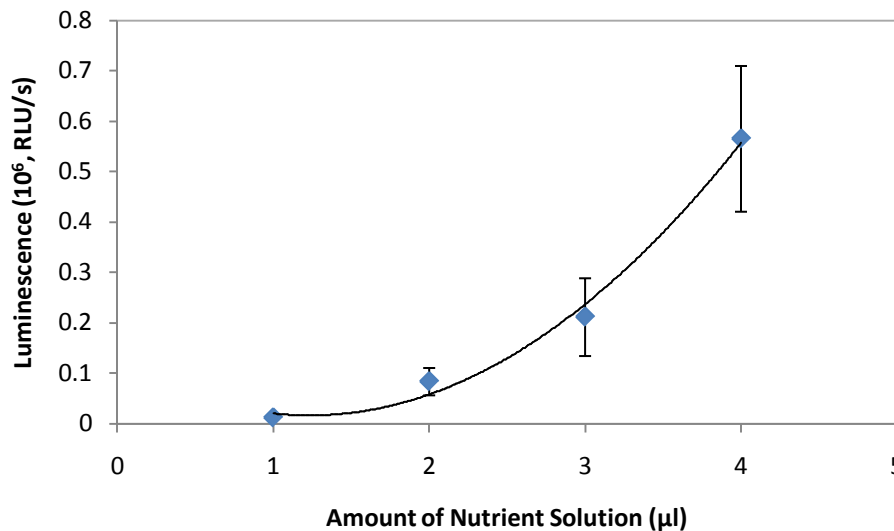


Figure 2-3. Effect of the amount of the nutrient solution added in intervals of time on protein expression yield. The x axis indicates the amount of the nutrient solution added every 10 minutes. The total reaction time was one hour. The line is the best fit of the exponential regression.

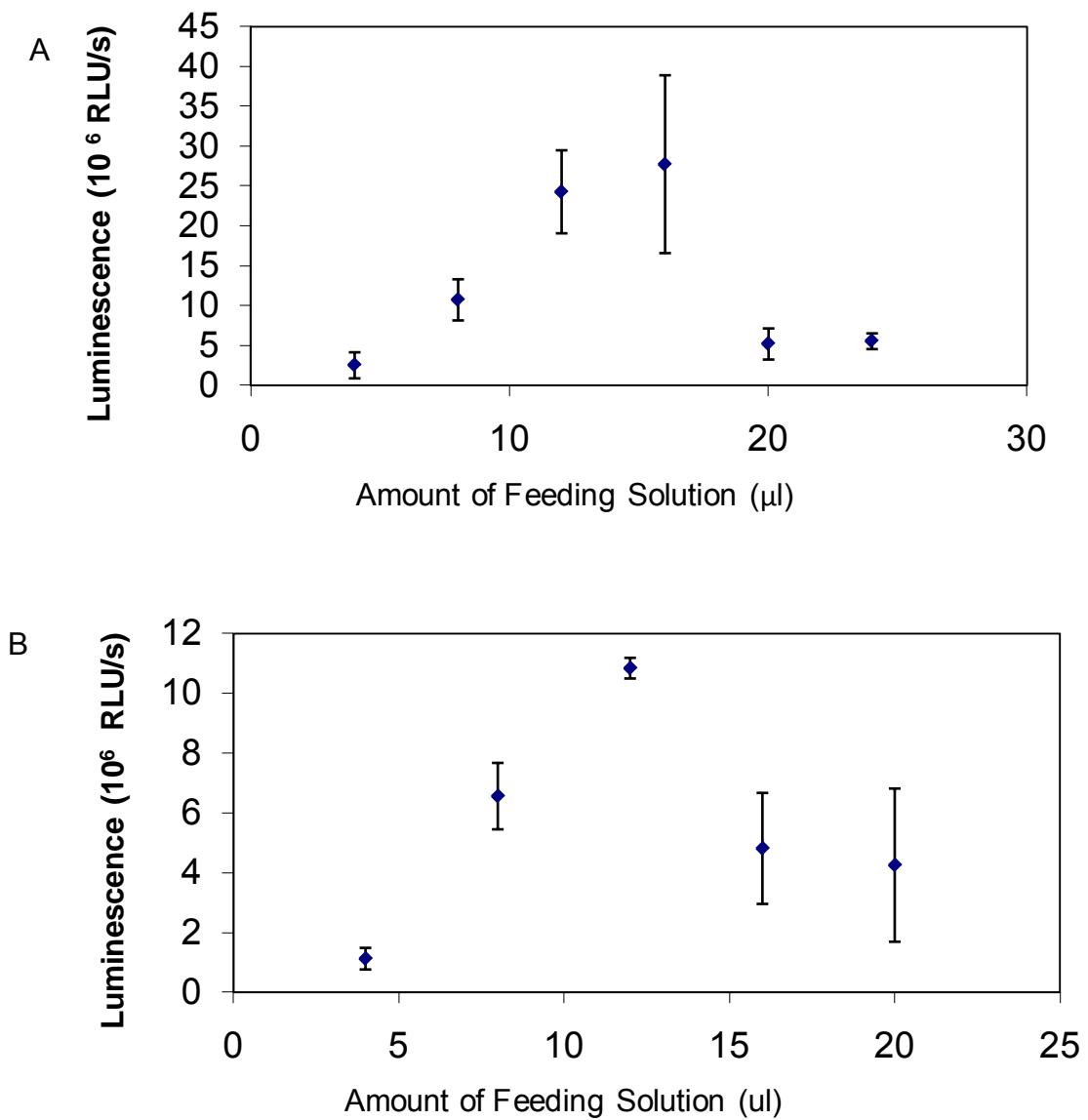


Figure 2-4. Effects of the amount of the nutrient solution added at once on protein expression yield. The nutrient solution was added using a syringe pump. The reaction time of each experiment was 30 minutes. Experiments were carried out in either the passive pumping devices A or in a microcentrifuge tube B.

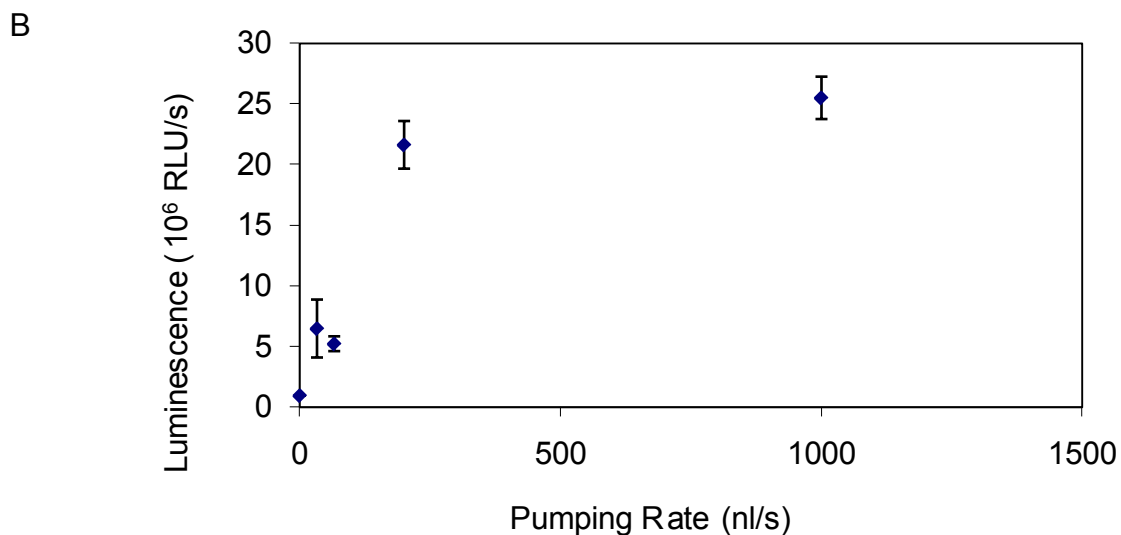
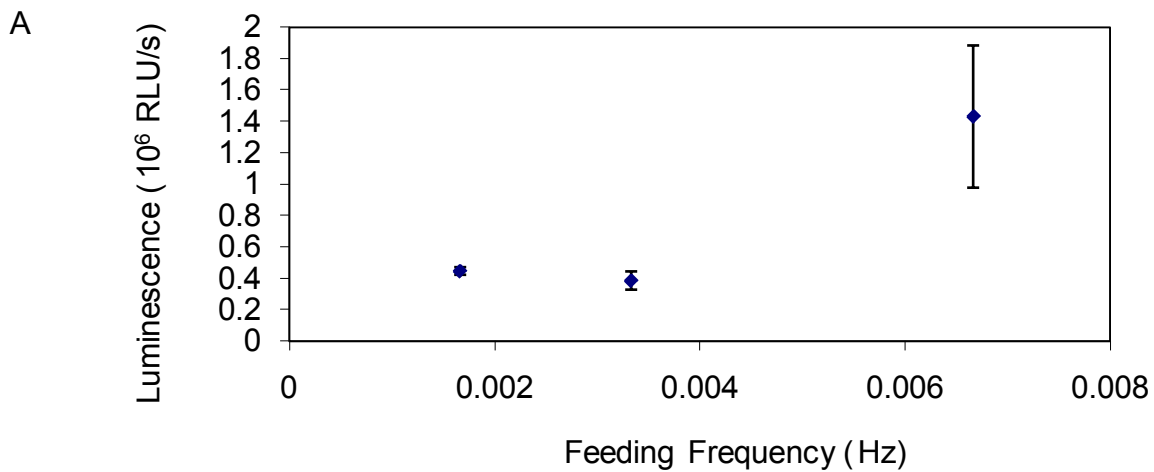


Figure 2-5. Effect of feeding frequency and pumping rate on protein synthesis yield. A) Effect of the feeding frequency of the nutrient solution on protein production. A total volume of 24  $\mu\text{L}$  of the nutrient solution was added by pipetting 1, 2, and 4  $\mu\text{L}$  at a time interval of 2.5, 5, and 10 minutes, respectively, over a period of one hour. B) Effects of the delivery rate of the nutrient solution on protein production when a syringe pump was used. A total volume of 12  $\mu\text{L}$  of the nutrient solution was delivered into the inlets of different channels of the device using various delivery rates.

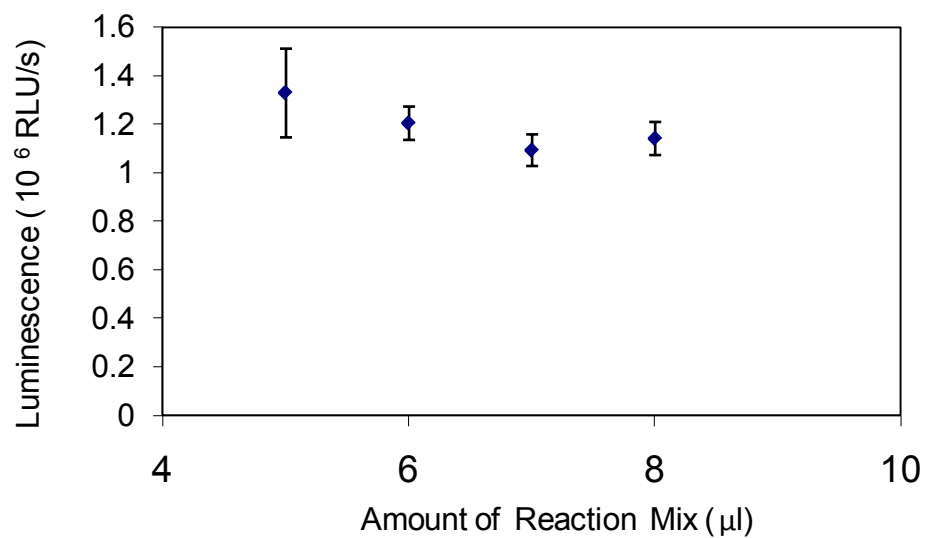


Figure 2-6. Effect of the amount of the expression solution on protein production. The same amount (12 μL) of the nutrient solution was added using a syringe pump with a delivery rate of 1000 nL/s while the amount of the expression solution varied as indicated.

## CHAPTER 3 DESIGN, OPTIMIZATION, AND FABRICATION OF A DEVICE FOR MINIATURIZED CONTINUOUS EXCHANGE CELL-FREE PROTEIN SYNTHESIS

### 3.1 Introduction

Cell-free protein synthesis (CFPS) has become an attractive alternative to conventional, cell-based protein expression systems. Continuous exchange cell-free (CECF) protein synthesis has been proven the most efficient format for CFPS. It has been shown that protein synthesis yield was much higher than any other CFPS system, including continuous flow cell-free (CFCF) protein synthesis and the batch format.<sup>25</sup> CECF protein synthesis is dependent upon simple diffusion of nutrients and energy components on one hand, and inhibitory protein synthesis byproducts on the other through a semi-permeable membrane. This process ensures the protein synthesis reaction lasting for a longer period of time, and as a result increasing the amount of protein produced by this process. The major advantage of CECF protein synthesis is its relatively simple setup since it does not require any external apparatus which is needed in other formats.

In this chapter, we discuss the design optimization and the fabrication of a device that contains multiple units for CECF protein synthesis. The optimization was performed by studying the effects of the membranes used, the volumetric ratio between the reaction mix and feeding solution, and the exchange surface area between the reaction mix and feeding solution in a miniaturized CECF setup.

In addition to the device's ability to carry out multiple CECF reactions in parallel, the device will follow the standards of the Society of Biomolecular Screening (SBS) so that it can be utilized with commercial measurement and dispensing equipment.

## **3.2 Materials**

Polycarbonate sheet was purchased from McMaster-Carr (Atlanta, Ga). Polypropylene sheets were purchased from Plastruct Canada (Ontario, Ca). Rapid Translation System (RTS) 100 Wheat Germ CECF and RTS 500 Ecoli CECF kits were purchased from Roche Applied Science, Mannheim, Germany. Sylgard 184 silicone elastomer kit was purchased from Dow Corning (Midland, MI)

Flat sheet dialysis membranes were purchased from Spectrum Laboratories (Rancho Dominguez, Ca). Regenerated cellulose membrane with differentiated filtration and a cutoff of 10, 000 daltons was purchased from Millipore (Billerica, Ma).

Polycarbonate sheet membrane with a 20,000 dalton cutoff was purchased from GE health care (Piscataway, NJ). Luciferase T7 control vector, recombinant luciferase, luciferase assay reagent, and nuclease free water were purchased from Promega (Madison, Wi).

## **3.3 Methods**

### **3.3.1 Prototype Device Fabrication**

A previously designed device was used as a starting point for our optimization process, the device shown in figure (3-1) has three components: a top part and bottom part milled by a CNC milling machine, and a regenerated cellulose membrane that separates the two parts. The top part has 3 mm diameter wells that are surrounded by two lunar shaped openings to allow access through the cellulose membrane. The bottom part has a diameter of 9 mm. The well in the top part is for protein synthesis. the openings in the top plate also allow access to the bottom part. The larger wells in the bottom part are designed to hold the feeding solution that provides the protein expression machinery with nutrients through a membrane.

The three layers (top part, membrane, and bottom part) were assembled together using microstamping technique.<sup>97</sup> In brief, poly(dimethylsiloxane) (PDMS) mixture was prepared according to the manufacturer's instruction (Sylgard 184, Dow Corning), followed by spinning it on a plate using a spinner (Laurell Technologies). The top layer with access holes and reaction chambers was then in contact with the thin PDMS layer, transferring a pattern of PDMS onto the bottom of the top layer. Similarly, a thin PDMS layer was transferred on the top contact area of the bottom layer with the feeding chambers. Three layers were immediately assembled together, fastened using C-clamps, and then cured in an oven at 60°C overnight. The access holes were connected to the feeding chamber by piercing through the local membrane

### **3.3.2 Protein Expression**

Luciferase was expressed using RTS 100 wheat germ kit (Roche). The reaction solution for protein expression and the feeding solution of nutrients were prepared according to the manufacturer's instructions. The reaction solution was composed of 15 µl wheat germ lysate, 15 µl reaction mix, 4 µl amino acids, 1 µl methionine, and 15 µl containing 2 µg of an individual DNA vector. For negative controls, the DNA vector was replaced with the same volume of nuclease free water. The feeding solution was prepared by combining 900 µl feeding mix (provided in the kit), 80 µl amino acids, and 20 µl methionine.

### **3.3.3 Luciferase Detection**

Luciferase was detected by adding the protein expression product to a 384 well white microplate, and programming a Mithras microplate reader (Berthold Technologies, Germany) to inject luciferase assay reagent, shake the microplate for 2 seconds, and read luminescence over 10 seconds.

### **3.3.4 Membranes**

Different types of membranes were tested in the device. The membranes varied by molecular weight cutoff and thickness as described in table 3-1. The thicknesses of the membranes were measured using a Dektak 150 profilometer as reported in table 2. A sample of each membrane was fixed on a microscope slide with an adhesive tape at the ends and the profilometer was used to scan the profile of the membrane.

All membranes were bonded using PDMS as describe above except for the cellulose membrane from Millipore which did not bind well when PDMS was attempted. Instead two-part epoxy (Epoxy Technology, Billerica, Ma) was used as follows. The two parts of the epoxy were mixed at a ratio of 10:1. A thin film of the mixture was created on a glass plate, by wrapping two pieces of thin wire on both ends of a razor. The razor was used to facilitate the removal of extra epoxy, by passing it on top of the epoxy mixture. Epoxy was transferred onto the two parts of the device by placing the two parts on top of the thin epoxy layer. In order to compare the effect of using different membranes, different devices were made using different membranes and the protein synthesis yield for each device was measured.

### **3.3.5 Reaction Mix and Feeding Solution Volume Ratio**

In order to take advantage of CECF protein synthesis the device needed to be optimized for maximum protein expression yield using the least amount of reagents. Although miniaturization in the device had been previously achieved,<sup>98</sup> the optimum ratio of the reaction mix to feeding solution was not studied. To achieve that goal multiple devices were designed so that all parameters are kept constant except for the amount of feeding solution.

The parameters that were kept constant include the exchange surface area between the reaction chamber and the feeding chamber, the size of the reaction chamber, and the amount of reaction mix used. That was accomplished by maintaining the same design and only varying the depth of the feeding chamber. The effect of the ratio was studied by expressing luciferase in the different devices. Relative protein synthesis yield was deduced from the luminescence resulting from the luciferase synthesized.

### **3.3.6 Exchange Surface Area of Membrane**

When the system is miniaturized the membrane surface area, and exchange rate, could have a greater effect on protein synthesis yield since the duration of the reaction is shorter, which is due to faster depletion of resources because of the small volumes used, faster enzymatic reactions, and possible evaporation.

The effect of the surface area was studied by designing different devices with all parameters constant except for the surface exchange area through the membrane between the two chambers. The parameters that were kept constant included the amount of both feeding solution and reaction mix, and the size of each chamber. The parameters that were changed were the dimensions of the feeding chamber whose depth changed as its cross sectional area decreased to maintain the same volume, and at the same time to maintain the same difference in liquid level between the reaction mix and the feeding solution in order to eliminate any possible effect from the difference in hydrostatic pressure. The parameters used for each device are shown in table 3-3.

### 3.3.7 96 Well-Plate Design

One of the applications of the device is high throughput screening. In order to achieve that goal, the device should be compatible with commercial dispensing and detection instrumentation.

Guidelines for regular microplates were set by the Society of Biomolecular Screening (SBS) and the American National Standards Institute (ANSI). Guidelines include rules for the height of a microplate (Figure 3-2), the location of the wells, and the shape and outline of the microplate. For the design to be compatible with commercial microplate readers and give an accurate reading, without damaging the plate reader, the device needs to follow these guidelines.

The device was designed to take luminescence/fluorescence readings from the top well. The surface area of the top well was maximized and the center of the top well was placed at the center location of a commercial 384 well-plate. To gain access to the feeding chamber and to prevent air entrapment in that chamber three access holes were designed to fit a pipette tip (see figure 3-3). Because the design needed to accommodate the top well and the three access holes, 96 wells were designed with the size and location corresponding to 384 well-plates, hence for each 4 wells in a 384 well plate only one was used that corresponds to the well in the first quadrant.

The well in the bottom plate was designed to encompass both the top well and the three access holes for filling. It was designed to accommodate 200  $\mu$ l of liquid to fulfill the 1:20 ratio under the assumption that 10  $\mu$ l of protein synthesis reaction mix will be used in a 50  $\mu$ l top well. The extra volume in the top well will accommodate the assay reagents if needed.

### **3.3.8 PDMS Thickness**

Although literature is available on the properties of spinning photoresist and other substances on Silicon, little was reported on the effect of spinning speed on PDMS thickness on plastic. Therefore, we studied the thickness of PDMS when it was spin coated on polycarbonate and polypropylene.

10 mg of monomer was prepared by mixing the elastomer and the hardener at a ratio of 10:1. The Laurel spinner was set at different speeds and the mixture was spun for 15 seconds. The film was cured in an oven overnight at 60° C. The cured PDMS was cut at two different locations from the center, and the thickness at each location was measured using a Dektak 150 profilometer.

### **3.3.9 Device Fabrication**

The device design is shown in figures (3-3 and 3-4). They were machined in polypropylene sheets (Plastruct Canada, Ontario, Ca) by TMR engineering, Micanopy, Florida. Afterwards, the machined parts were assembled with the regenerated cellulose membrane using the microstamping technique described above

### **3.3.10 Device Tests**

In order to test the device's ability of carrying out continuous exchange cell-free protein synthesis, 10 µl reaction mix with luciferase vector was pipetted into the top well, and 200 µl was added to the bottom well through the access holes. Two control experiments were performed at the same time, 10 µl reaction mix with luciferase vector was incubated in a microcentrifuge, and another 10 µl reaction mix was also incubated with 200 µl feeding solution in a microcentrifuge tube.

### **3.3.10.1 The dispensing test**

This test was done to verify if the device's design truly matches microplate standards. The test was done by injecting water in all 96 wells of the fabricated device, and comparing the amount of water injected in each of the wells with the wells in the corresponding location in a commercial 384 well-plate.

### **3.3.10.2 Luminescence measurement**

This test was done to compare the luminescence signal between a 384 well plate and the device by injecting 20  $\mu$ l luciferase assay reagent to 10  $\mu$ l of recombinant luciferase at a concentration of 100 nM. The signals were compared between the device and a commercial micorplate. The difference was probably due to the difference in absorbance and reflectance properties of the materials used for commercial microplates and the polypropylene used for the device.

### **3.3.11 Protein Purification**

Nickel-nitriloacetic acid (Ni-NTA) agarose magnetic beads from Qiagen (Valencia, Ca) were used to purify the histidine-tagged proteins, including (GFP), and (GUS). This was done by aliquoting five reaction products (10  $\mu$ l each) into a microcentrifuge with 5  $\mu$ l of Ni-NTA magnetic bead suspension. The mixture was incubated on microcentrifuge turner for 90 minutes.

A microcentrifuge tube magnet was used to immobilize the beads and the supernatant was removed. The beads were then washed by adding 25  $\mu$ l washing buffer, which was prepared by mixing 50 mM sodium phosphate, 300 mM sodium chloride, 20 mM imidazole, 0.05% Tween 20. The mixture was adjusted to a pH of 8 by adding sodium hydroxide. The beads and the washing buffer were incubated on a microcentrifuge turner for 30 minutes.

The microcentrifuge magnet was used again to immobilize the beads while removing the washing buffer using a pipette, afterwards, 50 µl elution buffer (50 mM sodium phosphate, 300 mM sodium chloride, 200 mM Imidazole, 0.05% Tween 20, pH8) was added to the beads and the mixture was incubated on the microcentrifuge turner for 5 minutes. The beads were immobilized using the magnet and the elution buffer with the purified protein was removed.

The relative amount of GFP in supernatants and beads was estimated by measuring fluorescence using excitation and emission wavelengths of 485 nm and 535 respectively. Glucoronidase (GUS) purification was verified by running a 15% polyacrylamide gel and staining it with coomassie brilliant blue stain.

### **3.4 Results**

#### **3.4.1 Membrane Effect**

The effect of using different membranes for CECF protein synthesis is shown in figure (3-5). It has been reported that the optimum membrane cutoff to be used in CECF protein synthesis is in the range between 8,000 - 14,000 daltons.<sup>10, 17, 99</sup> Most of the membranes used lied within this range. What was expected was that different membranes with the same cutoff would result in similar protein synthesis yield, however this was not the case. The polycarbonate membrane from GE with a cutoff of 20 KD was expected to result in the lowest protein synthesis yield, because of its large pores that would not be able to maintain the concentrations of the different components at an optimum, nor will it able to encapsulate important protein synthesis components in the reaction chamber. However the 10 KD cutoff membrane from Millipore did not produce much higher protein synthesis yield than the 20 KD cutoff GE membrane. At the same time, two different membranes with the same material from Spectrum Labs with the

same cutoff value of 6-8 KD resulted in completely different yields. One difference between the two membranes was their size: one was in a large sheet format (240 mm x 240 mm), and the other was in a 33 mm diameter disk format. The other difference was the thickness of the two membranes. The production of a large sheet required the material to be sturdy hence a thicker sheet was manufactured. The thickness of the membranes was measured as reported in table 3-2. The thicker membrane slows diffusion down and reduces protein synthesis yield. This is in agreement with Darcy's law  $J = (c_o - c_i) D/L$ . Where J is the flux  $c_o$  is the chemical concentration outside the membrane,  $c_i$  is the concentration inside the membrane, D is the diffusion coefficient, and L is the membrane thickness. In words Darcy's law states that the flux is inversely proportional to the membrane's thickness when there is diffusion across a porous membrane.<sup>100</sup>

### **3.4.2 Reaction Mix and Feeding Solution Ratio**

The goal of this study is to optimize the amount of feeding solution that would achieve maximum protein synthesis. Reports of the ratio between the reaction mix and the feeding solution range from 1:5 to 1: 100 depending on the system and the setup.<sup>23</sup> Results show that any amount of feeding solution greater than 200  $\mu$ l (with 10  $\mu$ l reaction mix) would result in a maximum protein synthesis yield (Figure 3-6). The figure shows that any amount of feeding solution more than 200  $\mu$ l is not going to have a significant effect on the amount of protein synthesized. Hence the optimum ratio between the protein synthesis reaction mix and the feeding solution for our system and setup is 1:20.

### **3.4.3 Membrane Surface Area**

In conventional CECF protein synthesis systems, the amount of reagents used is much larger than what is used in our device. As a result conventional systems are less susceptible to evaporation and surface tension issues than miniaturized devices. This, in addition to the larger reaction volumes, allows the reaction in a conventional system to last for longer periods of time. For the miniaturized device, it is expected that increasing the surface area of the membrane will increase the exchange rate of reagents between the feeding and reaction chambers, resulting in a greater protein synthesis yield.

Figure 3-7 shows that the greater the surface area the greater the luminescence signal indicating a larger amount of luciferase is synthesized when the surface area is increased.

### **3.4.4 PDMS for Microstamping**

For microstamping, polydimethylsiloxane (PDMS) needs to fulfill two conditions: the first is to minimize the amount of PDMS to prevent the small features of the micromilled parts from being clogged with excess PDMS; the second is to have enough PDMS to bond the layers without the obstruction of the burrs which usually result from milling.

The increase of spinning speed results in a decrease of the thickness of the PDMS layer formed. An inverse linear relationship can be observed in figure 3-8A between the spinning speed and PDMS thickness.<sup>101-102</sup> In addition, the results also shows that the thickness for all the speeds, except the lowest speed, is the same at the two distances (2 cm, 4 cm) taken from the center. At the lowest speed the thickness was a little larger at 2 cm due to a smaller centrifugal force.

There was no clear relationship between spinning acceleration and PDMS thickness when the final speed is constant (Figure 3-8B). However, the uniformity of thickness at 2 cm and 4 cm from the center decreased at very high or very low acceleration values.

### **3.4.5 Device Fabrication and Testing**

A picture of the fabricated device is shown in figure (3-9). The protein synthesis yield in the device was compared to that of the same amount of reaction mix in a tube – the batch process format; and with that of the same amount of reaction mix with the same amount of feeding solution (Figure 3-10) The results show that the device resulted in a 65 times increase in protein synthesis yield from the batch format and 22 times increase over the addition of the feeding solution to the reaction mix. In addition, the device showed at least 25 times higher protein synthesis yield than the unoptimized device previously published.<sup>98</sup>

The device can fit in commercial plate reader without the utilization of the “Height adjustment” option that the particular model had. In other words, the device is compatible with a wider range of commercial plate readers, even the ones that had no height adjustment option. The device also showed no problems in the dispensing test. The 20  $\mu$ l of water was successfully injected in the device in the same manner equal amounts of water were dispensed in the same locations in a 384 microplate.

The luminescence signal obtained from the luciferase assay in the device was distinguishable and statistically different from the negative control. However, the signal from the device was equivalent to one forth the signal from the same assay in a conventional microplate (figure 3-11). This should not be a problem if all samples are measured in the same device for drug screening and other applications since the

signals are standardized. The signal from protein synthesis without a feeding solution, which is a minimum of protein synthesized can easily be distinguished from a negative control in the same device as seen in figure 3-12.

### **3.4.6 Protein Purification**

Protein purification: was successful at a retrieval rate of 75% which was estimated by measuring the fluorescence signal of expressed GFP. Table 3-4 shows the percentage of fluorescence signal (relative to total fluorescent signal before purification). The experiment shows that 20% of the protein is washed out by the washing step.

Figure 3-13 shows the loss of protein from GUS purification during the wash step from lane 3 that has the wash solution. The same lane also shows remnants from the protein reaction mix demonstrating the tradeoff between the degree of purification and the degree of protein loss.

## **3.5 Conclusion**

Different parameters were studied for optimizing exchange between the feeding chamber and reaction chamber in continuous exchange cell-free protein synthesis. The studies showed that increasing the surface area, reducing the thickness of the dialysis membrane, and maintaining a ratio equal to or greater than 1:20 between the reaction mix and feeding solution would maximize the amount of protein synthesized.

Based on the optimized design, fabrication parameters and the accepted microplate standards, a 96-well device was designed and fabricated for 96 separate CECF protein synthesis reactions. The device was shown to be compatible with commercial dispensing and reading apparatuses. The amount of protein synthesized in the device was 65 times more than that synthesized in a conventional microplate.

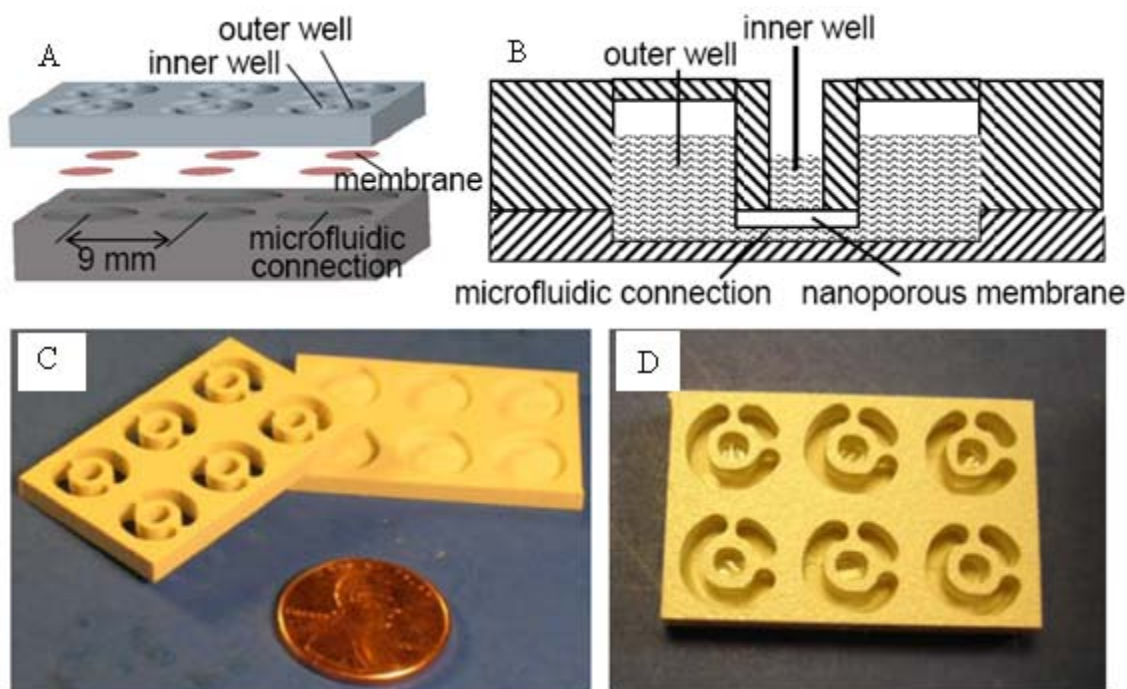


Figure 3-1. Original device used for optimization experiments. A) is a ProEngineer model for the device showing the inner well, outer well and membrane location. B) side view of each unit in the device. C) the two plastic micromachined parts constituting two layers. D) a fully assembled 6-well device

Table 3-1. List of membranes tested for cell free protein synthesis

Source	Material	Cutoff	Shape	Adhesive for bonding
Spectrum	Regenerated Cellulose	6- 8 KDa	Disk 33 mm diameter	PDMS
Spectrum	Regenerated Cellulose	6- 8 KDa	Sheet	PDMS
Millipore	Regenerated Cellulose with differentiated filtration	10 KDa	Disk 150 mm	Epoxy
GE	Polycarbonate	20 KDa	Sheet	PDMS

Table 3-2. Thickness of each membrane measured

Membrane	Thickness ( $\mu\text{m}$ )
GE polycarbonate	6
Spectrum Disk	42- 48
Spectrum Sheet	76
Millipore	235

Table 3-3. Surface area of membranes and their corresponding bottom well depth

Surface area of membrane ( $\text{mm}^2$ )	Adjusted bottom well depth (mm)
4.95	0.91
5.66	1.08
6.63	1.26
7.78	1.4
8.48	1.48
9.19	1.54



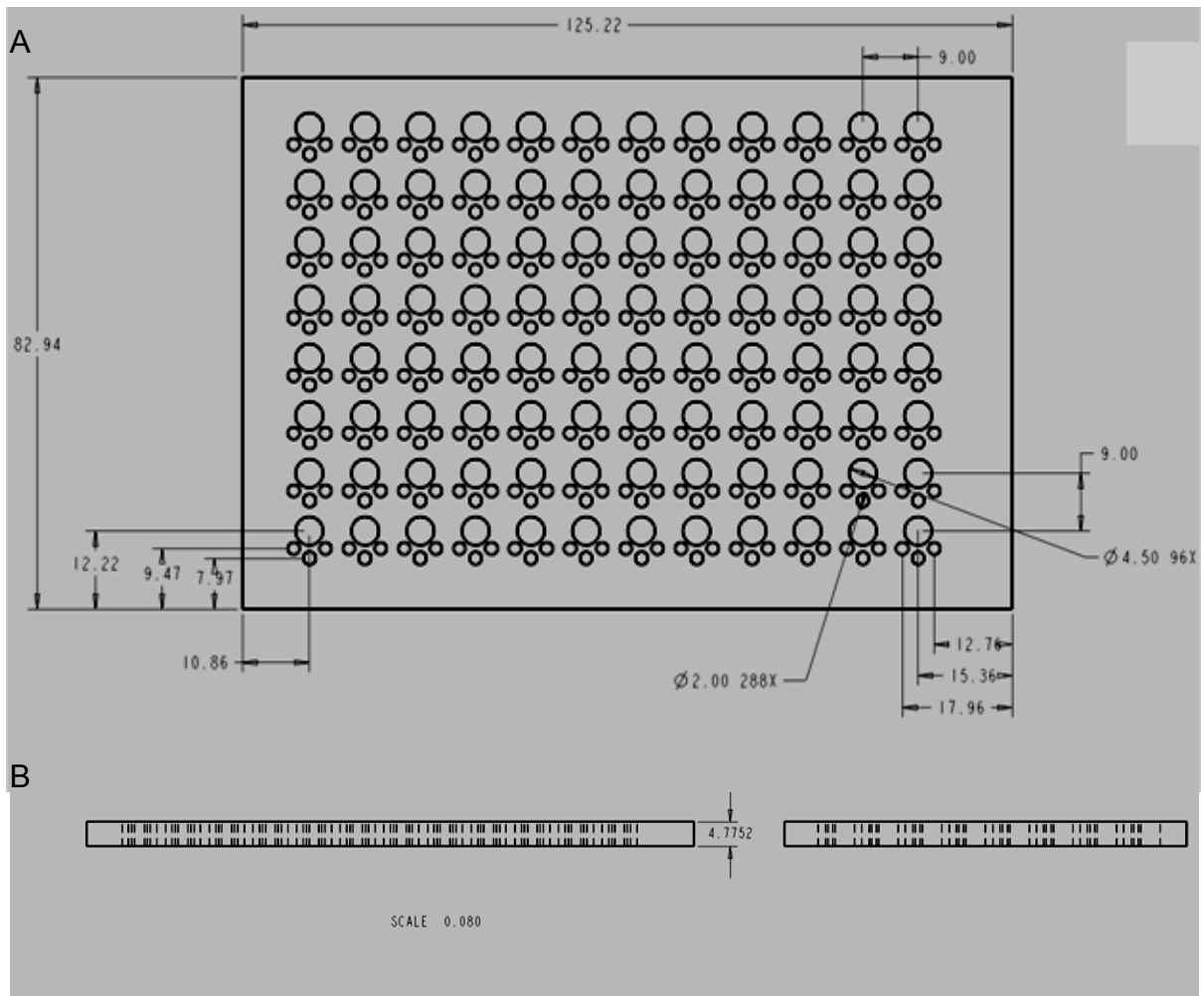


Figure 3-3. Design of top plate. A) Top view of the design of the top layer of the 96-well CECF device. B) Side view of the same part from both the longitudinal and the horizontal dimensions.

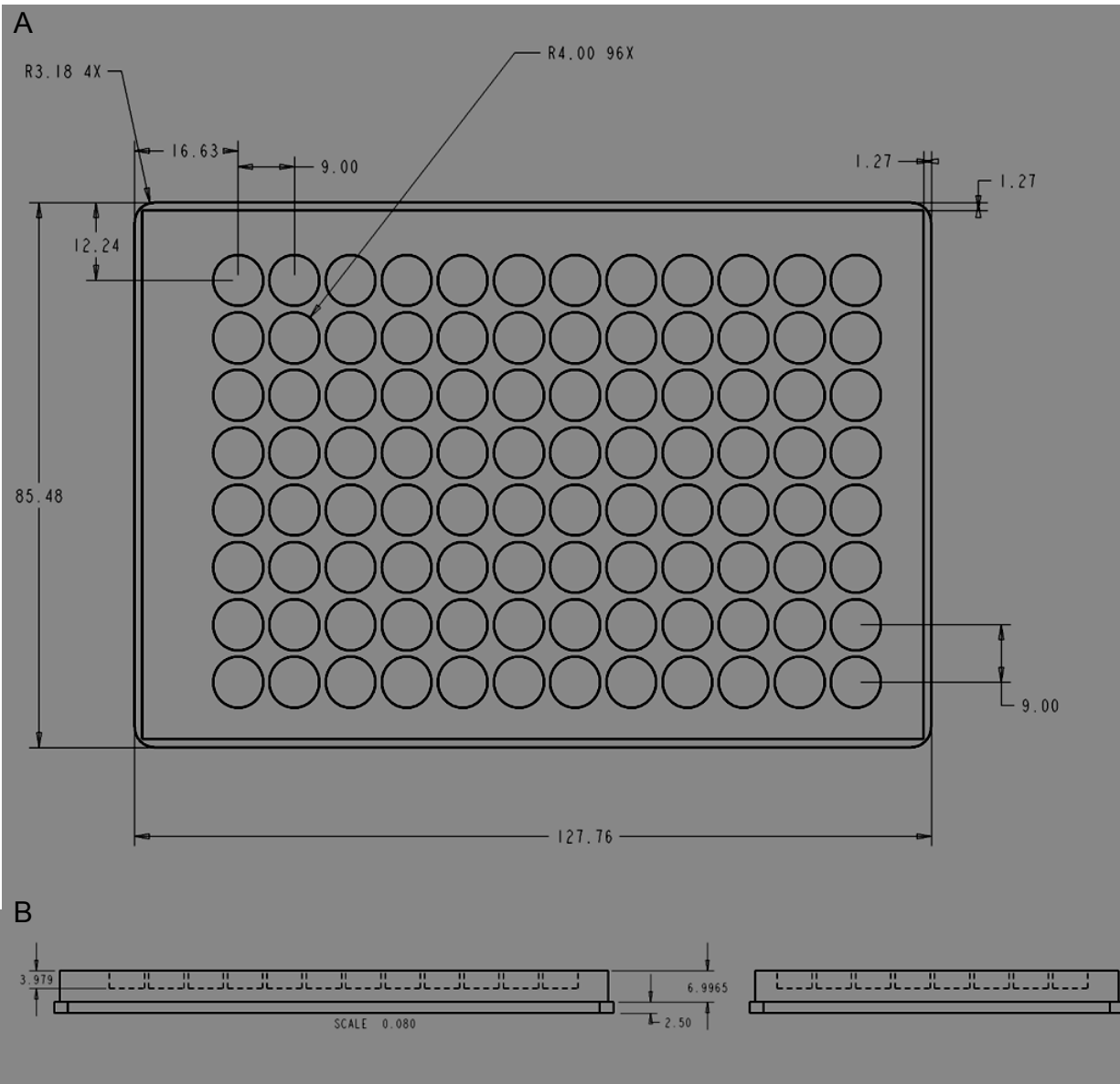


Figure 3-4. Bottom part design. A) Top view of the bottom plate of the 96-well CECF device. B) Side views of the bottom plate.

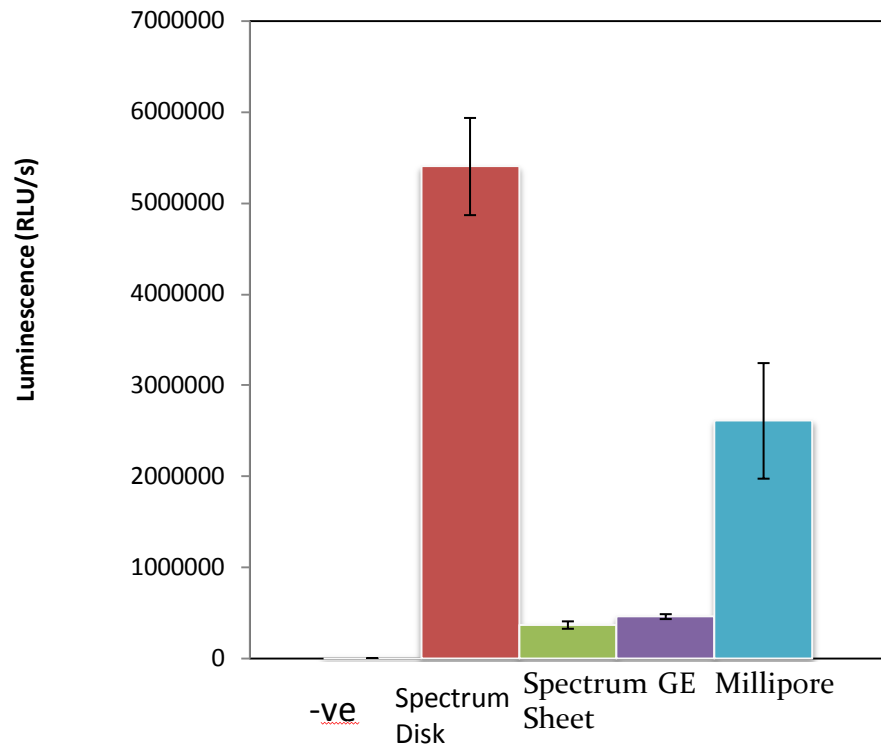


Figure 3-5. Effect of different membranes on protein expression yield in CECF devices.

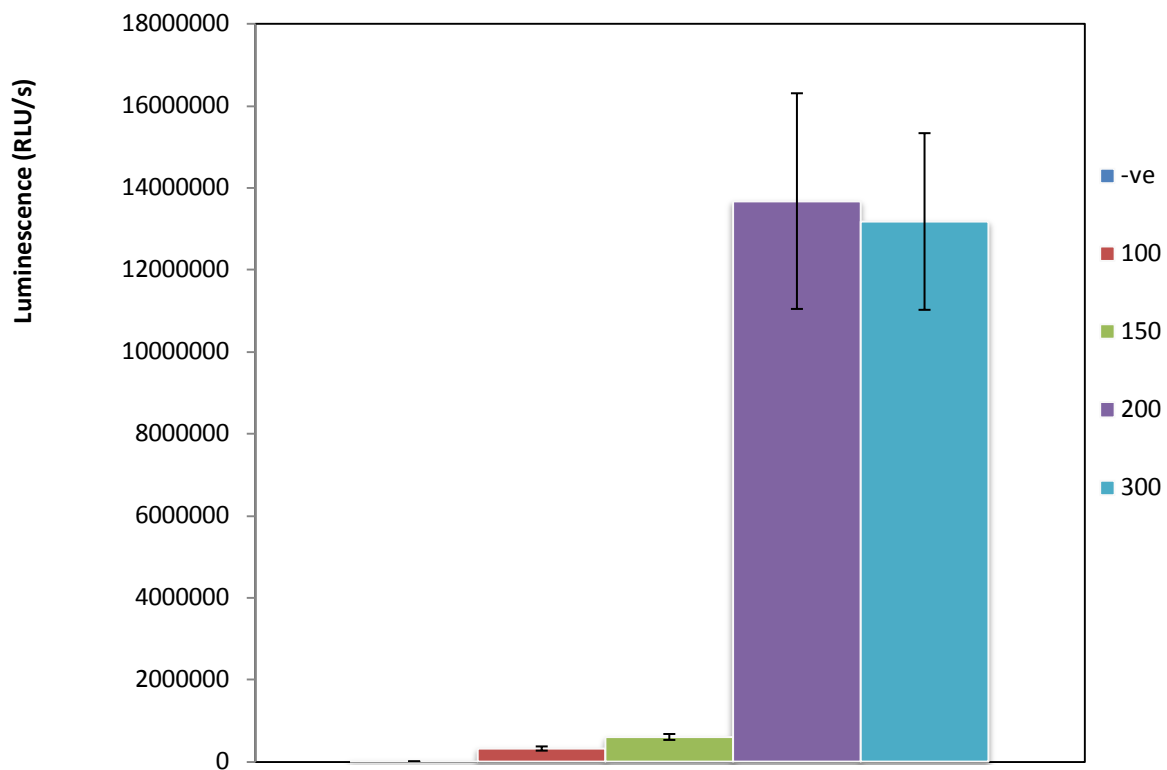


Figure 3-6. Effect of using different amounts of feeding solution on protein synthesis yield. The same amount of reaction mix was used in the CECF device.

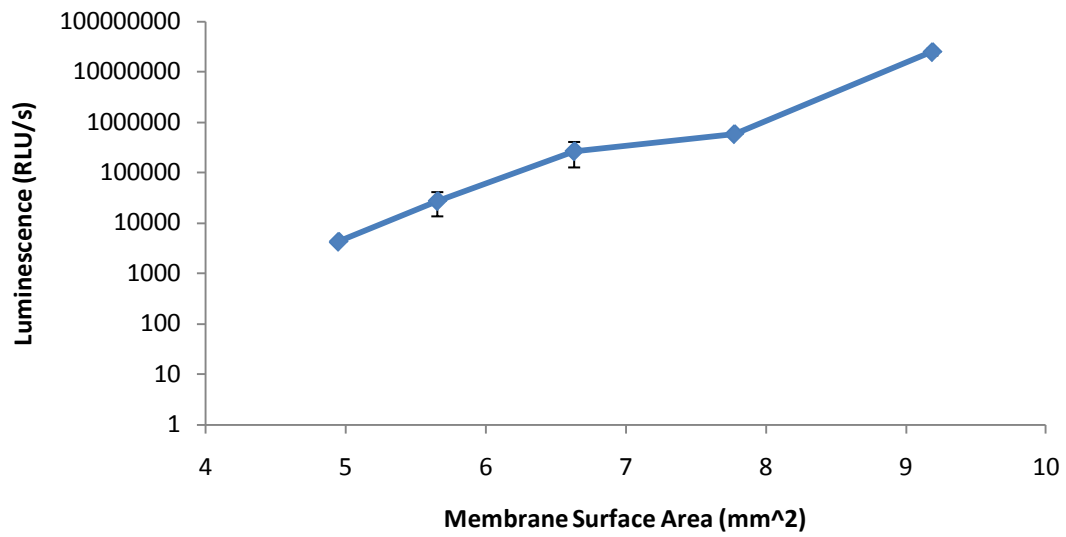


Figure 3-7. Effect of the surface area of the membrane on protein expression yield.

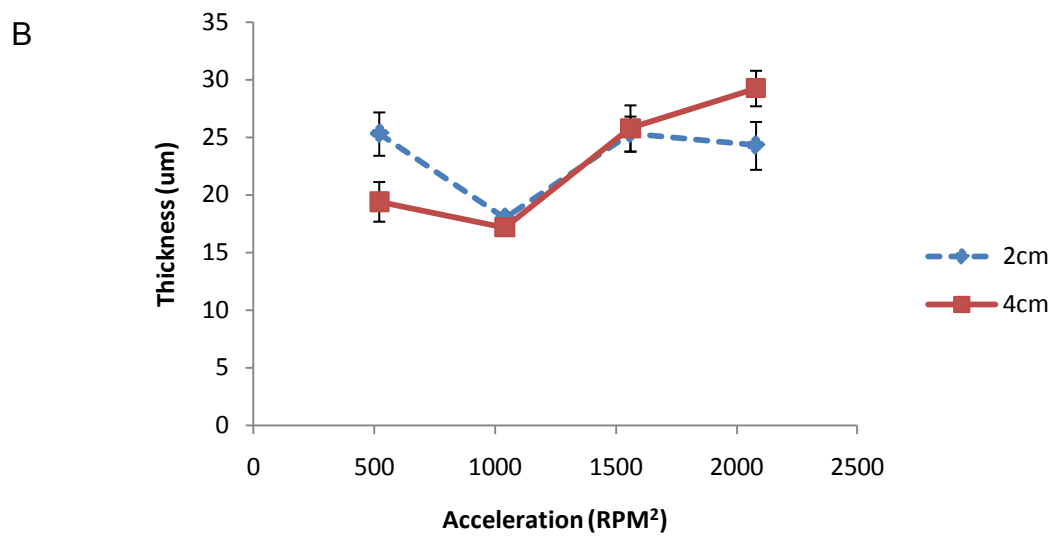
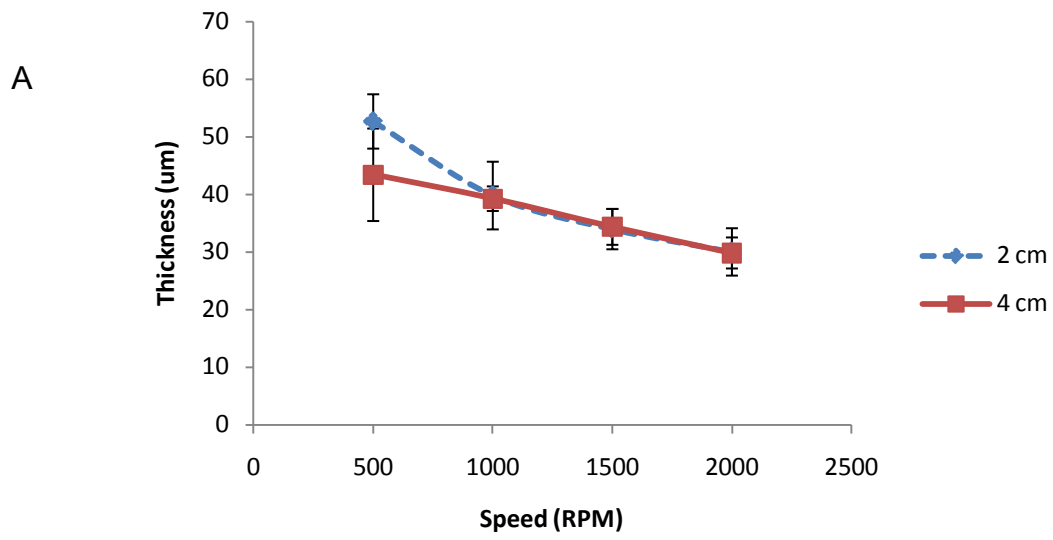


Figure 3-8. Effect of spinning parameters on PDMS thickness. A) Effect of spinning speed on the thickness of PDMS layer formed on a polycarbonate substrate. B) Effect acceleration on the thickness of PDMS

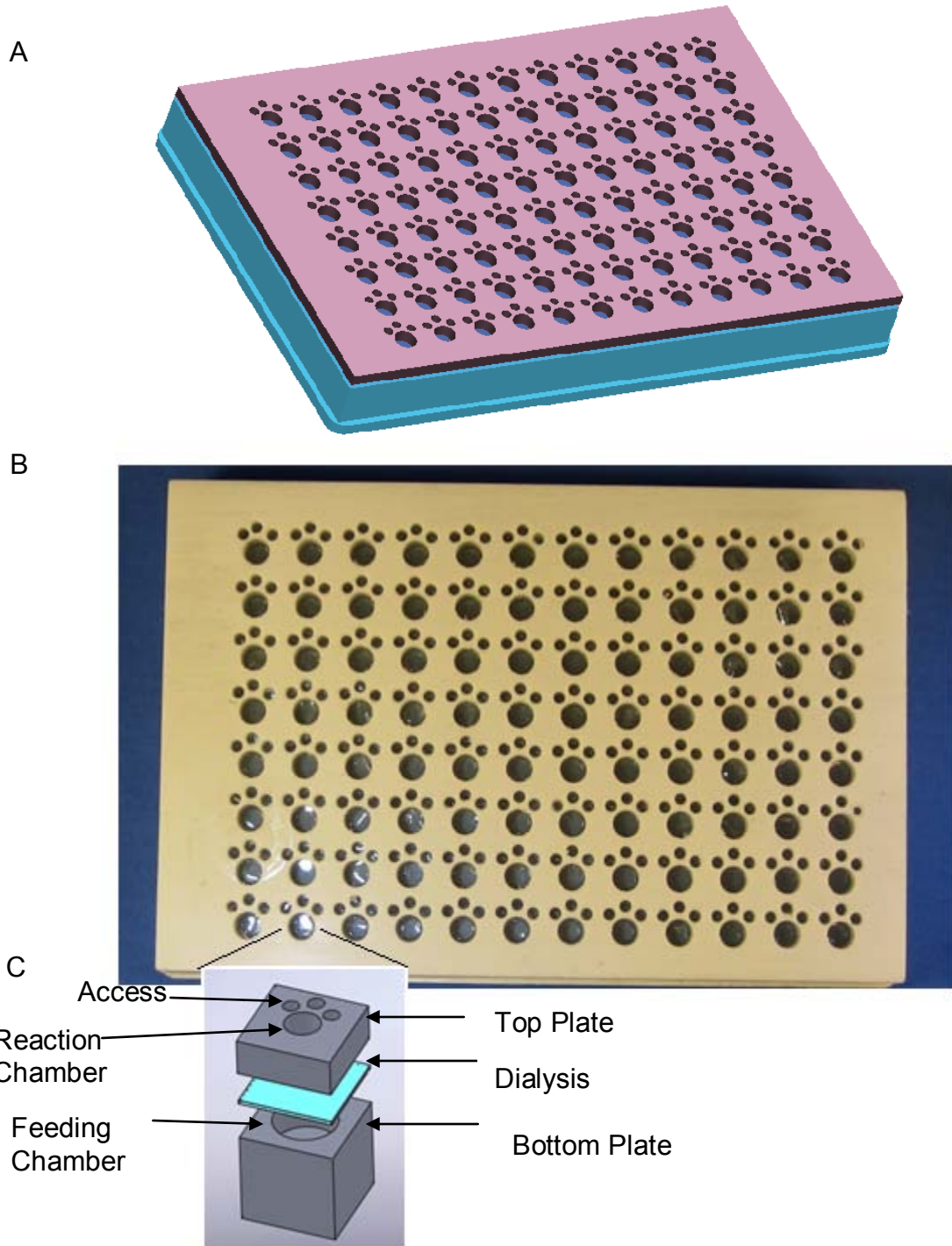


Figure 3-9. Model and picture of 96-well fluidic device. A) model of assembled 96-well CECF protein synthesis device. B) Picture of assembled device. C) Blow up model of a single well

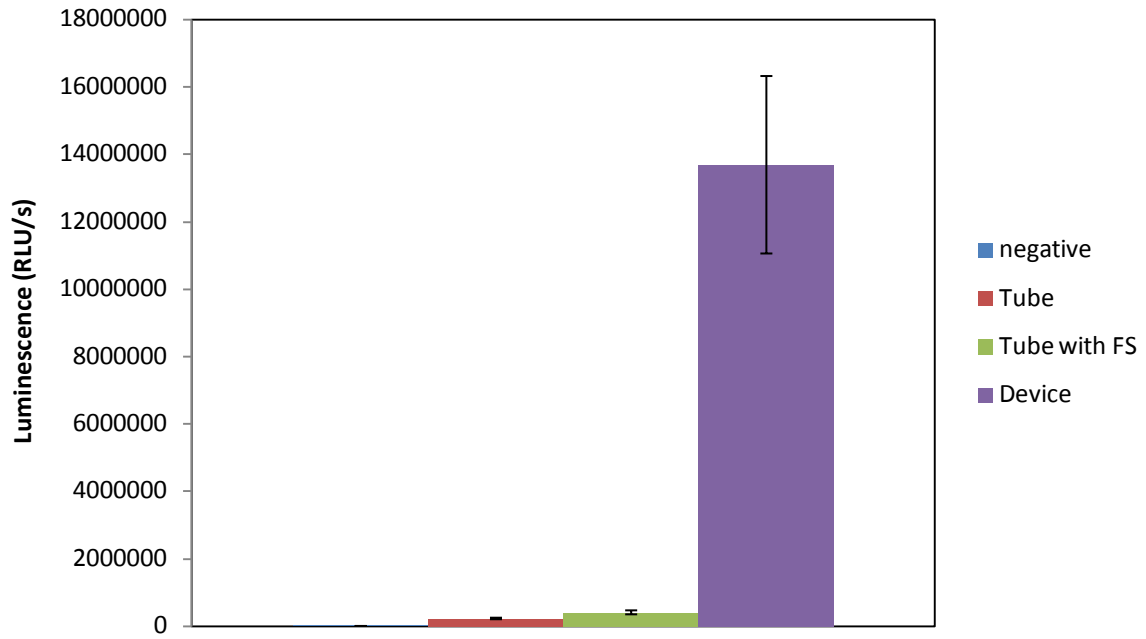


Figure 3-10. Comparison of protein synthesis yield between regular 384 well-plate and fluidic device

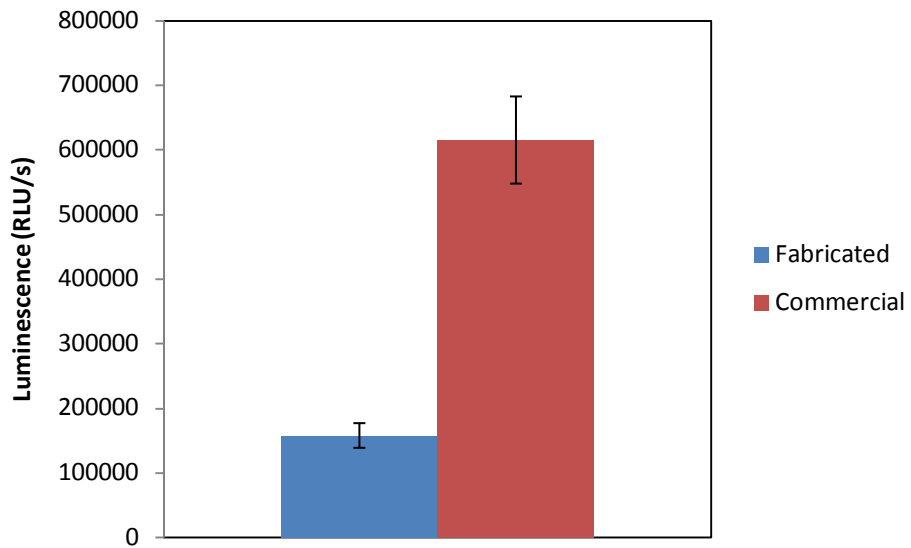


Figure 3-11. Comparison in luminescence signal between the device and a commercial 384 well-plate

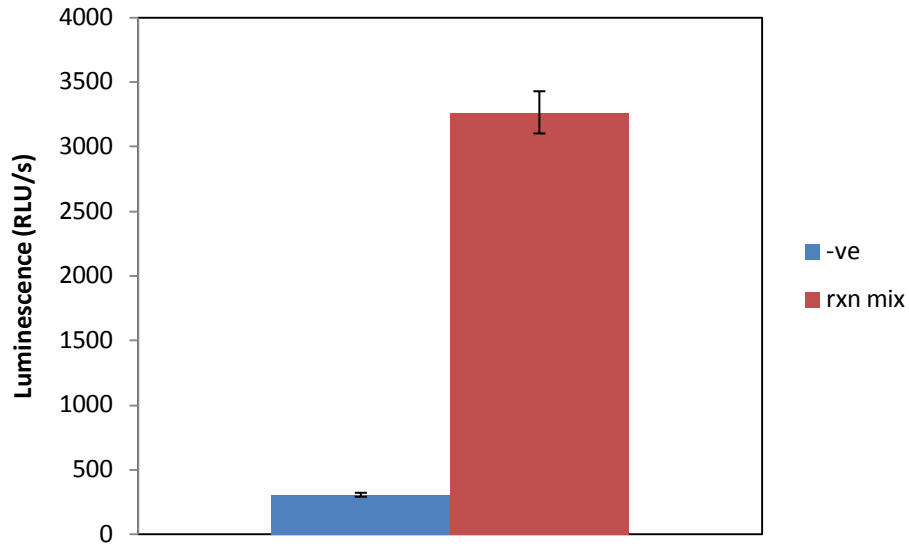


Figure 3-12. Difference in luminescence signal between a reaction mix with luciferase expressed and reaction mix with no DNA when the signal is read from a device.

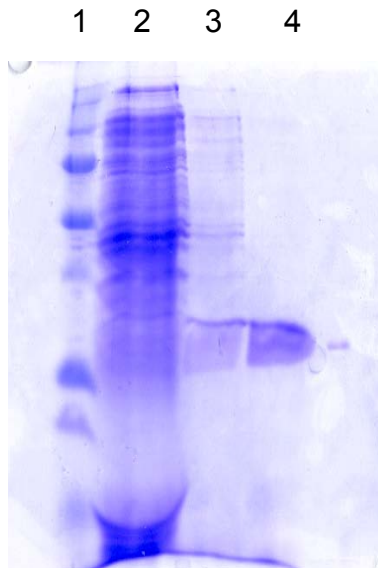


Figure 3-13. Gel of GUS purification results. The different lanes represent: 1) is the protein ladder. 2) Reaction mix with GUS expression. 3) Wash solution after wash. 4) Purified GUS.

Table 3-4. Results for Green Fluorescent Protein (GFP) purification

Step	Percentage of total fluorescence
Initial Supernatant after bead incubation	5%
Wash solution and beads	90%
Wash solution after removing from beads	20%
Elution solution	75%
Beads after elution	5%

## CHAPTER 4 HIGH THROUGHPUT PROTEIN SYNTHESIS AND DETECTION

### 4.1 Introduction

The fast, efficient, and simultaneous synthesis of multiple proteins in parallel has been a need and its importance has increased exponentially over the past few years. This importance stemmed from the close relationship between genes and their corresponding protein structure, function, and the need to match the high throughput format of gene discovery with that of protein analysis.

Over the past two years around two thousand genomes were under study including genomes of three primates, the human genome being the most relevant.<sup>65</sup> This genomic revolution led to a need for a better understanding of proteins which led to an increase in research for discovering new probes for screening for protein function and functional protein arrays. Another important application for protein synthesis is screening for new potential drugs or drug targets, both of which are usually proteins.<sup>63</sup>

One of the advantages of cell-free protein synthesis (CFPS) described in the previous chapters is that it provides the ability for miniaturization<sup>98, 103</sup> enabling high throughput protein synthesis and screening. In addition, CFPS allows the automation of protein synthesis, detection, and purification steps.<sup>104</sup> This in turn increases the accuracy of the experiments by reducing handling steps, reducing the amount of time required when compared to conventional cellular methods.

This chapter describes the use of the fluidic device described in chapter 3 for high-throughput protein synthesis. The experimental results show the advantage of using the device over a conventional microplate. CFPS is also used for synthesizing multiple

optically detectable proteins. Results demonstrate the possibility of using the system for enzyme engineering and enzyme screening.

## **4.2 Materials and Methods**

### **4.2.1 Plasmid Construction and Expression**

Control vectors of green fluorescent protein (GFP) which is the control vector for the RTS 500 E Coli kit and glucoronidase (GUS), the control vector for RTS 100 Wheat Germ kit were digested using restriction enzymes (Not1 and BamH1). The restriction reaction contained 20  $\mu\text{l}$  of plasmid with a concentration of  $1\mu\text{g}/\mu\text{l}$ , 5  $\mu\text{l}$  of 10X buffer, 2  $\mu\text{l}$  NotI enzyme, 2  $\mu\text{l}$  BamHI, and 21  $\mu\text{l}$  of water to have a total volume of 50  $\mu\text{l}$ . The reaction mixture was incubated in a water bath at 37° for 2 hours and ran on an agarose gel. The gel showed that GUS had restriction sites for both Not1 and BamH1 while GFP had only a restriction site for Not1.(Figure 4-1). As a consequence GUS was cut with the two restriction enzymes and ran on an agarose gel at 90 volts for 70 minutes. The vector fragment in which the new gene will be inserted was cut out from the gel and extracted using the Wizard SV gel and PCR cleanup system kit (Promega, Madison, Wi) as follows; an equal amount of membrane binding solution is added to the gel and the combination is incubated in a 50° water bath for 10 minutes to dissolve the gel. The resulting solution is poured into a column provided in the kit and was spun in a centrifuge at 2000 rotations per minute (rpm). The filtrate is discarded and the column is washed by adding 700  $\mu\text{l}$  wash solution to it and centrifuging it for 1 minute at 16000 g. The washing step was repeated with 500  $\mu\text{l}$  of wash buffer. The mini column is then transferred to a 1.5 ml microcentrifuge tube and 50  $\mu\text{l}$  water was added to it and centrifuged at 16000 g for 1 minute to dissolve the plasmid into the water.

The beta-lactamase ( $\beta$ -lac) gene was obtained from the PUC 18 vector (Figure4-2 a) by using polymerase chain reaction (PCR). At the beginning primers were designed to copy the gene from the vector and at the same time add the restriction sites of Not1 and BamH1. This was done so that the gene would be inserted in the correct orientation to be expressed in the cell-free protein synthesis system and can be transcribed efficiently by the T7 polymerase used in the system. The primers used were : 5'-AAAAGCGGCCGCATGAGTATTCAACATTTCCGTG- 3' and 5'-GGTCGGATCCTTACCAATGCTTAATCAGTG- 3'. The primers included regions necessary for PCR and the remaining bases include the restriction sites for Not1 and BamH1.

A PCR reaction was prepared by mixing the following components: 0.5  $\mu$ l plasmid template DNA, 5  $\mu$ l 10X PCR buffer, 0.5  $\mu$ l from each primer, 2.5  $\mu$ l dimethylsulfoxide (DMSO), 1  $\mu$ l deoxynucleotide triphosphates (dNTPs), 0.5 Taq polymerase enzyme, and 39.5  $\mu$ l water. The reaction was then incubated in a PCR machine. It is worth noting that multiple melting temperatures ( $T_m$ ) were tested for getting maximum PCR products, the optimum temperature was 65°C.

After the verification and cleaning of the PCR product by running the PCR mixture on an agarose gel, the fragment from the gel was cut and extracted using Wizard SV gel and PCR cleanup system as described above. The fragment was added to the purified GUS vector, followed by the ligation reaction: 3  $\mu$ l 10X ligation buffer, 2  $\mu$ l vector, 4  $\mu$ l insert sequence from digested PCR fragment, 1  $\mu$ l ligase enzyme, and 20  $\mu$ l water. The reaction was incubated overnight at 4° C.

Pretreated DH5 $\alpha$  E coli cells were transformed with the ligation mixture as follows, 50  $\mu$ l of cells were taken from a -80 $^{\circ}$  freezer, the cells were thawed on ice for five minutes, the ligation mixture was added and the whole mixture was transferred to a glass tube and incubated on ice for thirty minutes. The glass tube was then put in a 42 $^{\circ}$  water bath for two minutes to heat shock the bacteria and allow it to take up the plasmids, the tube was then put on ice for 5 minutes to cool off the temperature. Afterwards, 1- 1.5 ml of L-broth liquid media was added to the tube which was incubated in a 37 $^{\circ}$  shaker for an hour to allow the bacteria to grow.

Two agar plates with ampicillin at a concentration of 100  $\mu$ g/ml were used. The first one was plated with 100  $\mu$ l of media containing transformed DH5 $\alpha$ . The remaining amount of DH5 $\alpha$  was transferred to a microcentrifuge and centrifuged at 10 000 RPM for one minute. The supernatant was discarded and the pellet was resuspended and plated on the second agar plate. The two plates were incubated at 37 $^{\circ}$  overnight. Colonies were selected from the two plates with a sterile stick. Each colony is grown into a glass tube containing L-broth with ampicillin at a concentration of 100 $\mu$ g/ml and incubated in a shaker at 37 $^{\circ}$  overnight.

Wizard Plus Miniprep system from Promega (Madison, Wi) was used to perform a miniprep on the grown bacterial colonies. The contents of each of the glass tubes were then poured into a microcentrifuge tube and spun for 1 minute at top speed to collect the cells and remove the supernatant. The cells were resuspended in 250  $\mu$ l resuspension buffer and vortexed for complete resuspension. 250  $\mu$ l of cell lysis buffer was added to the resuspended cells followed by adding 350  $\mu$ l neutralization buffer to precipitate the protein content of the cells.

The microcentrifuge tubes were spun at maximum speed for 10 minutes. A spin column was inserted in a collection tube for each of the spun microcentrifuge tubes, the supernatant was poured into the column, and the microcentrifuge tube was discarded. The spin column and the collection tube were then spun at maximum speed for 1 minute and the precipitate was discarded, 750  $\mu$ l of washing solution was added to the spin column, then spun at maximum speed for one minute. The precipitate was discarded and the washing process was repeated with 250  $\mu$ l washing solution. The spin column was removed from the collection tube and inserted into a 1.5 ml microcentrifuge tube and they were spun at maximum speed for 1 minute after adding 100  $\mu$ l of water to dissolve the DNA bound to the spin column's membrane.

Samples of the extracted plasmids were digested using the restriction enzymes Not1 and BamH1 in a reaction as described above. The digestion reactions were ran on an agarose gel to verify which colonies had the correct plasmid (Figure 4-3). Glycerol was added to cells containing the correct plasmid, the cells were saved at -80° C for future use.

Alkaline phosphatase gene sequence was PCR- amplified from *Pseudomonas Aeruginosa* chromosomal DNA using the primers 5'-AGGGAGCGGCCGCATGACCCCAGGTTATCCCCTCGCCCTC-3' and 5'- TCGTTCGGATCCGATCAGTCGCGCAGGTTTCAGTGCGC-3'. The conditions used for the PCR reaction were the same as described above for the  $\beta$ -lactamase gene except that the PCR reaction contained 2  $\mu$ l of template DNA instead of 0.5  $\mu$ l because genomic DNA was used instead of plasmid DNA.

The amplified PCR fragment was cleaned as described above. It was then cloned into the pGEM vector using the pGEM-T easy vector system from Promega (Madison, WI). The reaction was set up as follows; 5  $\mu$ l of 2X rapid ligation buffer, 1.5  $\mu$ l T4 DNA ligase, 1.5  $\mu$ l pGEM vector, and 1.5  $\mu$ l PCR fragment. The mixture was incubated at 4  $^{\circ}$ C overnight. The pGEM insertion was done to ascertain that the correct fragment was cut out for ligation with vector at Not1 and BamH1 restriction sites. Cutting the PCR fragment with the restriction enzymes would be difficult to test since the size of the DNA fragment is almost identical and cannot be distinguished from the uncut PCR fragment, however cutting the pGEM vector with the PCR fragment inserted using the Not1 and BamH1 restriction enzyme would enable the assertion of obtaining the correct cut fragment.

The pGEM vector with the PCR insert plasmid was then transformed into DH5 $\alpha$  cells as described above. The cells were plated on an ampicillin plate that was also plated with X-gal for Blue-White screening. Since both the pGEM vector and the PCR fragment have blunt ends the pGEM vector could self-ligate without containing the insert. At the same time it would still have the Ampicillin gene which would provide cells with self-ligated pGEM vector with Ampicillin resistance. In order to differentiate colonies that have the self-ligated pGEM vector from colonies that have the pGEM vector with the PCR fragment Blue-White screening is necessary. The pGEM vector is opened in the middle of the  $\beta$ -galactosidase gene where the target DNA vector should be inserted. When pGEM self-ligates,  $\beta$ -galactosidase is intact, the enzyme is synthesized and it cleaves X-gal, resulting in the blue insoluble chemical 5-bromo-4-chloro-3-hydroxyindole, which turns the colors of the colonies with the self-ligated plasmid blue.

Colonies containing the PCR insert did not turn blue and remained white. These colonies were picked and grown in L-broth containing 100 µg/ ml ampicillin as described earlier.

Plasmids from each colony were digested with the restriction enzyme Not1 and BamH1 and the AP gene was cut out from the gel and purified as described above. Cloning into pGEM vector was done to guarantee that the digestion reaction has occurred properly after having some problem in cloning the gene directly into the vector extracted from the GUS control vector. A ligation reaction similar to the one described above for β-lactamase cloning was set up with the extracted fragment containing alkaline phosphatase gene. The resulting plasmid was transformed into DH5α cells, which were afterwards plated for ampicillin selection. Colonies were grown overnight, and finally a miniprep was performed.

Plasmid DNA from the miniprep was digested using the restriction enzyme Pst1. This restriction enzyme was found to cut the AP gene at two locations resulting in a 500 bp fragment and hence was used to verify the presence of the correct plasmid (Figure 4-4).

5 µl samples of each solution containing the constructed plasmid was diluted in 95 µl water in a cuvette. The mixture was measured using a spectrophotometer at an absorbance wavelength of 260 nm. The result was multiplied by 20 – counting for the 20 times dilution- to obtain the plasmid concentration.

#### **4.2.2 Protein Expression**

Luciferase, β-glucuronidase, alkaline phosphatase, β-lactamase, and β-galactosidase were expressed using RTS 100 wheat germ kit (Roche). The reaction solution for protein expression and the feeding solution of nutrients were prepared

according to the manufacturer's instruction. The reaction solution was composed of 15  $\mu$ l wheat germ lysate, 15  $\mu$ l reaction mix, 4  $\mu$ l amino acids, 1  $\mu$ l methionine, and 15  $\mu$ l containing 2  $\mu$ g of an individual DNA vector, except for AP vector for which 4  $\mu$ g were added. An optimization experiment was carried out to find the correct amount of AP used in case there was any contamination from the plasmid construction and amplification steps. For negative controls, the DNA vector was replaced with the same volume of nuclease free water. The feeding solution was prepared by combining 900  $\mu$ l feeding mix (provided in the kit), 80  $\mu$ l amino acids, and 20  $\mu$ l methionine.

DNA vectors that were not constructed as described above were purchased. Vectors of luciferase (Figure 4-2 b), glucuronidase, and  $\beta$ -galactosidase (p-DNR LacZ) (Figure 4-2 c) were obtained from Promega, Roche, and Clontech, respectively. (Figure 4-5)

Green fluorescent protein (GFP) was expressed in the RTS 500 E. coli kit. The reaction solution was composed of a 10  $\mu$ l solution from a mixture containing 2  $\mu$ g of GFP vector and 40  $\mu$ l aliquot of a mixture, which was prepared by mixing 0.525 ml E coli lysate, 0.225 ml reaction mix, 0.27 ml amino acid mix without methionine, and 30  $\mu$ l methionine. The feeding solution was prepared by adding 2.65 ml amino acids without methionine and 0.3 ml methionine to 8.1 ml feeding mix. Coexpression reaction mix solution was prepared as described previously with each protein expressed separately except that plasmid DNA from all 6 constructs was added. 0.33  $\mu$ g plasmid from each protein except for alkaline phosphatase DNA from which 0.66  $\mu$ g were added. All Coexpression experiments were carried out in the Wheat Germ system except for the test where GFP was measured which was expressed in the E Coli system.

To carry out protein expression in the fluidic microplate device, 10  $\mu$ l of the reaction solution was pipetted to a reaction chamber and 200  $\mu$ l of the feeding solution was added to the feeding chamber through one of the access holes. The device was sealed using PCR tape to prevent evaporation. For comparison, a standard 384-well microplate was used and 10  $\mu$ l of the same reaction solution was pipetted to one well. The microplate was also sealed with PCR tape. Both the device and the microplate were placed on an orbital shaker for four hours, rotating at a speed of 30 rpm. The synthesized proteins were then analyzed as discussed below, though GFP samples were kept still at room temperature for two additional hours, allowing them to fold completely to have fluorescent property.

#### **4.2.3 Detection of Glucuronidase (GUS)**

For the detection of GUS Marker Gene  $\beta$ -Glucuronidase (GUS) Reporter Gene Activity Detection Kit (Eugene, Co) was used. The kit was made for the detection of GUS expression in plant cells hence the procedure needed to be optimized for the cell-free format in which GUS was expressed. A Mithras LB940 microplate reader (Berthold Technologies, Bad Wildbad, Germany) was used to measure the fluorescent signal which results from the catalysis of 4-methylumbelliferyl  $\beta$ -D-glucuronide (4-MUG), a fluorogenic GUS substrate whose catalysis results in a fluorescent signal at an excitation and emission wavelengths of 355 nm and 460 nm respectively.<sup>105</sup>

The optimum concentration of 4-methylumbelliferyl  $\beta$ -D-glucuronide (4-MUG) was found to be 100  $\mu$ M when the amount added is 30  $\mu$ l to accommodate the size of the well in the designed device. Although the enzymatic assay was reported to take 2-3 hours, the high concentration of GUS in the cell-free system was found to speed up the reaction. Only 6-8 minutes was needed since the fluorescence signal from the

enzymatic reaction was measured over 2 hours, only to find that the signal reached a plateau after 6 minutes(Figure 4-6). The final protocol followed was to add 30  $\mu$ l of 100  $\mu$ M GUS to the protein expression mix, incubating the reaction for 6-10 minutes at room temperature, and finally measuring and averaging the fluorescence signal over 10 seconds.

#### **4.2.4 B-Galactosidase (LacZ) Detection**

Fluorescein mono- $\beta$ -D-Galactopyranoside (FMGal) (MarkerGene Technologies, Eugene, Co), a fluorogenic LacZ substrate, was used to detect LacZ synthesis.<sup>106-107</sup> The fluorescent signal was measured at an excitation and emission wavelengths of 485 nm and 535 nm respectively. The concentration of 200  $\mu$ M was used as recommended by the manufacturer. In order to evaluate the enzymatic reaction incubation time, a kinetic assay was performed to measure fluorescence after adding the substrate to protein expression mix was done. The reaction needed an incubation time in the range of 10- 15 minutes (Figure 4-7). The final protocol was to add 30  $\mu$ M FMGal to the protein expression mix after the reaction, incubate for 10- 15 minute, then measure and average the fluorescence signal for 10 seconds.

#### **4.2.5 Alkaline Phosphatase (AP) Detection**

3-Phenylumbelliferone 7-O-phosphate hemipyridinium (MarkerGene Technologies, Eugene, Co), a substrate that emits a fluorescent signal after being cleaved by AP, was used for its detection. The optimum concentration reported in literature<sup>108</sup> was 10  $\mu$ M when 30  $\mu$ l were added to the protein expression mix. Excitation and emission filters used had the wavelengths of 355 nm and 460 nm respectively. The enzyme turnover was very fast and the maximum signal could be reached instantaneously. No incubation period was necessary and the signal was stable to up to 30 minutes.

#### 4.2.6 B-Lactamase (B-Lac) Detection

$\beta$ -lactamase was measured using m- [[(phenylacetyl)glycyl]oxy]benzoic acid<sup>109-110</sup> (Calbiochem, San Diego, Ca), a chromogenic  $\beta$ -lactamase substrate that changes color upon being catalyzed. This reaction can be followed spectrophotometrically at a wavelength of 314 nm. To measure  $\beta$ -lactamase expression in-vitro, 90  $\mu$ l 2 mM m- [[(phenylacetyl)glycyl]oxy]benzoic acid was added to 10  $\mu$ l expression product. To optimize the amount of time for the catalysis reaction to take place the mixture was transferred to a cuvette and absorbance was measured using a BioRad spectrophotometer every minute for 15 minutes. To prove the specificity of the reaction 90  $\mu$ l of substrate was added to 10  $\mu$ l luciferase expression product and the absorbance signal of the mixture was measured under the same conditions. The two absorbance signal curves for  $\beta$ -Lac and luciferase using beta lactamase substrate is shown in figure (4-8). The result shows that the reaction takes around 5 minutes to reach a plateau. As a result, for  $\beta$ -Lac measurement, the protein expression mix and substrate were incubated for 5 minutes before absorbance measurement.

### 4.3 Results

#### 4.3.1 Luciferase Expression Yield

Measuring the luminescence signal from luciferase expression over time in a regular microplate and in the 96-well device fundamentally compares cell-free protein expression between two formats. The regular microplate represents the batch format, in which all protein expression components are mixed together, whereas the 96-well device represents the continuous exchange format, in which the reaction is continuously supplied with amino acids, ATP, GTP, and other energy components. It is also supplied with amino acids through a semipermeable membrane.<sup>10</sup> The membrane also maintains

the concentration gradient of anions and cations that have an optimum concentration in the protein synthesis process, the effect of maintaining this concentration has been discussed particularly for  $Mg^{+2}$  ions which are needed at a higher concentration for transcription than they are for translation,<sup>111</sup> and has been shown as the reason why coupled transcription/translation systems usually give a lower yield than uncoupled systems<sup>13</sup>. The bottom well also provides an outlet for the reaction's byproducts which can suppress the process if their concentrations increase. This continuous supply of reagents allows the reaction to last for a longer period of time and hence increases the protein synthesis yield as shown in figure (4-9). The protein synthesis reaction seized thirty minutes after the beginning of the reaction in the batch format. In contrast, the CECF format where the reaction lasted more than four hours and led to 52 times greater protein yield for luciferase.

#### **4.3.2 Protein Expression Levels**

The improvement in protein expression yield in the device over a conventional microplate differed from one protein to the other. This is shown in figure (4-10) and reported in Table4-1. For example luciferase and GFP had a very big improvement in yield as indicated by the amplification factor in luminescence signal for luciferase (52.37) and fluorescence signal for GFP (44.75). On the other hand the increase in AP and  $\beta$ -galactosidase expression was only (1.4) times and (2.85) times, respectively (Table 4-1). The variation in the improvement in protein expression yield when is most evident when comparing GUS and  $\beta$ -lactamase. GUS was not detected when expressing it in the regular microplate, there was no statistical difference in the signal between the negative control and the samples expressed in a conventional microplate. In other words GUS can only be detected when expressed in the device. On

the other hand,  $\beta$ -lactamase expression is not improved much when using the device. This variation is expected to be due to the plasmids used. Plasmids that have given higher protein yields were optimized for cell-free protein synthesis systems with a T7 polymerase promoter. On the other hand  $\beta$ -galactosidase plasmid also had a T7 promoter, but it was designed for cell-based systems. It had no T7 terminator and the untranslated regions (UTR) are expected to be significantly different.

Figures (4-11) and (4-12) show that extending protein synthesis time through the utilization of the CECF format improved protein expression yield. As a result, the positive signal can be more distinguishable from the background that results from using the protein's specific enzymatic assay. The relevance in displaying a negative control lies in the fact that the reaction mix's components could have a catalytic effect on the various enzymatic substrates used. In order to prove the presence of the protein expressed the signal from the expression product has to be statistically distinguishable from the negative control.<sup>112</sup> Detecting a protein using its enzymatic assay without harvesting is not only more rapid and more practical for high throughput screening,<sup>32, 113</sup> but would also give a more accurate measurement of the true amount of protein expressed since purifying the protein always results with some loss. Most importantly, these assays would prove that the expressed proteins are in their correct conformation by showing their functionality in catalyzing their specific substrates.<sup>114</sup>

Figures (4-11) and (4-12) also show the specificity of the assays to their corresponding proteins, where enzymes could not catalyze substrates specific to other enzymes. This demonstrates the possible application of the system in enzyme fingerprinting and functional screening.

### 4.3.3 Co-Expression

We expressed all six proteins in the same reaction—by adding all 6 plasmids to the same reaction—both in a microplate and in the 96-well device, and applied the different detection assays to detect each protein. All the proteins except for AP were detected only when the co-expression was carried out in the device (Figure 4-13). It can also be observed that the percentage of protein yield from co-expression differs from one protein to the other when compared to proteins' individual expression. For example, GFP yield from coexpression was 9.6 % of the protein expression yield when of individual GFP expression. This was not expected since GFP and its co-expression measurement were both done in the E coli based kit, to which only the GFP plasmid is compatible. On the other hand, AP yield from the co-expression reaction in the device was 80% of the individual AP expression yield in the device.(Table 4-2)

Expressing multiple proteins in the same reaction might have many applications such as studying protein-protein interactions and post-translational modification. It can also be used in the expression of multi subunit proteins. Coexpression was necessary for the successful expression of properly folded soluble membrane proteins <sup>73</sup> as demonstrated in Chapter 5.

## 4.4 Conclusion

In this chapter, the 96-well fluidic device in chapter 3 was used for high-throughput protein synthesis. Six optically detectable proteins were expressed namely; GFP, luciferase, GUS,  $\beta$ -galactosidase,  $\beta$ -lactamase, and alkaline phosphatase. Their corresponding enzymatic assays (except for GFP) were used for their detection, not only ascertaining successful polypeptide expression but also correct conformation and function. Their corresponding assays were optimized for applications in a cell-free

environment and their specificity was also demonstrated by comparing them with a negative control and by using them with different protein expression products.

The superiority of the device was shown by comparing it to a regular microplate. An improvement in protein synthesis yield was as high as 87 times for GUS. The importance of using the device was also demonstrated for GUS where it was only successfully expressed in the device and had no statistically significant expression levels in a regular microplate. The necessity of optimizing the plasmid used for cell-free protein expression was evident by the protein synthesis yield discrepancy between an optimized plasmid such as GFP or GUS and an unoptimized plasmid such as  $\beta$ -lac or AP.

Finally, the device was successfully used for increasing protein synthesis yield in both a prokaryotic (E coli) based system and a eukaryotic (wheat germ) based system, showing the flexibility of the device and the possibility of using it in expressing different types of proteins with different expression restrictions. This device can be used for high throughput protein synthesis, for enzyme screening and fingerprinting, and other applications as demonstrated in chapter 5.

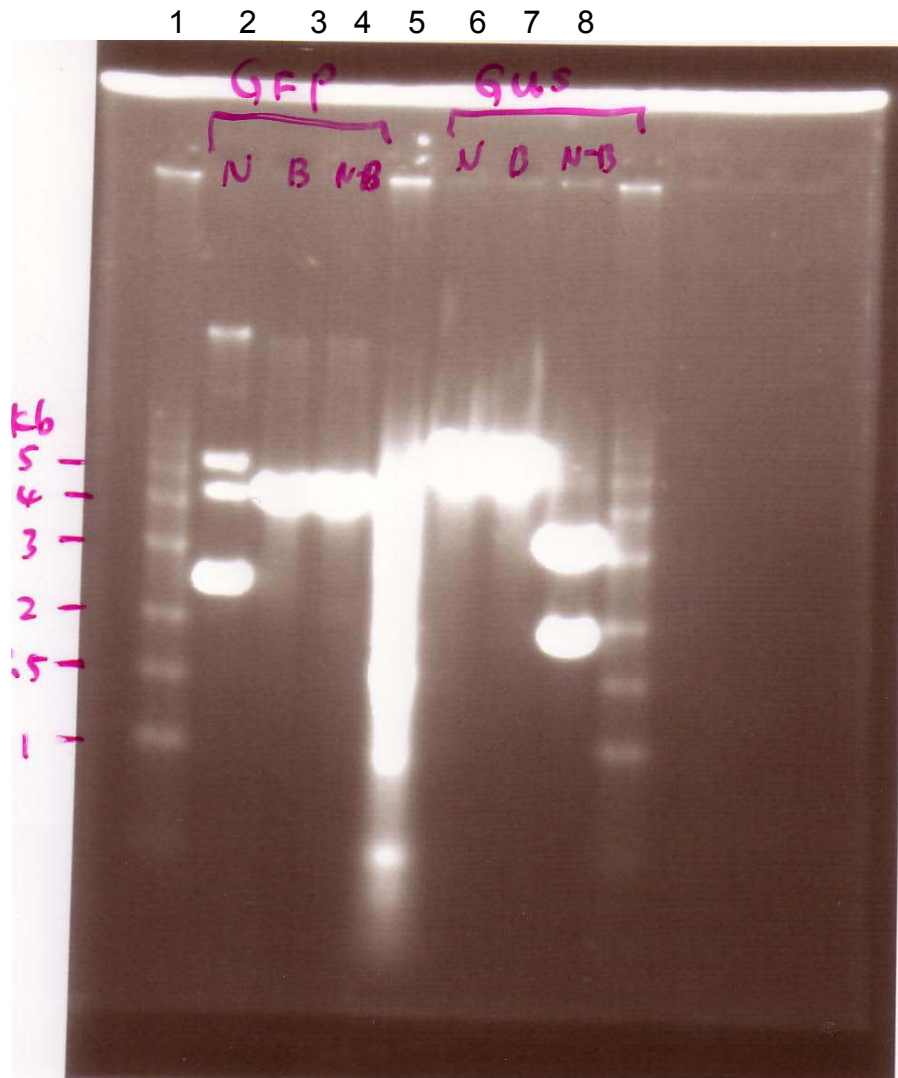


Figure 4-1. Screening for restriction sites in GFP and GUS vectors. Lanes 1,5,9: 1 Kb ladder. Lane 2 has the GFP vector cut with Not1. Lane 3 GFP vector cut with BamH1. Lane 4 GFP cut with Not1 and Bam H1. Lane 6 GUS cut with Not1. Lane 7 Gus cut with BamH1. Lane 8 GUS cut with Not1 and BamH1.

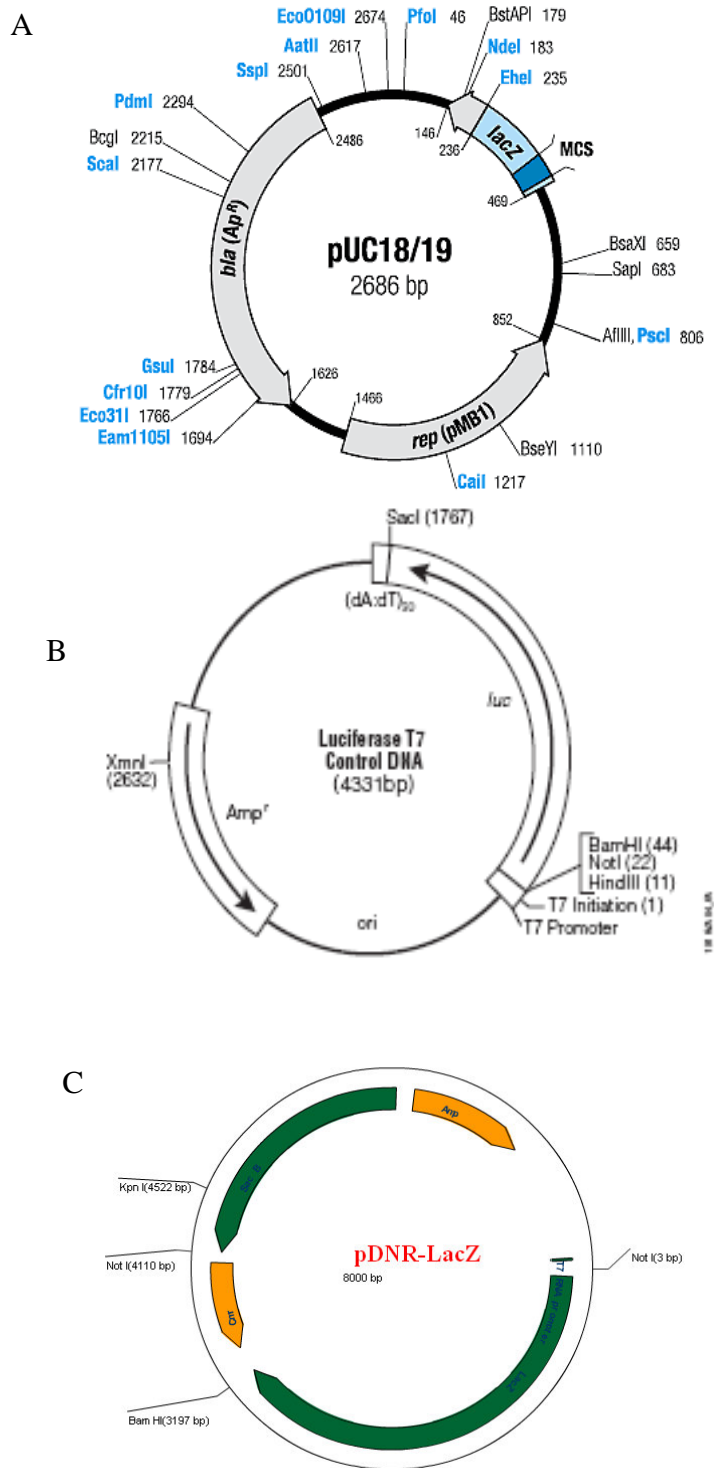


Figure 4-2. Vector maps for plasmids used for PCR and protein expression. A) puc 18 vector from which  $\beta$ -lactamase gene was amplified. B) Luciferase T7 control vector. C) pDNR  $\beta$ -Galactosidase vector drawn using EZ plasmid map V1.9 (UT Austin)

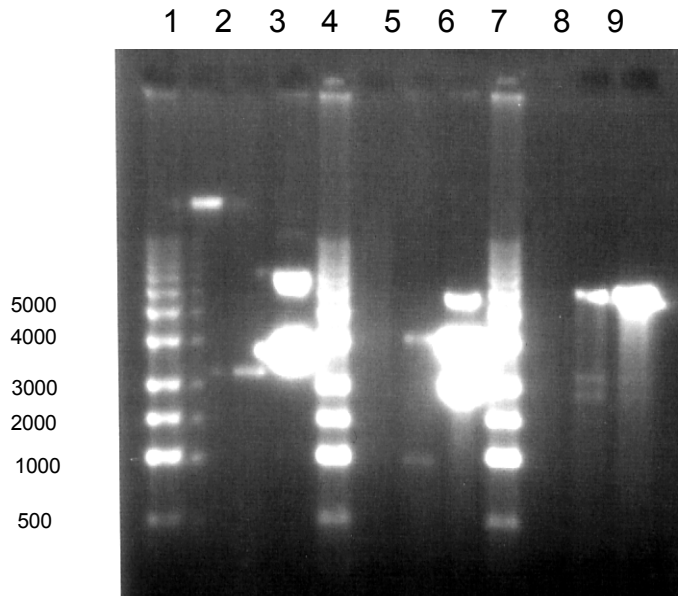


Figure 4-3. Screening for colony containing correct  $\beta$ -lactamase gene. Lanes 1,5,9 are ladders. Lanes 2,6,10 are undigested DNA. Lanes 3,7, 11 are digested DNA were the desired 1 kb band is in lane 7, lanes 4,8,12 are digested GUS vector as a control

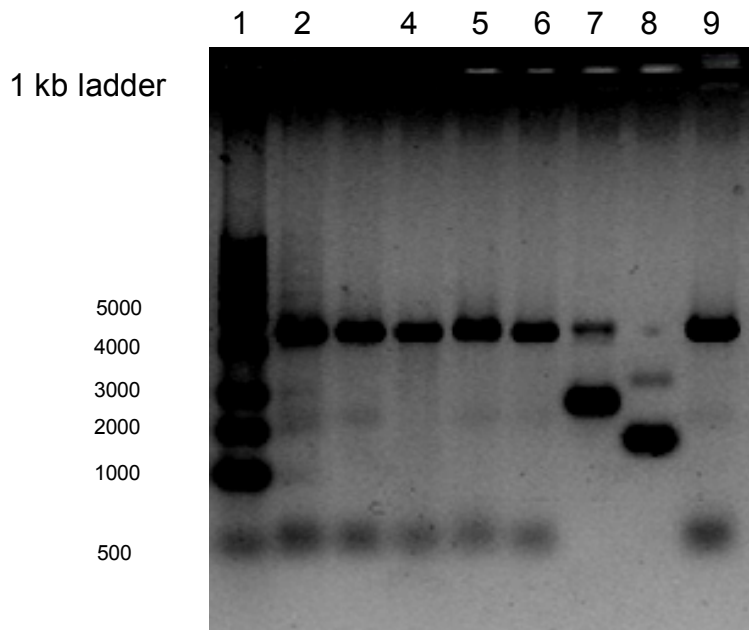


Figure 4-4. Screening for colonies containing correct alkaline phosphatase gene. Lane 1 contains 1 Kb ladder (unit is base pair). lanes 2 through 9 contain plasmids purified from different grown colonies cut with restriction enzyme Pst1 which should cut a 500 bp segment from the AP gene. All colonies except that in 7 and 8 contain the correct vector.

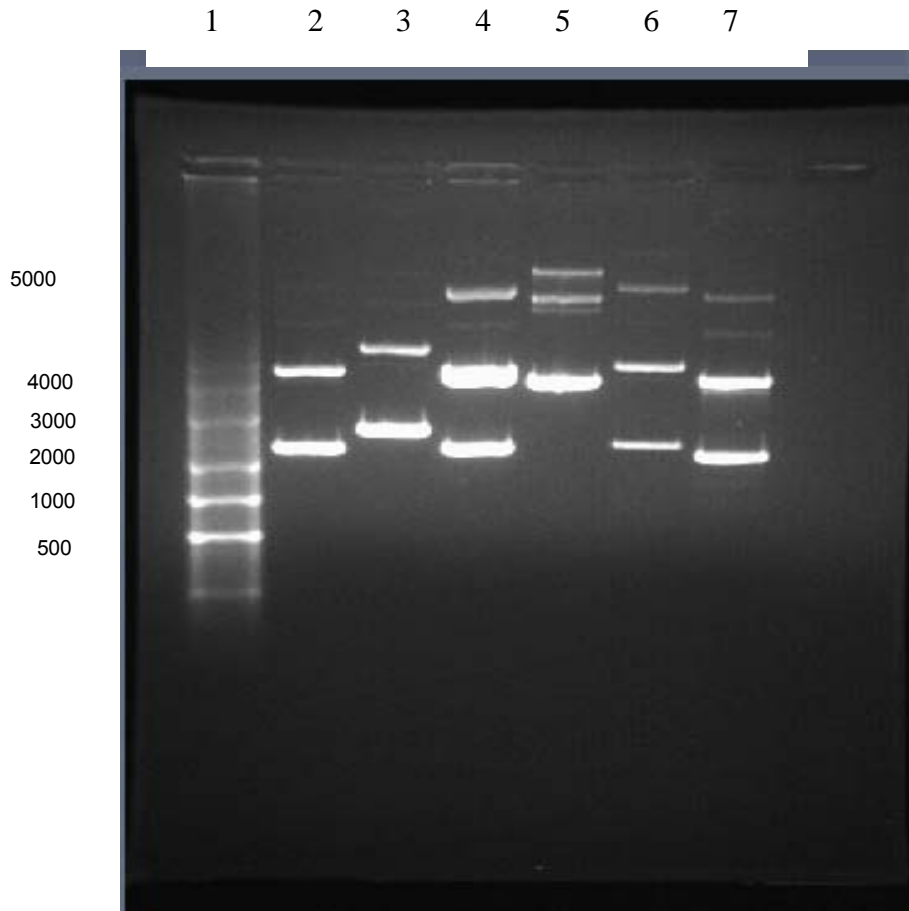


Figure 4-5. Agarose gel of all plasmids run the first lane is the ladder afterwards the plasmids are in order: GFP, GUS, luciferase,  $\beta$ -galactosidase,  $\beta$ -lactamase, and alkaline phosphatase

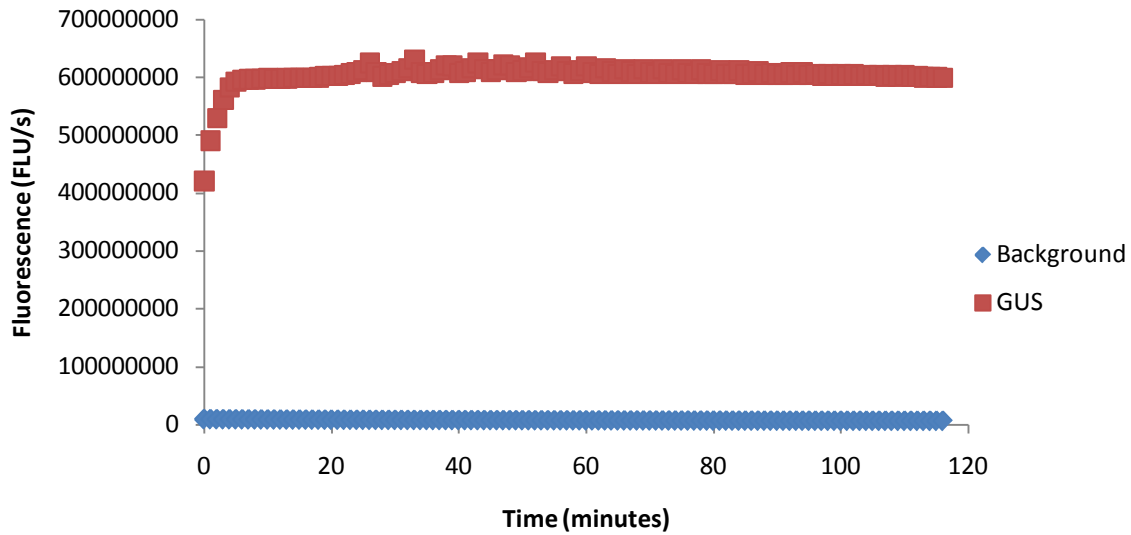


Figure 4-6. GUS enzyme kinetics with its substrate 4-methylumbelliferyl  $\beta$ -D-glucuronide (4-MUG). 4-MUG was added to a negative control containing reaction mix without plasmid and another containing GUS vector.

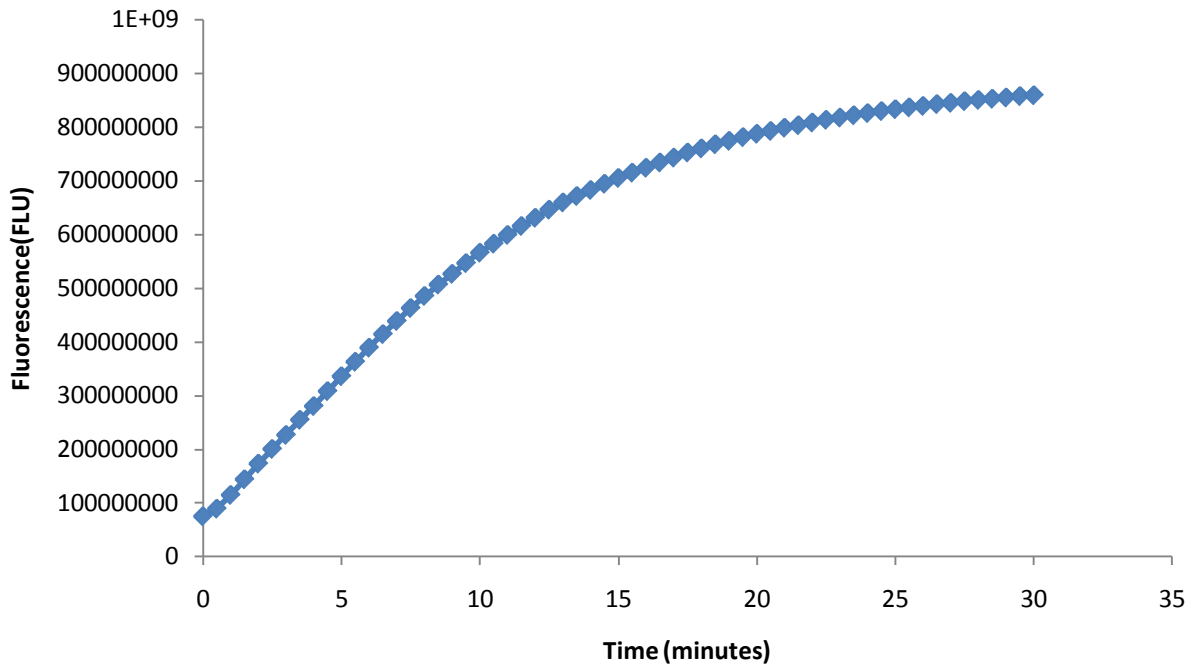


Figure 4-7. Enzyme kinetics of  $\beta$ -Galactosidase with its substrate Fluorescein mono- $\beta$ -D-Galactopyranoside (FMGal).

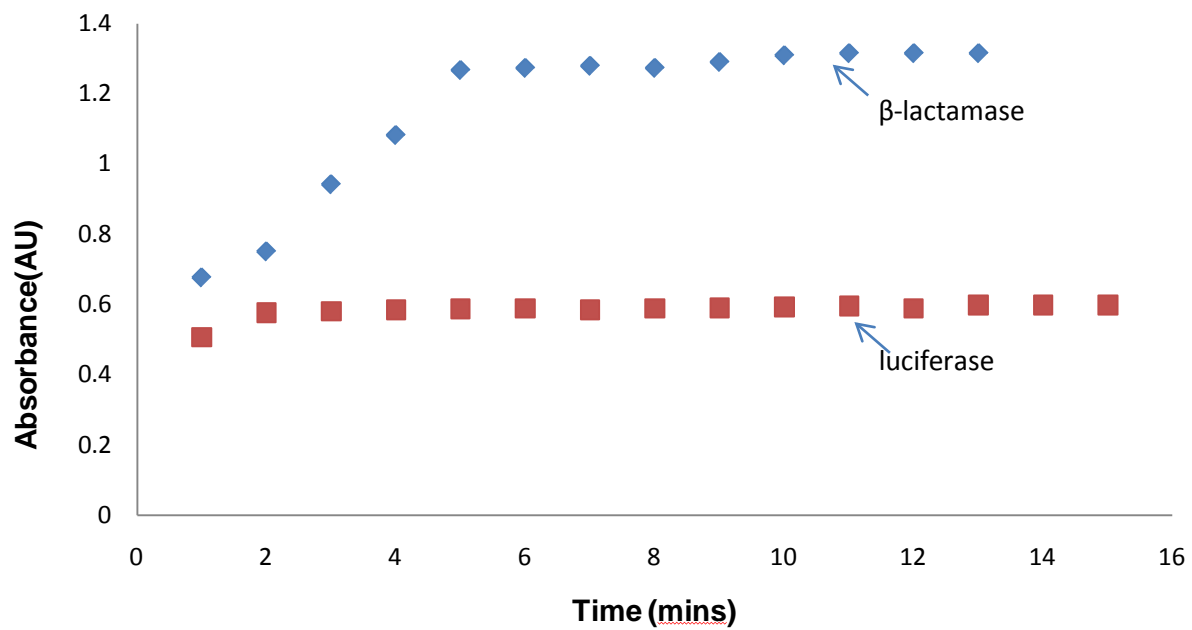


Figure 4-8.  $\beta$ -lactamase detection using m-[[Phenylacetyl]glycyl]oxy]benzoic acid which was added to the reaction product of  $\beta$ -lactamase. This was compared to the reaction product of luciferase.

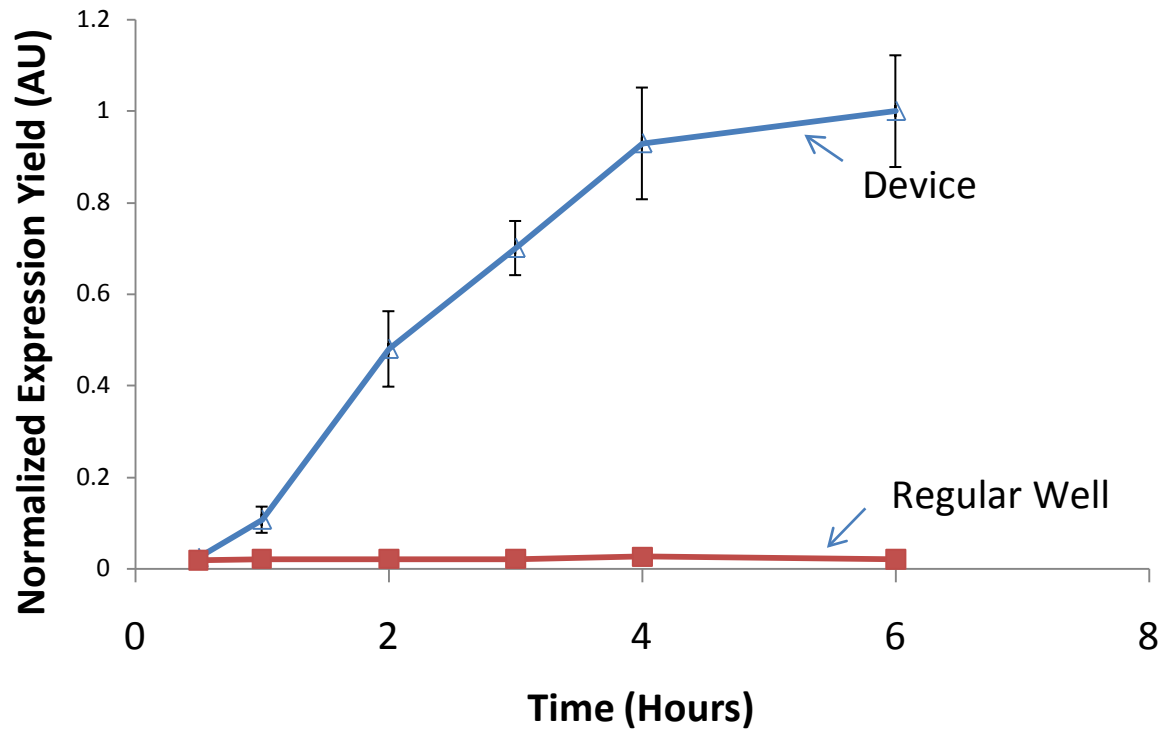


Figure 4-9. Luciferase expression over time. Triangles represents luciferase expression in the 96 well device and the squares represent expression in a regular 96 well-plate. This figure shows that using the 96-well fluidic device extend protein synthesis reaction time and increases protein synthesis yield.

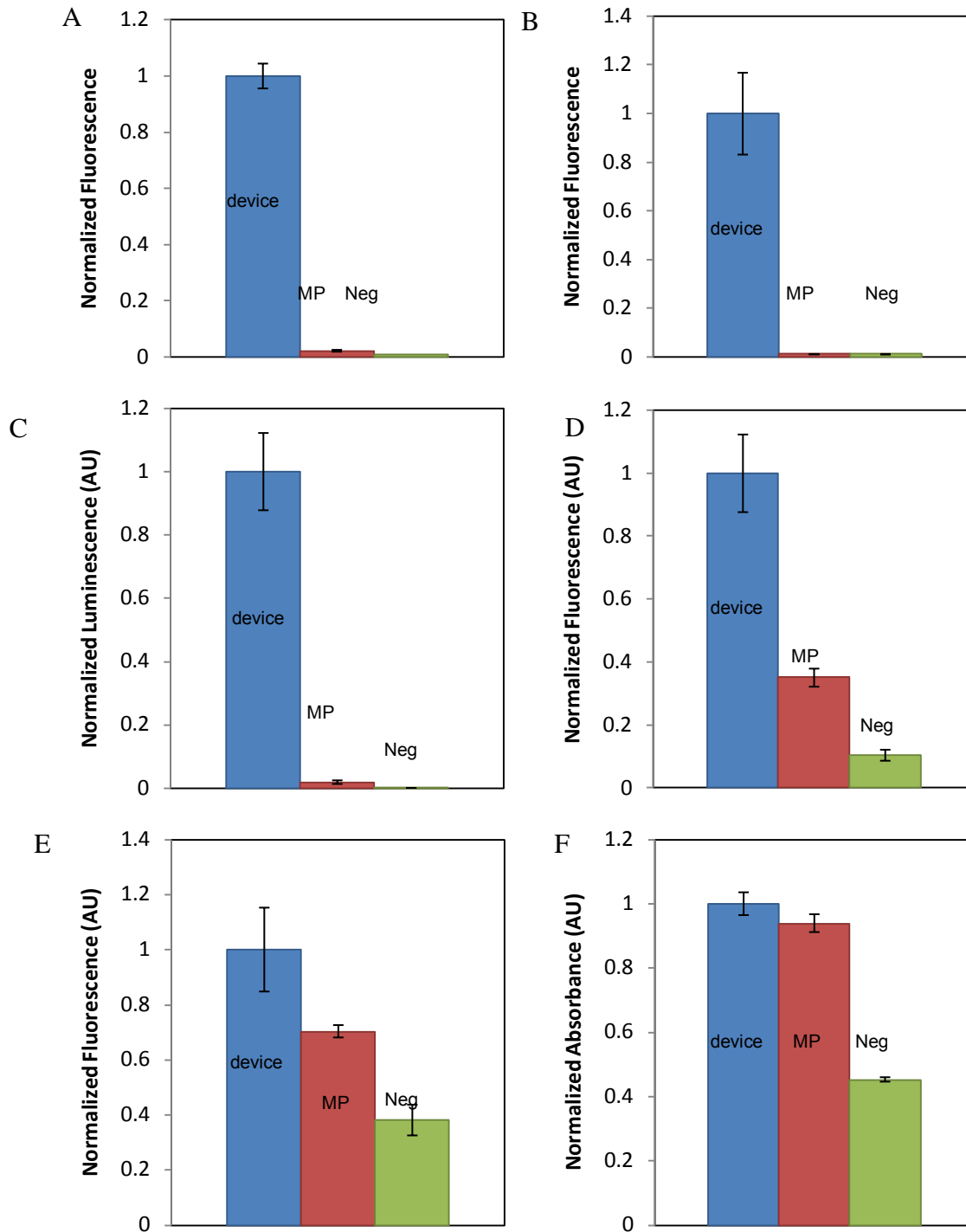


Figure 4-10. Comparison between protein expression yield for each of the six proteins. For each protein a value is given for expression in the device, in a regular microplate (MP), and a negative value where no DNA is added. A) GFP, B) GUS C)Luciferase, D) LacZ E)AP, F) BLac.

Table 4-1. Comparison in protein synthesis yield between device and conventional microplate.

Protein	Device	Regular well	Negative	Amplification
Green fluorescent protein (GFP)	9163648	204770	92749	44.75
Glucoronidase (GUS)	50216325	578202	567482	86.85
Luciferase	59381261	1133778	427	52
$\beta$ -Galactosidase	404715	142080	42365	2.85
Alkaline phosphatase (AP)	56818101	39955264	21631131	1.4
B- lactamase	1.03	0.97	0.43	1.06

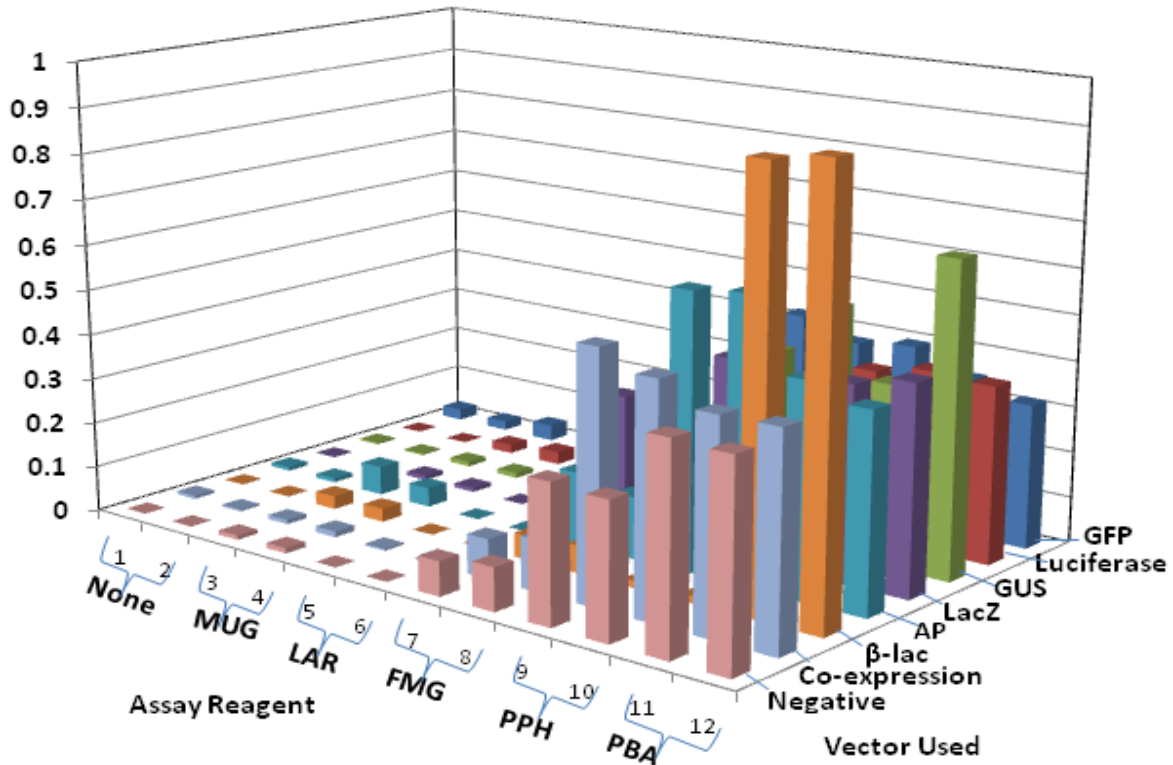


Figure 4-11. Expression of 6 different proteins in a conventional microplate and the detection of each of them with assays specific for each protein expressed. In addition, a negative control with no DNA and a coexpression with all 6 proteins is presented. These experiments were done in a regular microplate. Proteins expressed were green fluorescent protein (GFP), luciferase,  $\beta$ -glucuronidase (GUS),  $\beta$ -galactosidase (lacZ), alkaline phosphatase (AP), and  $\beta$ -lactamase ( $\beta$ -lac). The assay reagents for detecting the proteins expressed were 4-methylumbelliferyl  $\beta$ -D-glucuronide (MUG), luciferase assay reagent (LAR), fluorescein mono- $\beta$ -D-Galactopyranoside (FMG), 3-phenylumbelliferone 7-O-phosphate hemipyridinium (PPM), and m-[[[(phenylacetyl)glycyl]oxy]benzoic acid (PBA).

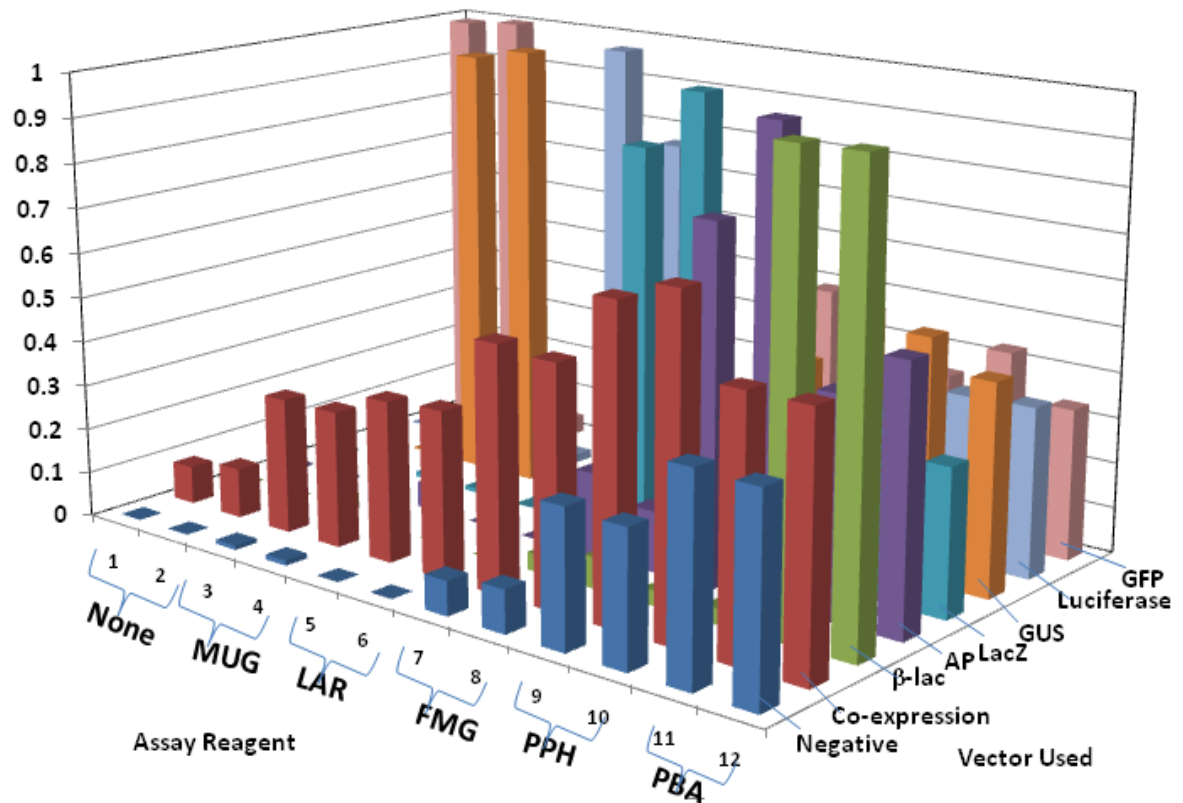


Figure 4-12. Expression of 6 different proteins in the fluidic device and the detection of each of them with assays specific for each of the proteins. In addition a negative control with no DNA and a test with all 6 proteins coexpressed is presented). These experiments were done in the 96- well device. Proteins were green fluorescent protein (GFP), luciferase,  $\beta$ -glucuronidase (GUS),  $\beta$ -galactosidase (lacZ), alkaline phosphatase (AP), and  $\beta$ -lactamase ( $\beta$ -lac). The assay reagents for detecting the proteins expressed were 4-methylumbelliferyl  $\beta$ -D-glucuronide (MUG), luciferase assay reagent (LAR), fluorescein mono- $\beta$ -D-Galactopyranoside (FMG), 3-phenylumbelliferone 7-O-phosphate hemipyridinium (PPM), and m-[(phenylacetyl)glycyl]oxy]benzoic acid (PBA).

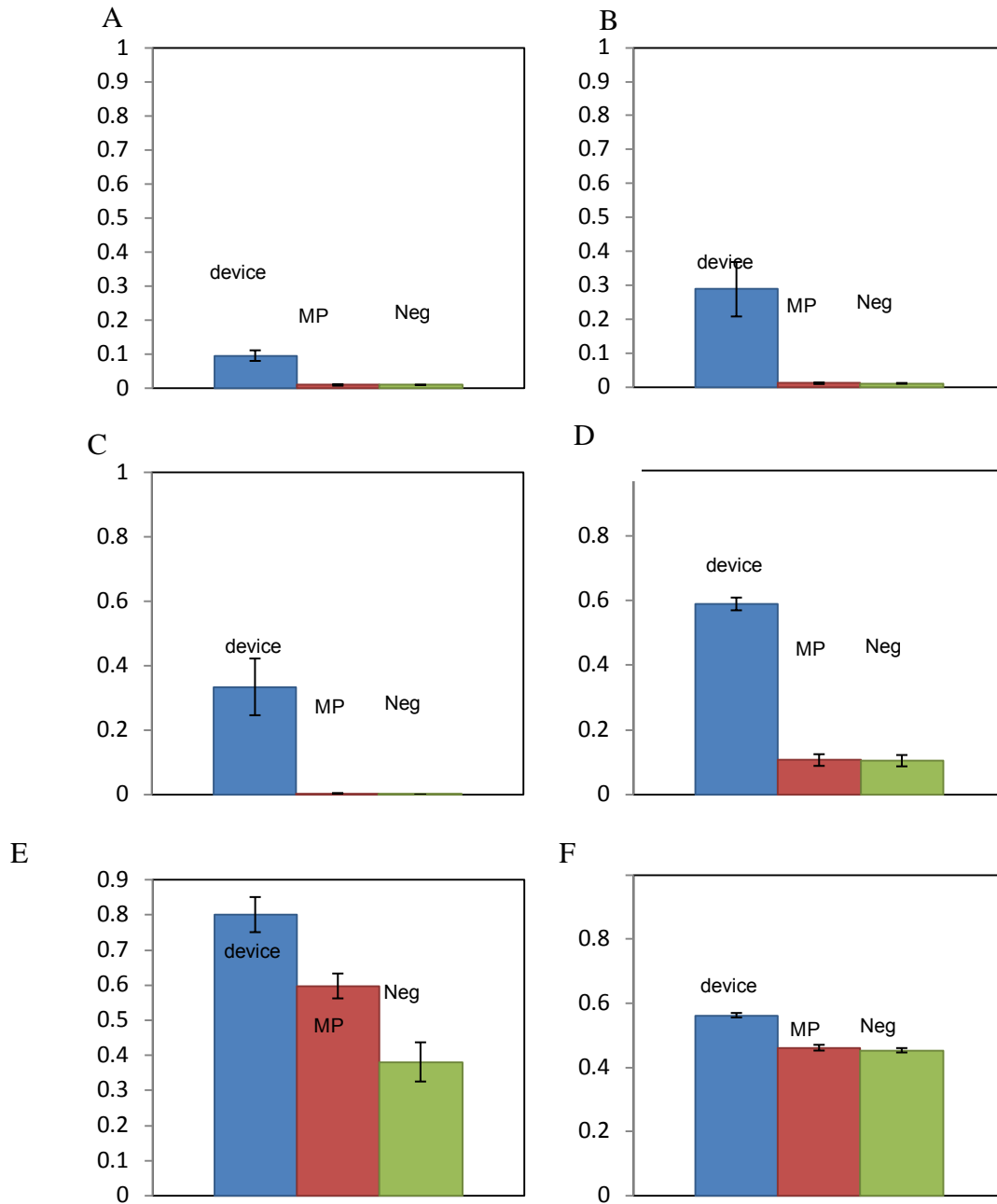


Figure 4-13. Detection of different protein levels when all are expressed in the same reaction both in the 96- well device and a regular 96- well plate. Note that the data is normalized to the maximum in figure 5 to relate the yield with the maximum. A) GFP, B) GUS C)Luciferase, D) LacZ E)AP, F) BLac

Table 4-2. Values comparing protein synthesis yield indicated by the signal from each assay when all proteins are coexpressed in the same reaction

Protein	Device	Regular well	Negative	Amplification
Green fluorescent protein (GFP)	881021	43952	92749	20.05
Glucoronidase (GUS)	14483424	585477	567483	24.74
Luciferase	19846715	225067	427	88.18
$\beta$ -Galactosidase	238355	43163	42365	5.52
Alkaline phosphatase (AP)	45474453	33927339	21631131	1.34
$\beta$ -lactamase	0.56	0.46	0.45	1.2

## CHAPTER 5 MEMBRANE PROTEIN EXPRESSION & DRUG SCREENING

### 5.1 Introduction

A great amount of research aims for in vitro screening and detection of therapeutic drugs.<sup>115</sup> Half of human drug targets are membrane proteins<sup>76</sup> and 28% are enzymes<sup>116</sup> making these two categories of proteins the major targets for drug screening. The main bottleneck in the process of drug screening is the production of functional protein targets that can be used for screening for new drugs.

Membrane proteins constitute one third of proteins found in the human genome project. They have roles in cell-cell communication, signal transduction, transport, and recognition.<sup>116</sup> There are many problems in studying these proteins the, first lies in the difficulty in obtaining sufficient quantities of proteins because of complexity in expressing them.<sup>117</sup> The second problem is maintaining the protein's function when they are solubilized, for which detergents are usually used.<sup>118</sup> If the proteins are not in a soluble form they usually aggregate or unfold,<sup>119</sup> and sometimes they disintegrate from the membranes they were embedded in.<sup>120</sup>

On the enzymatic side of drug screening,  $\beta$ -lactamases are the major source for bacterial resistance to antibiotics. Resistance is achieved through hydrolyzing the amide bond in  $\beta$ -lactam antibiotics such as Ampicillin (Figure 5-1A) causing the antimicrobial agents to be ineffective.<sup>82</sup> Since such antibiotics represent more than 65% of the world antibiotic market, and are usually combined with  $\beta$ -lactamase inhibitors, screening for inhibitors especially enzymes with continuous mutations<sup>84</sup> requires a quick and effective method.

The main  $\beta$ -lactamase inhibitors used with antibiotics include clavulanate acid, sulbactam, and its derivative tazobactam.

### **5.1.1 Clavulanate Acid**

Clavulanate acid (Fig 5-1B) is the first  $\beta$ -lactamase inhibitor described in literature.<sup>88</sup> Clavulanic acid was described as a suicide inhibitor which binds irreversibly to the enzyme after being cleaved by  $\beta$ -lactamase.

Clavulanate acid was the first  $\beta$ -lactamase inhibitor that was approved as a drug by the Food and Drug Administration (FDA). When mixing it with Amoxicillin at a ratio of 2:1 results with the antibiotic commercially known as Augmentin. This drug has been shown to be effective in treating respiratory infections, soft tissue infections and skin infections, urinary tract infections, and chancroid.<sup>121</sup>

Another popular antibiotic that contains clavulanate acid is Timentin, a combination of clavulanate acid and ticarcillin. Timentin is used to treat respiratory infections, pneumonia, and urinary tract infections.<sup>121</sup>

### **5.1.2 Sulbactam**

Sulbactam is a highly potent specific inhibitor of a wide range of  $\beta$ -lactamase enzymes that was first described in the 1970s. Its structure contains a  $\beta$ -lactam ring (Figure 5-1C) that is hydrolyzed by  $\beta$ -lactamase, creating a covalent bond between the enzyme and its inhibitor and irreversibly deactivating the enzyme (Figure 5-2).

Some commercial drugs contain a combination of sulbactam and amoxicillin, sulbactam and cefoperazone, and sulbactam and ampicillin known commercially as Unasyn.

### 5.1.3 Tazobactam

Tazobactam (Figure 5-1D) is another  $\beta$ -lactamase inhibitor which is a derivative of Sulbactam and it was first described in the 1980s. Tazobactam's most popular commercial drug is known as Zosyn that combines it with piperacillin.

Tazobactam has been developed to be more potent than both clavulanate and sulbactam in inhibiting class C  $\beta$ -lactamases. Sulbactam is the least resistant inhibitor against class C  $\beta$ -lactamases and tazobactam has been designed to replace sulbactam against bacteria that produce this class of enzymes. In vitro and in vivo studies have varying reports as to whether clavulanate acid or tazobactam are more potent inhibitor against class C  $\beta$ -lactamases. Some sources describe clavulanate as being more superior,<sup>122</sup> and others describe tazobactam as the more potent.<sup>123</sup> Although these studies seem to compare the same factors, in vivo studies tested the minimum concentration of the inhibitor for cell survival, while in vitro studies discussed the enzymes potency in catalyzing its substrate in the presence of different inhibitors. The in vivo studies also included many factors that would affect the outcome of the experiment that were not related to the enzyme. These factors include the permeability of the cell membrane, since the permeability may vary among different inhibitors.

The evolution of more antibiotic resistant bacteria cannot only be solved by the development of drugs that inhibit the resistance mechanism. The challenge also requires finding new drugs that can be used as antibiotics. One of the major sets of antibiotics is protein synthesis inhibitors. Protein synthesis inhibitors consist of a very broad set of compounds. In spite their long history of being used as antibiotics, little effort is being made to discover new inhibitors and to understand their mechanisms of

action. In addition, protein synthesis inhibitors have also been studied as antitumor drug candidates.

In this chapter the fluidic plate described in chapter 3 and used in chapter 4 for high-throughput protein synthesis demonstrated in chapter 4 will be used for other applications. One is the synthesis of soluble and insoluble membrane proteins, by using nanolipoproteins to provide a lipid bilayer for bacteriorhodopsin to insert itself and form a soluble structure. The second application is using  $\beta$ -lactamase, as an example for enzyme inhibitor screening, and for drug screening. Finally, the open nature of cell-free protein synthesis is taken advantage of to ascertain the physiological target of protein synthesis inhibitors as a proof of concept for discovering new proteins synthesis inhibitors and understanding their mechanism.

## **5.2 Materials and Methods**

### **5.2.1 Membrane Protein Expression**

Membrane protein expression required additional preparation of lipid micelles and cofactors to obtain correctly folded, functional membrane protein.

#### **5.2.1.1 Vesicle and retinal preparation**

A solution of 1,2-dimyristoyl-sn-glycero-3-phosphocholine (DMPC) (Avanti Polar Lipids, Alabaster, Al) in dnase/rnase free water at a concentration of 68 mg/ml was sonicated using a vibra cell probe sonicator at a power of 6 watts until the solution turned clear in color (Figure 5-3). The mixture was centrifuged at top speed for two minutes to remove any metal remnants from sonication, and the supernatant was saved. A 10 mM all trans-retinal (Sigma-Aldrich, St Louis, Mo) solution was prepared in 100% ethanol.

### **5.2.1.2 Protein expression**

Protein expression reaction mix and feeding solutions were prepared based on the manufacturer's recommendation for the RTS 100 CECF E Coli kit. In short, the reaction mix was made by mixing 0.525 E coli lysate, 0.225 ml reaction mix, 0.27 amino acids without methionine, and 30  $\mu$ l methionine. The feeding solution was made by mixing 8.1 ml feeding mix, 2.65 ml amino acids without methionine, and 0.3 ml methionine.

The working reaction mix was prepared by adding DMPC vesicles to a final concentration of 2 mg/ml, retinal to a final concentration of 50  $\mu$ M, and 5 $\mu$ g/ml of each plasmid to the reaction mix.

To start the protein expression reaction in the device, 200  $\mu$ l of the feeding solution was added to the feeding chamber of the device, 10  $\mu$ l of the working reaction mix was added to the reaction chamber. The device was sealed with PCR tape to prevent evaporation.

### **5.2.1.3 SDS PAGE and Western blotting**

For coomassie staining, aliquots of the total reaction mix, the soluble fraction after centrifugation, and the pellet after centrifugation were diluted at a ratio of 1:20 in 2 X sodium dodecyl sulphate (SDS) sample loading buffer. The loading buffer was prepared as follow: mix 15 ml 20% SDS, 1.5 ml 0.1% bromphenol blue (BPB), 11 ml deionized water, and 10 ml 4X stacking gel buffer which contains Tris base and 20% SDS. The sample in the SDS loading buffer was heated at 99 $^{\circ}$  C for ten minutes to denature. Afterwards, the samples were loaded onto a 15% acrylamide gel, a Precision Plus protein standard ladder from Biorad was ran with the samples in a Mini-Protean III Cell system from Biorad. The samples were electrophoresed at 150 V for 3 hours in PAGE

electrophoresis buffer which was made by mixing 14.4 g/l glycine, 3.03 Tris base g/l, and 20% SDS at a concentration of 5 ml/l.

The gel was transferred to a container that had the comassie blue stain (1.25 g Brilliant Blue R Coomassie concentrate (Sigma), 450 ml methanol, 100 ml acetic acid, and 450 ml deionized water). The gel was incubated in the stain and put on an orbital shaker at 20 RPM for an hour. The CBB stain was removed and the gel was rinsed with deionized water twice. The gel was then incubated in CBB destaining solution which was prepared by mixing 300 ml methanol, 100 ml acetic acid, and 600 ml deionized water. The incubation was on an orbital shaker at 20 RPM for overnight.

In order to dry the gel to save it, two cellulose sheets were rinsed with water, and the gel was placed between the two sheets which were spread on a plastic board. Bubbles between the two sheets and around the gel were squeezed out to avoid cracking the gel. Finally, frames were added onto the white board to stabilize the sheets and the gel and the assembly was left to dry overnight.

For the western blot the samples were mixed in sample loading buffer in a ratio of 1:100. After treating the samples and electrophoresing them as described above, the gel was soaked in transfer buffer containing 3.03 g of Tris base, 14.41 g glycine, 200 ml methanol, and deionized water. At the same time a set of thick and thin filter paper was soaked in the same transfer buffer, and (Polyvinylidene Fluoride) PVDF membrane was soaked in methanol. Finally, the gel was placed beneath the nitrocellulose membrane and both were place between the soaked filter paper, assembled, and a current of 220 mA was run for 30 minutes.

The PVDF membrane was blocked with 5% fat free milk in PBS-Tween washing buffer for one hour. Afterwards it was incubated in 1:50 000 anti-his-peroxidase mouse monoclonal antibody (Roche) in blocking solution over night. The membrane was then washed with washing buffer for 15 minutes, and this step was repeated three times. Finally a mix of 1:40 ECL Plus western blotting detection reagents (GE Healthcare Life Sciences) was added to the membrane and incubated for 5 minutes. The membrane was then exposed on 9x10 inch Kodak film and the film was processed.

### 5.2.2 B-Lactamase Inhibition Assays

Three different  $\beta$ -lactamase inhibitors were used; tazobactam and potassium clavulanate from Sigma (St. Louis, Mo), and sulbactam from Astatech Inc (Bristol, Pa). In addition, cefotaxime (Sigma) -a 3rd generation cephalosporin- was chosen as a negative control (Figure 5-4). This chemical was chosen because of the presence of a beta-lactam ring in its structure. B-lactamases usually hydrolyze beta-lactam rings hence their substrates and inhibitors usually contain this ring. However, in the case of cefotaxime, the chemical is too large to inhibit beta-lactamase or to be catalyzed by it.<sup>84</sup>

A series of concentrations for each of the inhibitors and control were prepared. for Each measurement 5  $\mu$ l of solution containing a particular inhibitor was added to the reaction mix after the protein expression reaction is done, the mixture was incubated for 15 minutes as recommended in literature.<sup>87</sup> A similar series of concentrations was prepared without adding the plasmid encoding beta-lactamase to the reaction mix before adding the inhibitors and cefotaxime. These samples served as a negative control. Afterwards the mixture was added to 85  $\mu$ l of 2 mM m-[[[(phenylacetyl)glycyl]oxy]benzoic acid and measurements were taken as described in

chapter 4. Percent inhibition was calculated by subtracting the corresponding negative control and then normalized against the positive control.

### **5.2.3 Protein Synthesis Inhibitor Target Selection and Design**

The protein synthesis inhibitors (PSI) were selected based on the following criteria: firstly the target of the PSI should be known and studied before, secondly the physiological target had to be small and restricted in a limited region; finally the PSI should be able to bind to its target in its secondary structure. Based on these criteria ricin (Sigma Aldrich Mo), hygromycin B (EMD Biosciences, NJ), and sparsomycin (Developmental Therapeutics Program (DTP) NCI/NIH) were chosen as PSIs.

Ricin binds to the ricin/ sarcin rRNA loop in the ribosome. It has been shown to catalyze the depurination of the second adenine in a GAGA sequence in the loop shown in figure 5-5 A.<sup>124-126</sup> Hygromycin B binds to a specific sequence in the 16S rRNA that is preserved across species (Figure 5-5 B).<sup>127</sup> Sparsomycin binds to a specific sequence in the peptidyl transferase loop in 23S-like rRNA (Figure 5-5 C), inhibiting elongation.<sup>128</sup> The RNA sequences used to design the targets were compatible with the real target with the addition of a few extra bases to further stabilize the secondary structure. For testing ricin's target two additional aptamers were used. One has the same structure as the native target. However it has a point mutation where the adenine that ricin target is exchanged with a guanine, chosen because both nucleic acids are purines and are of a more similar structure. The second additional aptamer used was an inhibiting aptamer published by Ellington.<sup>124</sup> A negative control that was also used is the binding site of a different PSI sparsomycin. The same sparsomycin target was used with its corresponding inhibitor sparsomycin with hygromycin b target as a negative control.

After designing the targets according to literature, RNA sequences shown in table 5-1 were ordered from Integrated DNA Technologies. RNA aptamers were resuspended in 1x phosphate-buffered saline and 5 mM MgCl<sub>2</sub>, adequate concentrations were prepared and the mixtures were heated to 95°. These solutions were added to the protein expression mix at the beginning of the reaction before adding the PSI. The 96 well device was used as described above with luciferase.

### **5.3 Results and Discussion**

#### **5.3.1 Miniaturization of the Membrane Protein Expression Assay**

The device was able to miniaturize by 100 times the assay for synthesizing the membrane protein bacteriorhodopsin in a cell free format that has been previously reported.<sup>76</sup> This is not only beneficial in terms of reducing cost by two orders of magnitude but it is also more practical for running parallel membrane protein reactions for high throughput applications such as drug screening. The need for the device arises from the fact that the commercial devices available are designed for large scale continuous exchange cell-free protein synthesis reactions and cannot be applied for small scale or parallel reactions, leaving the batch format as the only possible format for miniaturization. When CECF is performed in the device, however, protein synthesis yield increased as shown in figure 5-6. In figure 5-6 A, bacteriorhodopsin and apolipoprotein were coexpressed in batch format in a tube and the same reaction was carried out in the device in figure 5-6 B. The amount of proteins expressed in the batch format was too low to detect the change in color to purple as a result of the expression of bacteriorhodopsin. However, the purple shade could be clearly seen in the protein expression mix from the device after being aliquoted into a microcentrifuge tube.

### 5.3.2 Membrane Proteins' Solubility

The coexpression of nanolipoproteins and bacteriorhodopsin in the same solution is facilitated by nanolipoproteins' ability to form lipid bilayer patches from lipid micelles, which would increase the bacteriorhodopsin lipid bilayer solubility. Figure 5-7 shows pictures of microcentrifuge tubes containing different cell-free protein synthesis reaction mix expressing different combinations of plasmids. These were aliquoted from the 96-well device and centrifuged to separate soluble and insoluble materials for visualization. The tube containing negative control with no plasmid and the tube containing apolipoprotein plasmid showed no color, although the expression of apolipoprotein was verified by coomassie stained gel and Western blot (figure 5-8). The tube in figure 5-7 containing bacteriorhodopsin plasmid shows a purple pellet and clear supernatant. This result shows that bacteriorhodopsin is correctly folded, and also shows that it is mostly insoluble when expressed on its own. The tube containing bacteriorhodopsin plasmid and apolipoprotein plasmid has a purple supernatant, showing that bacteriorhodopsin's solubility increases when expressed with the apolipoprotein lipid complex. The contents of the supernatant, pellet, and total protein expression mix were analyzed and are shown in figure 5-8. The gel and blot show that apolipoprotein is expressed and is completely soluble since it is not detected in the pellet after centrifuging the mix neither in the gel nor in the blot. The figure also shows that bacteriorhodopsin is insoluble when expressed on its own since it is only detected in the pellet and cannot be detected in the supernatant. The increase of bacteriorhodopsin solubility when being coexpressed with apolipoprotein is also shown in figure 5-8 since both bacteriorhodopsin and apolipoprotein are present in the supernatant.

### 5.3.3 B-Lactamase Inhibitor Detection as an Example for Drug Screening

B-Lactamase inhibition was chosen to demonstrate the utilization of the expressed proteins and their corresponding assays in applications such as drug screening. To test the effect of the inhibitors on the enzymatic assay of  $\beta$ -lactamase and to determine the minimum inhibitory concentrations of inhibitors to be used, different dilutions of tazobactam and clavulanate acid were added and the kinetic readings were taken at each inhibitor concentration. (Figure 5-9, 5-10). These figures were used to pinpoint the range of inhibitor concentration to be used. Figure 5-11, shows the effect of the inhibitors on the enzyme.  $\beta$ -lactamase is most sensitive to the inhibitor clavulanate acid with an inhibition value of 3.46%/mM. Whereas tazobactam and sulbactam showed a sensitivity of 0.605%/mM and 0.246%/mM respectively. Cefotaxime, the negative control, had no effect on beta-lactamase's activity, in spite its possession of a beta-lactam ring. This ring is in the three other inhibitors and is the part that beta-lactamases catalyze in its substrates. However, cefotaxime is too large a compound to be catalyzed by the enzyme.

These results are in agreement with results obtained for the TEM-1 type  $\beta$ -lactamase which encoded on the puc-18 plasmid, from which the gene was cloned.<sup>85</sup> Clavulanic acid has been reported as the most effective  $\beta$ -lactamase inhibitor for TEM  $\beta$ -lactamases.<sup>121-122</sup> Tazobactam has been reported to be more effective than Sulbactam in some reports,<sup>122</sup> and less effective in others.<sup>121</sup> However, it is worth noting that the values obtained for the amount of inhibitor to achieve a certain level of inhibition are greater in our experiments, and even differ between sources. This can be easily explained by the amount of enzyme and the need for a greater amount of inhibitor to suppress greater amounts of enzyme.<sup>87</sup> It is expected that more  $\beta$ -lactamase would

be expressed in the described cell-free system than in regular bacterial systems because the gene is cloned after the T7 promoter for the purpose of increasing the expression yield. This can be proven by the fact that TEM-1  $\beta$ -lactamase gene is present in all six vectors expressed but it is only cloned under the T7 polymerase promoter in the  $\beta$ -lactamase vector. These results prove the specificity of the assay and further show that it is more accurate than the use of bacterial systems to study beta-lactamase activity, since bacterial systems have many factors that can affect the cell's resistance to antibiotics. For example, pseudomonas is resistant to beta-lactam antibiotics through the presence of a secretion system which pumps the drugs out instead of having an enzyme that catalyzes them.<sup>129</sup>

#### **5.3.4 PSI Target Screening**

All three ricin aptamers (Figure 5-12) had an inhibitory effect on ricin, as they completely inhibit it at a range from 2 to 5 orders of magnitude of the amount of Ricin used. The inhibitory aptamer published by Ellington was the most effective (Figure 5-13). Hygromycin target partially inhibited the effect of Hygromycin on protein synthesis by partially retaining protein synthesis (Figure 5-14). The partial inhibition is shown by an increase in protein synthesis as the amount of aptamer increased. However, RNA did not completely inhibit hygromycin B which can be justified by two explanations. The first is that hygromycin is a small molecule and much greater amounts of RNA are needed to bind to it. The second is that ricin's mechanism is catalytic and has a higher turnover. This enzymatic activity and the fact that ricin does not remain bound to the RNA can explain the higher efficacy of the inhibitory aptamer. Sparsomycin, another small molecule, has shown a high specificity to its target which can be easily differentiated from its specificity to the same amounts of hygromycin B target, which was used as a

negative control (Figure 5-15). The differentiation of sparsomycin and its derivatives through its molecular target has a lot of potential for antitumor drug screening since sparsomycin has been reported as an effective antitumor drug for specific types of carcinomas such as leukemia.<sup>130</sup>

#### **5.4 Conclusion**

In this chapter, we have shown the applicability of continuous exchange cell-free protein synthesis in a fluidic device in high throughput drug screening. Firstly to demonstrate the possibility of screening for membrane protein related drugs, a soluble form of the membrane protein bacteriorhodopsin was successfully expressed by using nanolipoproteins as a scaffold in which bacteriorhodopsin inserts itself.

In addition, screening for  $\beta$ -lactamase inhibitors, an important component of most available antibiotics, was demonstrated by using the optical enzymatic assay to test for the degree of inhibition of  $\beta$ -lactamase activity. The assay did not only save a lot of time and effort, but was also more specific to the enzyme itself and excluded other factors that are found in cellular based experiments. The assay was also able to differentiate the potency of the different inhibitors by observing change in inhibition corresponding to the change in the inhibitors concentration where an estimate can be given by calculating the slope of the calibration curve between the inhibitor's concentration and the degree of inhibition corresponding to that change.

Finally, using the assay we were able to prove the ability of differentiating ribosomal RNA targets for PSI, which might be utilized for finding new drugs.

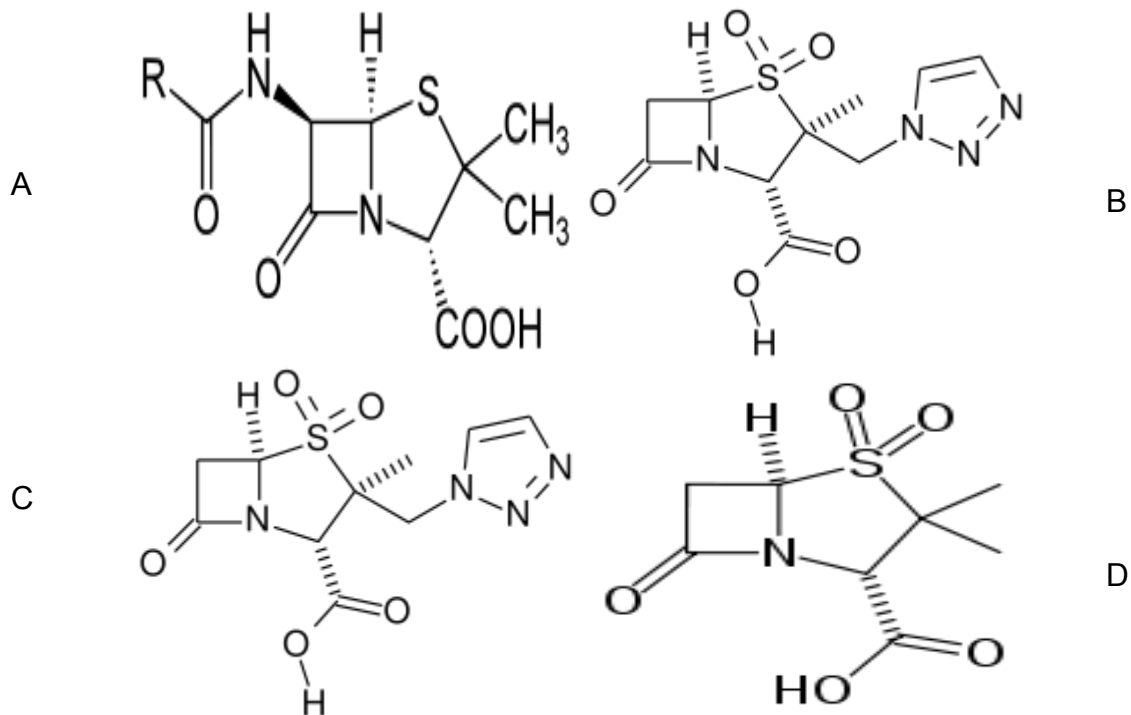


Figure 5-1. Structure of antibiotics and inhibitors with  $\beta$ -lactam ring. A) Penicillin core structure. B) Clavulanate Acid. C) Tazobactam. D) Sulbactam.

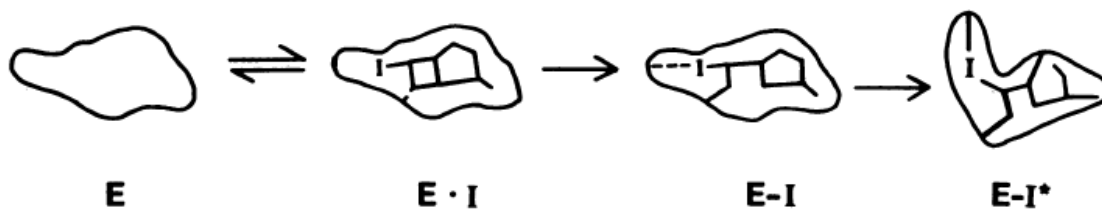


Figure 5-2. Mechanism of Sulbactam inhibition of  $\beta$ -lactamase [Clinical Microbiology Reviews, 1988, 1, 109-123, reproduced with permission from American Society for Microbiology]

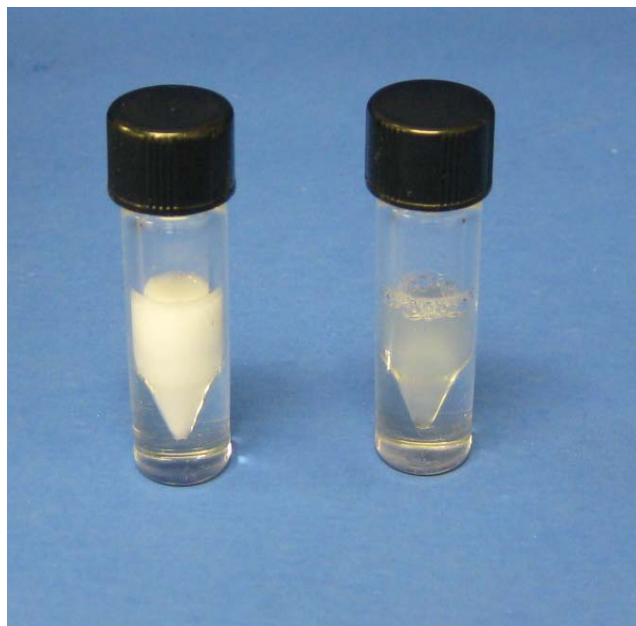


Figure 5-3. The change in color of DMPC solution after sonication. The formation of unilamellar micelles is characterized by a clear color.

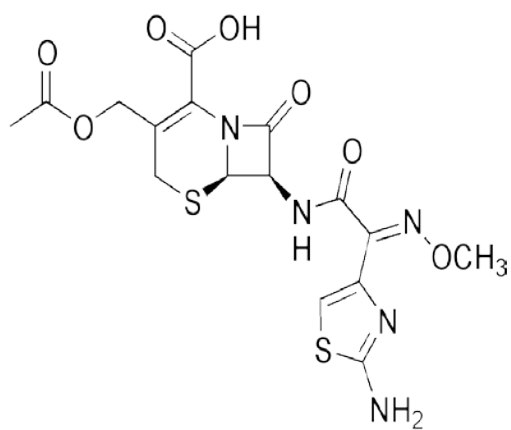


Figure 5-4. Cefotaxime structure.

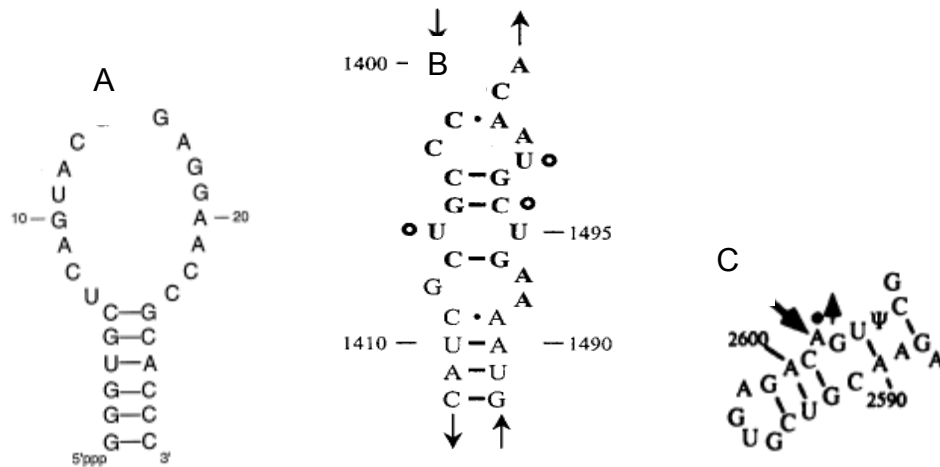


Figure 5-5. Ricin , hygromycin B, and sparsomycin targets A) ricin B) hygromycin B C) sparsomycin target

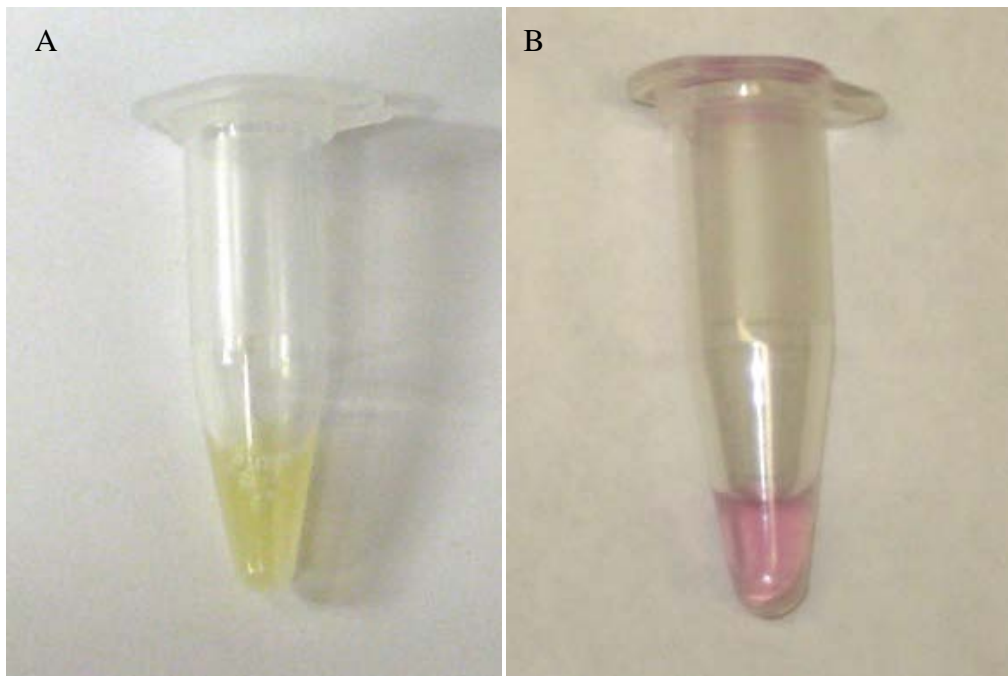


Figure 5-6. Comparison between coexpressin bacteriorhodopsin and apolipoprotein in batch format (A) and in CECF format in 96- well device (B).

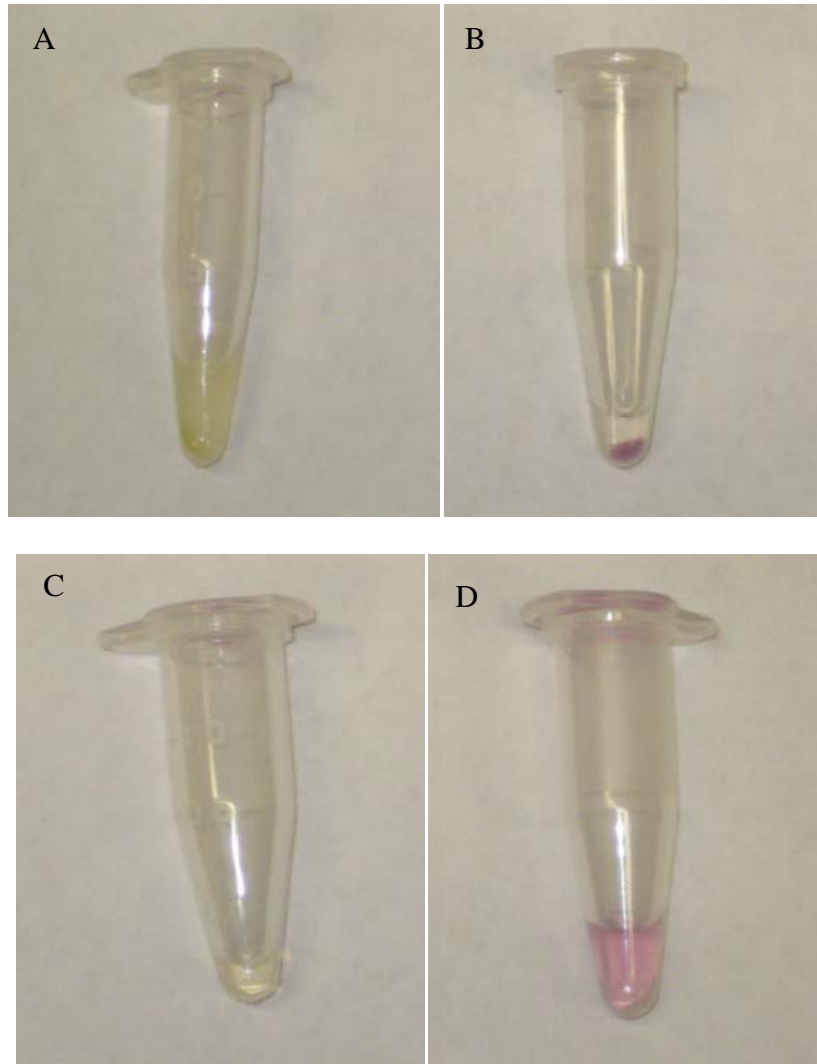


Figure 5-7. Pictures of microcentrifuge tubes containing centrifuged aliquots from 96-well device with protein synthesis reaction mix with different plasmids added at the beginning of the reaction. A: negative control with no plasmids added, B: bacteriorhodopsin, C: Apolipoproteins, D: bacteriorhodopsin and apolipoproteins.

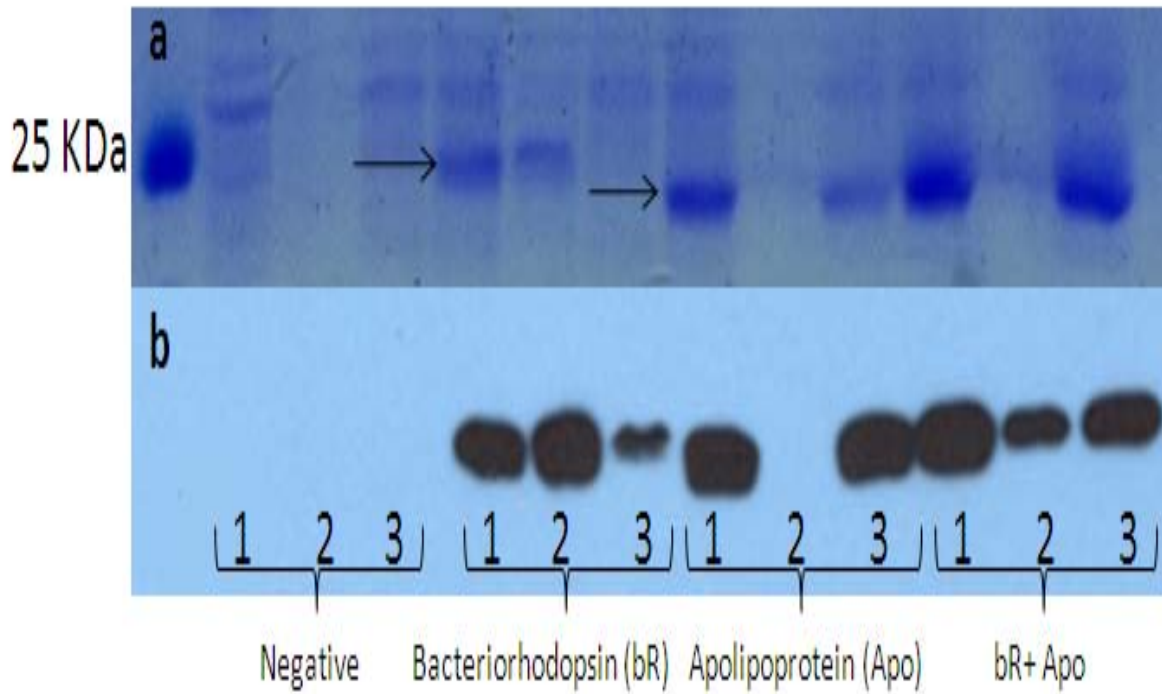


Figure 5-8. Protein gel and Western blot of membrane protein samples. Lanes: 1- ladder, 2- negative total, 3-negative pellet, 4- negative supernatant, 5- bacteriorhodopsin total, 6- bacteriorhodopsin pellet, 7- bacteriorhodopsin supernatant, 8- apolipoprotein total, 9 -apolipoprotein pellet, 10- apolipoprotein supernatant, 11 - bacteriorhodopsin & apolipoprotein total, 12 - bacteriorhodopsin & apolipoprotein pellet, 13 - bacteriorhodopsin & apolipoprotein supernatant

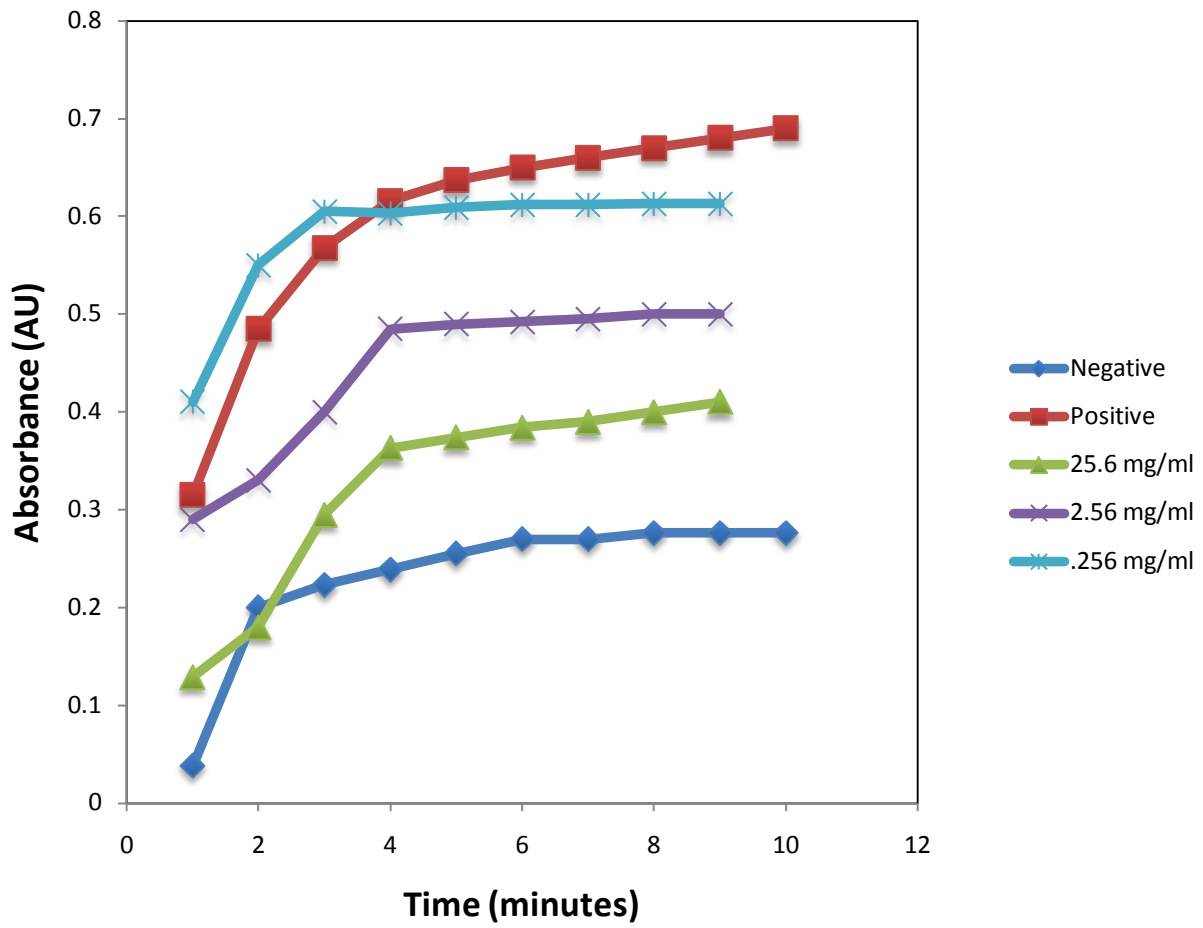


Figure 5-9. Kinetics of  $\beta$ -lactamase in the presence of different concentrations of the inhibitor tazobactam.

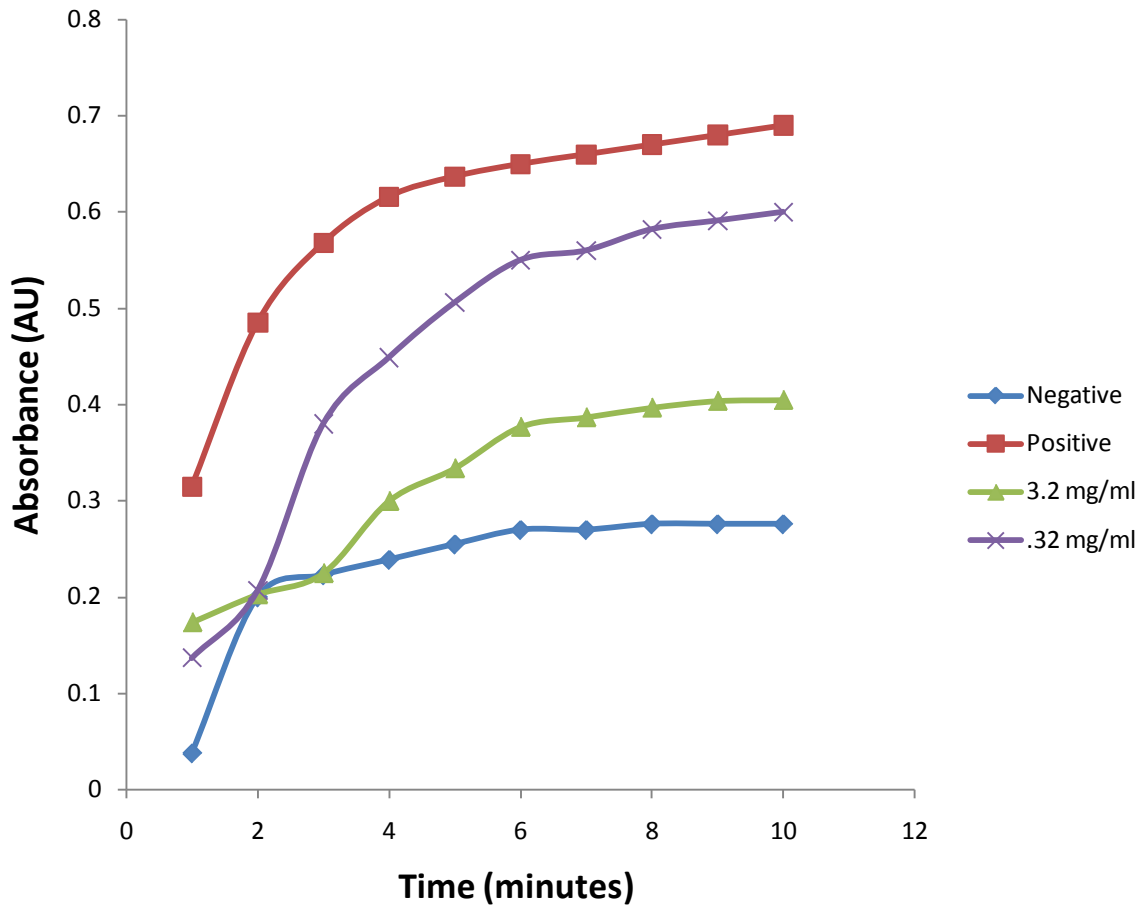


Figure 5-10. Kinetics of  $\beta$ -lactamase in the presence of different concentrations of the inhibitor clavulanate acid.

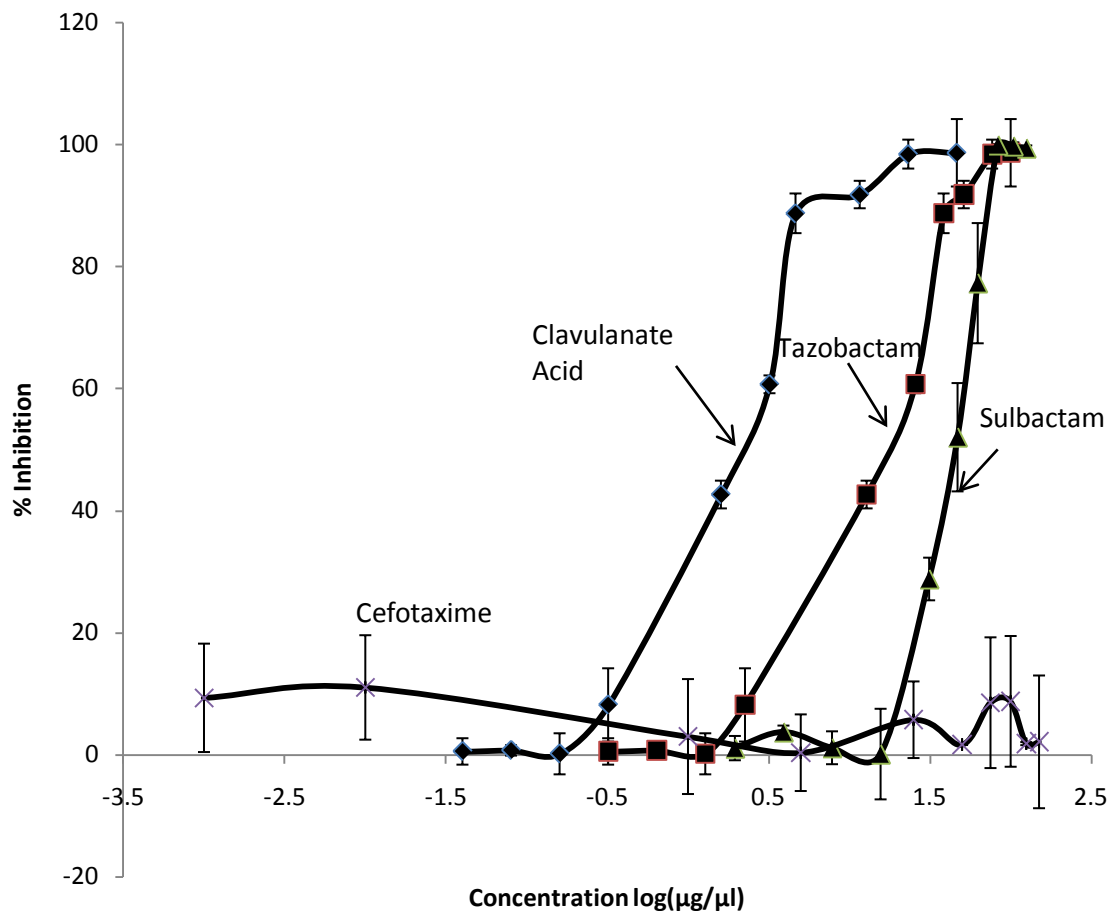


Figure 5-11. Calibration curves for three different  $\beta$ -lactamase inhibitors. Tazobactam, Clavulanate Acid, and Sulbactam. In addition the effect of Cefotaxime which has a beta-lactam ring however is neither a substrate or an inhibitor to beta lactamase was used as a demonstration of a negative control. Inhibition is presented by the reduction in the absorbance signal because of the inhibitors' effect which prevents the enzyme from catalyzing its substrate

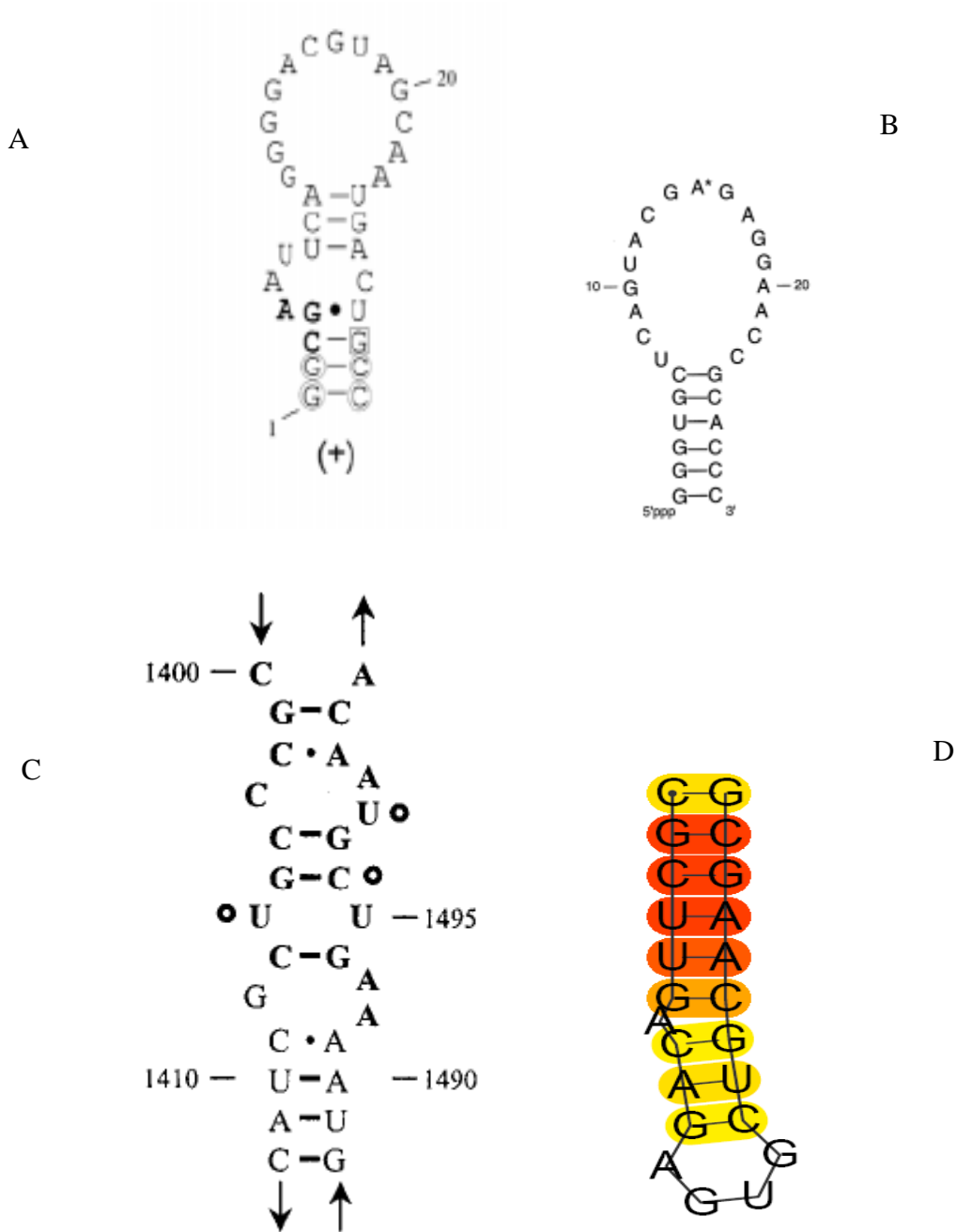


Figure 5-12. Structure of protein synthesis inhibitor targets and aptamers used. A) ricin inhibitory aptamer, B) ricin/ sarcin loop C) hygromycin B target D) sparsomycin target

Table 5-1. Table of sequences to synthesize the protein synthesis inhibitors (PSI) targets used

Aptamer name	Sequence
Hygromycin 1	5- rGrGrG rCrUrG rCrArC rUrGrC rCrCrG rCrC -3
Hygromycin 2	5- rGrGrC rArArU rGrCrU rGrArA rGrCrA rGrCrC rC -3
Ricin native loop	5-rGrGrG rGrUrG rCrUrC rArGrU rArCrG rArGrA rGrGrA rArCrC rGrCrA rCrCrC rC-3
Ricin inhibitory loop	5-rGrGrC rGrArA rUrUrC rArGrG rGrGrA rCrGrU rArGrC rArArU rGrArC rUrGrC rC-3
Ricin point mutation	5- rGrGrG rGrUrG rCrUrC rArGrU rArCrG rGrGrA rGrGrA rArCrC rGrCrA rCrCrC rC -3
Sparsomycin target	5'- rGrGrG rArArC rGrUrC rGrUrG rArGrA rCrArG rUrUrC rCrC - 3'

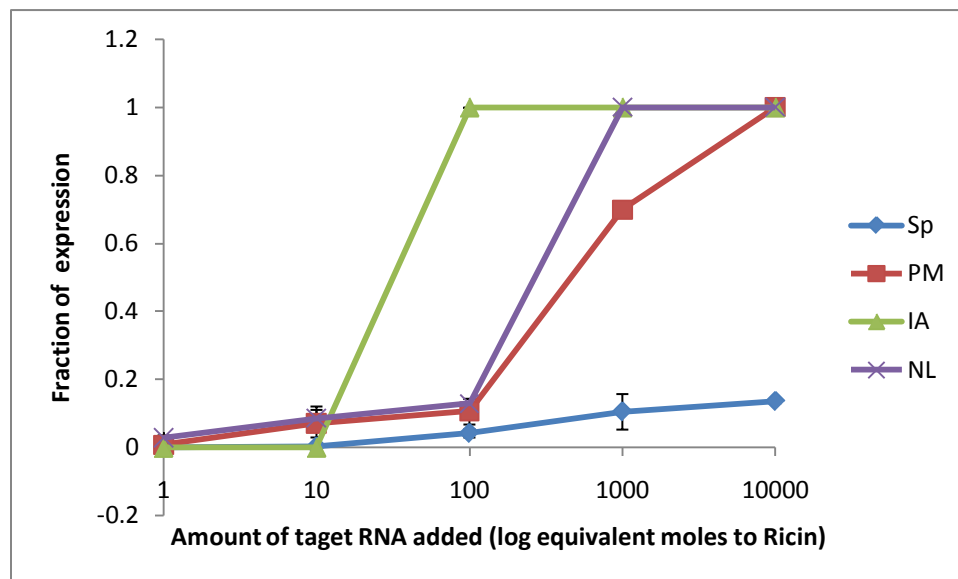


Figure 5-13. The effect of different RNA aptamers on ricin inhibition by. Sp: sparsomycin target. PM: point mutation. IA: inhibiting aptamer. NL: native loop.

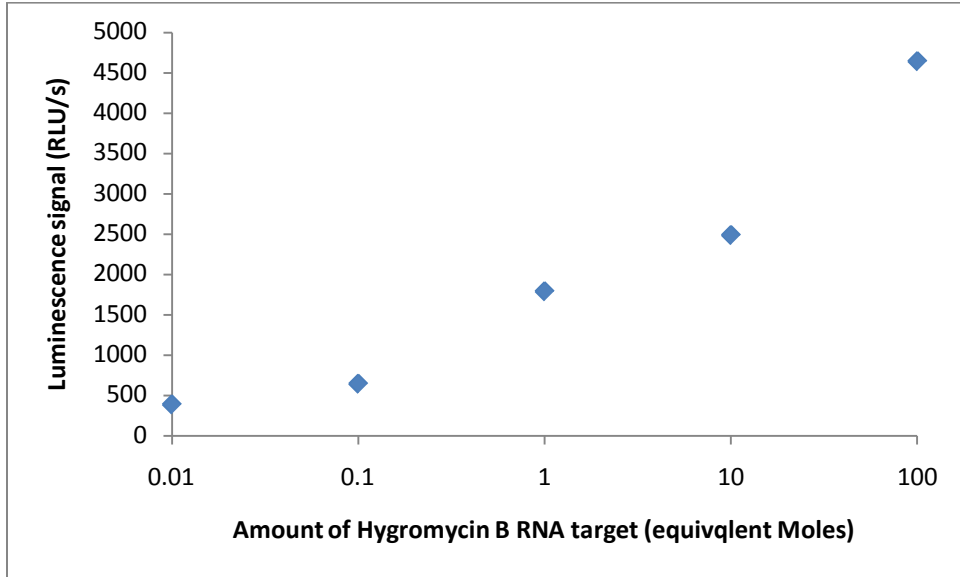


Figure 5-14. The effect of hygromycin B target on the level of protein synthesized, represented by the luminescence signal.

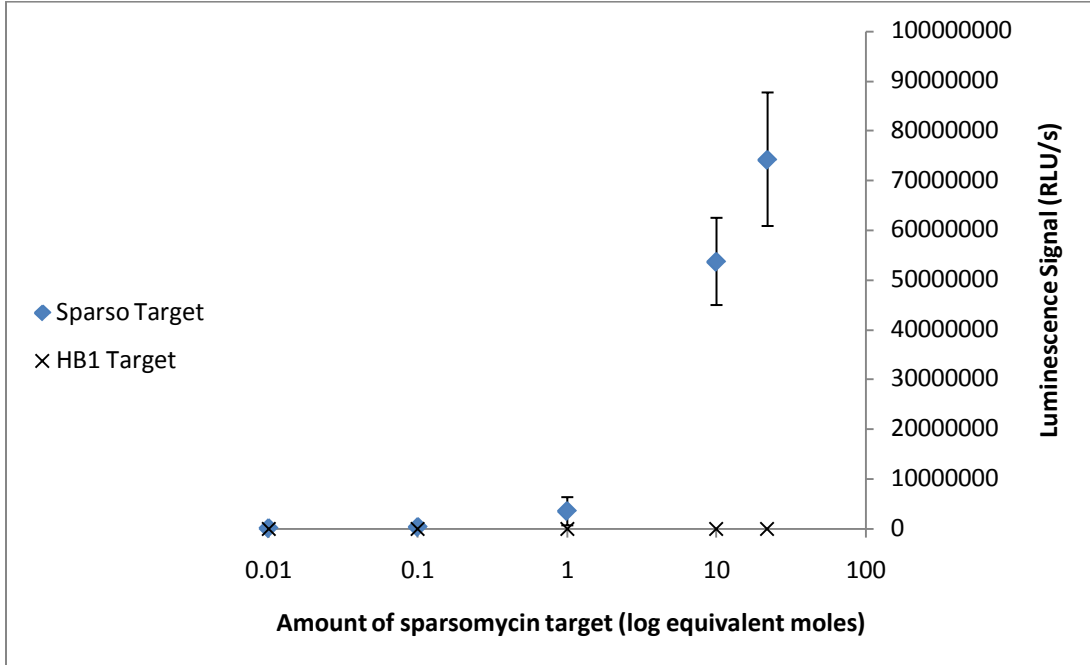


Figure 5-15. The effect of sparsomycin inhibition by sparsomycin target and hygromycin B target as a negative control.

## CHAPTER 6 CONCLUSION

The general objective for this research is to adapt microfluidic and bioMEMS platforms for enhancing the performance of cell-free protein synthesis. This was achieved by exploiting fluid manipulation for miniaturizing the reaction vessels to decrease reagent volume/cost, and allow for high throughput applications.

### 6.1 Assessment

This work was successful at achieving the following:

- Implementing the passive pumping mechanism and the microfluidic platforms developed by Beebe et al. for high-throughput protein synthesis and detection. This work also included an optimization process for applying the device to cell-free protein synthesis and found the defining factors that not only increased protein synthesis yield but also decreased the amount of reagents, hence decreasing cost. The work also included scientific analysis of the different variables that had a direct effect on protein synthesis yield.
- Miniaturizing continuous exchange cell-free (CECF) protein synthesis and optimizing the factors that enhance exchange between the reaction and feeding chambers and as a result increase protein synthesis rate and yield. These factors and other constraints were used to design a 96-unit fluidic device that was tested and verified to enhance protein synthesis yield and to fit commercial microplate readers.
- Demonstrating the application of the designed fluidic device for high throughput protein synthesis by expressing and optically detecting proteins. This work also adapted known cellular enzymatic assays for a miniaturized cell-free format and optimized the amounts of reagents used to reduce cost and enhance signal.
- Demonstrating the direct use of the fluidic device for other applications, including:
  - Using the device in combination with the newly developed nanolipoprotein technology to express soluble membrane proteins.
  - Using enzymes expressed in the device for enzyme and drug screening directly, without the need for harvesting
  - Utilizing the cell-free protein synthesis mechanism to screen or verify the physiological target of different protein synthesis inhibitors which are antitumor drug candidates.

The successful adaptation of microfluidic and bioMEMS devices such as the ones described in this research will simplify the complex processes in related fields. Such an adaptation will allow scientists to concentrate on obtaining new information instead of being impeded by traditional biological techniques that are both costly and time consuming.

Miniaturization and high throughput methods reduce time and increase efficiency. They also reduce reagent volume and cost and at the same time increase accuracy, and enable observations that are difficult if not impossible to do in a traditional format. Reducing cost by miniaturization and the use of cheaper materials such as plastics in combination with portability of the system and its ease of use provide the promise of point of care analysis systems that are accessible to a greater consumer arena. Such prospects have a lot of promise in a world where testing and obtaining therapies for diseases such as malaria and AIDS are defined by cost, transportation, and qualified medical personnel.

## **6.2 Future Work**

Although this research shows progress and cause for optimism, there is room for improvement

### **6.2.1 Evaporation Control**

Like many microfluidic applications, evaporation tends to be problematic for small liquid volumes because of a large surface area to volume ratio. In spite the use of PCR tape to seal the device, part of the reaction mix evaporates and condenses on the tape and is very difficult to retrieve. One solution is to limit the dead volume by reducing the size of the reaction chamber, however this would eliminate the possibility of adding

more assay reagents. Continuous addition of materials can also reduce the problem however it would increase reagent consumption.

A commonly used method is the addition of mineral oil on top of the reaction, however this would complicate additional assay reactions if needed. Another method that has been used is placing the microfluidic device in a highly humid closed environment, on the other hand this might cause the samples to get diluted in unwanted condensed water.<sup>131</sup>

A method that can be attempted to reduce evaporation is having a temperature gradient in the device, by lowering the temperature near the top of the well. This can be done by simply adding a cooling material on top of the well, or can be done specifically by having a network of channels with cooling liquid run near the top of the chamber. In addition, decreasing the dead volume might be a possibility, however, there would be a need to redesign the device so that the reaction chamber can be connected to an adjacent chamber. Reagents can be added to this chamber and the reaction mix can be pumped to it after the protein expression reaction is over.

### **6.2.2 In Situ Protein Purification**

In spite the success of using magnetic beads for purifying the expressed proteins, it would be more convenient to incorporate protein purification within the same device. This can be done by coating part of the device with Ni-NTA or a similar metal such as cobalt for which histidine tags have an affinity as discussed earlier. This can be challenging because most Ni-NTA coating techniques have been developed for materials such as silicon and glass. The fact that the fluidic device is made of polymers such as polypropylene and polycarbonate could make the coating process very complicated.

Another solution is to make the current device more compatible with magnetic separation platforms. With the current device requiring aliquoting samples from the device before purification because of difficulty in accessing the different wells with a magnet. However, the device's design can be adjusted to be compatible with magnetic platforms similar to those used with Ni collated microplates such as the ones manufactured by Qiagen.

A practical solution would be treating the surface of the plastics to enable the addition of metal chelating agents to which Ni or Co are bound, or by adding a layer of PDMS and treating it to become more hydrophylic to enable the addition of Ni chelates. Finally, Ni can be treated after sputtering it to the bottom of the feeding well of the device to acquire an ionic form to enable tag binding.

### **6.2.3 Automated Dispensing and Mixing**

Since microfluidics provides the opportunity for automation by utilizing its various components such as pumps, mixers, and valves. This enables automatically dispensing reagents (whether reaction or feeding solution) into different wells of the device. Automation would not only make the utilization of the device easier but would also increase the accuracy of dispensing different reagents by eliminating human error. This is especially important when handling small amounts in the order of microliters.

In addition, microfluidics can be used to enhance mixing especially in the feeding well. Although an orbital shaker is used in the current system to increase exchange between the two chambers. Pumps or mixers can lead to faster exchange and enhance protein synthesis yield. Other methods for enhancing mixing include using mini stir bars in the bottom well, and adding a heater to the bottom well for convective mixing.

#### **6.2.4 Universal Detection Method**

Although we demonstrated the ability to use high throughput screening for proteins with inherent fluorescence properties and proteins which have optically detectable assays, we still have to use traditional polyacrylamide separation and western blotting to detect proteins without such properties or assays. As mentioned earlier such techniques are not convenient for high throughput screening. Alternative techniques should be developed for universal detection. Some techniques that have been used are using fusion proteins, for example fusing all proteins with GFP.<sup>32</sup>

Another method would be to integrate more than one device, one for protein synthesis and another for protein separation where protein separation has been successfully carried out on chip format.

In conclusion, there is a lot of potential for developing fluidic platforms for applications in biotechnology. The emergence of the fields of microfluidics and biomems has raised the expectations of researchers to the extent that some projected that they will revolutionize research and development in biomedicine to the same degree that micromachining techniques revolutionized electronics. Although it is quite a leap, the possibilities of such interdisciplinary fields provide a great opportunity for advancement and innovation

## LIST OF REFERENCES

1. S. Yokoyama, *Curr. Opin. Chem. Biol.*, 2003, **7**, 39-43.
2. S. Graslund, P. Nordlund, J. Weigelt, J. Bray, O. Gileadi, S. Knapp, U. Oppermann, C. Arrowsmith, R. Hui, J. Ming, S. Dhe-Paganon, H. W. Park, A. Savchenko, A. Yee, A. Edwards, R. Vincentelli, C. Cambillau, R. Kim, S. H. Kim, Z. Rao, Y. Shi, T. C. Terwilliger, C. Y. Kim, L. W. Hung, G. S. Waldo, Y. Peleg, S. Albeck, T. Unger, O. Dym, J. Prilusky, J. L. Sussman, R. C. Stevens, S. A. Lesley, I. A. Wilson, A. Joachimiak, F. Collart, I. Dementieva, M. I. Donnelly, W. H. Eschenfeldt, Y. Kim, L. Stols, R. Wu, M. Zhou, S. K. Burley, J. S. Emtage, J. M. Sauder, D. Thompson, K. Bain, J. Luz, T. Gheyi, F. Zhang, S. Atwell, S. C. Almo, J. B. Bonanno, A. Fiser, S. Swaminathan, F. W. Studier, M. R. Chance, A. Sali, T. B. Acton, R. Xiao, L. Zhao, L. C. Ma, J. F. Hunt, L. Tong, K. Cunningham, M. Inouye, S. Anderson, H. Janjua, R. Shastry, C. K. Ho, D. Y. Wang, H. Wang, M. Jiang, G. T. Montelione, D. I. Stuart, R. J. Owens, S. Daenke, A. Schutz, U. Heinemann, S. Yokoyama, K. Bussow, K. C. Gunsalus, S. G. Consortium, B. Architecture Fonction Macromol, S. G. Ctr, C. S. G. Consortium, C. Integrated, S. Function, I. S. P. Ctr, S. Joint Ctr, Genomics, M. C. S. Genomics, X. R. C. New York Struct Genomi, N. E. S. G. Consortium, O. P. P. Facility, P. Sample, P. Facility, R. S. G. Max Delbruck Ctr Mol Med and S. C. Proteomics, *Nat. Methods*, 2008, **5**, 135-146.
3. S. Nallamsetty and D. S. Waugh, *Nat. Protocols*, 2007, **2**, 383-391.
4. O. Gileadi, S. Knapp, W. Lee, B. Marsden, S. Müller, F. Niesen, K. Kavanagh, L. Ball, F. von Delft, D. Doyle, U. Oppermann and M. Sundström, *J. Struct. Funct. Genomics.*, 2007, **8**, 107-119.
5. T. Cornvik, S.-L. Dahlroth, A. Magnusdottir, S. Flodin, B. Engvall, V. Lieu, M. Ekberg and P. Nordlund, *Proteins: Struct., Funct., Bioinf.*, 2006, **65**, 266-273.
6. N. H. Tolia and L. Joshua-Tor, *Nat. Methods*, 2006, **3**, 55-64.
7. M. W. Nirenberg and J. H. Matthaei, *Proc. Natl. Acad. Sci. U. S. A.*, 1961, **47**, 1588-1602.
8. G. Zubay, *Annu. Rev. Genet.*, 1973, **7**, 267-287.
9. F. Katzen, G. Chang and W. Kudlicki, *Trends Biotechnol.*, 2005, **23**, 150-156.
10. A. S. Spirin, *Trends Biotechnol.*, 2004, **22**, 538-545.
11. A. S. Spirin, V. I. Baranov, L. A. Ryabova, S. Y. Ovodov and Y. B. Alakhov, *Science*, 1988, **242**, 1162-1164.

12. T.-W. Kim, J.-W. Keum, I.-S. Oh, C.-Y. Choi, H.-C. Kim and D.-M. Kim, *J. Biotechnol.*, 2007, **130**, 389-393.
13. Y. Endo and T. Sawasaki, *Biotechnol. Adv.*, 2003, **21**, 695-713.
14. H. R. B. PELHAM and R. J. JACKSON, *Eur. J. Biochem.*, 1976, **67**, 247-256.
15. H. Nakano and T. Yamane, *Biotechnol. Adv.*, 1998, **16**, 367-384.
16. Y. Shimizu, A. Inoue, Y. Tomari, T. Suzuki, T. Yokogawa, K. Nishikawa and T. Ueda, *Nat. Biotechnol.*, 2001, **19**, 751-755.
17. D. M. Kim and C. Y. Choi, *Biotechnol. Progr.*, 1996, **12**, 645-649.
18. G. H. Hahn and D. M. Kim, *Anal. Biochem.*, 2006, **355**, 151-153.
19. G. H. Hahn, A. Asthana, D. M. Kim and D. P. Kim, *Anal. Biochem.*, 2007, **365**, 280-282.
20. M. N. Chekulayeva, O. V. Kurnasov, V. A. Shirokov and A. S. Spirin, *Biochem. Biophys. Res. Commun.*, 2001, **280**, 914-917.
21. P. Walter and G. Blobel, *Method Enzymol.*, 1983, **96**, 84-93.
22. A. S. Spirin, *Bioorg. Khim.*, 1992, **18**, 1394-1402.
23. D. Schwarz, V. Dotsch and F. Bernhard, *Proteomics*, 2008, **8**, 3933-3946.
24. Y. Endo, S. Otsuzuki, K. Ito and K. Miura, *J. Biotechnol.*, 1992, **25**, 221-230.
25. N. Nishimura, Y. Kitaoka and M. Niwano, *J. Ferment. Bioeng.*, 1995, **80**, 403-405.
26. T. Sawasaki, Y. Hasegawa, M. Tsuchimochi, N. Kamura, T. Ogasawara, T. Kuroita and Y. Endo, *FEBS Lett.*, 2002, **514**, 102-105.
27. V. Noireaux and A. Libchaber, *Proc. Natl. Acad. Sci. U. S. A.*, 2004, **101**, 17669-17674.
28. J. F. Hainfeld, W. Liu, C. M. R. Halsey, P. Freimuth and R. D. Powell, *J. Struct. Biol.*, 1999, **127**, 185-198.
29. V. Gaberc-Porekar and V. Menart, *Chem. Eng. Technol.*, 2005, **28**, 1306-1314.
30. J. Porath, J. Carlsson, I. Olsson and G. Belfrage, *Nature*, 1975, **258**, 598-599.

31. P. Braun and J. LaBaer, *Trends Biotechnol.*, 2003, **21**, 383-388.
32. M. A. Coleman, V. H. Lao, B. W. Segelke and P. T. Beernink, *J. Proteome Res.*, 2004, **3**, 1024-1032.
33. M. Y. He and M. J. Taussig, *Nucleic Acids Res.*, 2001, **29**, art. no.-e73.
34. M. Y. He, O. Stoevesandt and M. J. Taussig, *Curr. Opin. Biotechnol.*, 2008, **19**, 4-9.
35. G. M. Whitesides, *Nature*, 2006, **442**, 368-373.
36. Y. Luo, J. H. Qin and B. C. Lin, *Front. Biosci.*, 2009, **14**, 3913-3924.
37. A. Manz, C. Effenhauser, N. Burggraf, D. J. Harrison, K. Seiler and K. Fluri, *J. Micromech. Microeng.*, 1994, 257.
38. Z. M. Zhou, D. Y. Liu, R. T. Zhong, Z. P. Dai, D. P. Wu, H. Wang, Y. G. Du, Z. N. Xia, L. P. Zhang, X. D. Mei and B. C. Lin, *Electrophoresis*, 2004, **25**, 3032-3039.
39. J. H. Qin, F. C. Leung, Y. S. Fung, D. R. Zhu and B. C. Lin, *Anal. Bioanal. Chem.*, 2005, **381**, 812-819.
40. H. Chen and Z. H. Fan, *Electrophoresis*, 2009, **30**, 758-765.
41. W. C. Jackson, T. A. Bennett, B. S. Edwards, E. Prossnitz, G. P. Lopez and L. A. Sklar, *Biotechniques*, 2002, **33**, 220-226.
42. W. Zhan, J. Alvarez and R. M. Crooks, *Anal. Chem.*, 2003, **75**, 313-318.
43. S. H. Chen, Y. H. Lin, L. Y. Wang, C. C. Lin and G. B. Lee, *Anal. Chem.*, 2002, **74**, 5146-5153.
44. G. M. Walker and D. J. Beebe, *Lab on Chip*, 2002, **2**, 131- 134.
45. I. J. Chen, E. C. Eckstein and E. Lindner, *Lab Chip*, 2009, **9**, 107-114.
46. E. Berthier and D. J. Beebe, *Lab Chip*, 2007, **7**, 1475-1478.
47. P. Morier, C. Vollet, P. E. Michel, F. Reymond and J. S. Rossier, *Electrophoresis*, 2004, **25**, 3761-3768.
48. B. Yao, G. A. Luo, X. Feng, W. Wang, L. X. Chen and Y. M. Wang, *Lab Chip*, 2004, **4**, 603-607.

49. S. Saliterman, *Fundamentals of BioMEMS and Medical Microdevices*, Wiley-Interscience, Bellingham, Wa.
50. R. Bashir, *Adv. Drug Deliv. Rev.*, 2004, **56**, 1565-1586.
51. J. Hong, J. B. Edel and A. J. deMello, *Drug Discov. Today*, 2009, **14**, 134-146.
52. T. A. Franke and A. Wixforth, *Chemphyschem*, 2008, **9**, 2140-2156.
53. T. Chovan and A. Guttman, *Trends Biotechnol.*, 2002, **20**, 116-122.
54. T. J. Clark, P. H. McPherson and K. F. Buechler, *Point of Care*, 2002, **1**.
55. C. L. Hansen, E. Skordalakes, J. M. Berger and S. R. Quake, *Proc. Natl. Acad. Sci. U. S. A.*, 2002, **99**, 16531-16536.
56. C. Hansen and S. R. Quake, *Curr. Opin. Struc. Biol.*, 2003, **13**, 538-544.
57. A. S. Verkman, *Am. J. Physiol.-Cell Physiol.*, 2004, **286**, C465-C474.
58. G. W. Aherne, E. McDonald and P. Workman, *Breast Cancer Res.*, 2002, **4**, 148-154.
59. A. Roda, M. Guardigli, P. Pasini and M. Mirasoli, *Anal. Bioanal. Chem.*, 2003, **377**, 826-833.
60. D. A. Pereira and J. A. Williams, *Brit. J. Pharmacol.*, 2007, **152**, 53-61.
61. J. P. Goddard and J. L. Reymond, *Trends Biotechnol.*, 2004, **22**, 363-370.
62. J. P. Goddard and J. L. Reymond, *Curr. Opin. Biotechnol.*, 2004, **15**, 314-322.
63. J. L. Reymond, *Food Technol. Biotech.*, 2004, **42**, 265-269.
64. J. L. Reymond, V. S. Fluxa and N. Maillard, *Chem. Commun.*, 2009, 34-46.
65. B. F. Cravatt, A. T. Wright and J. W. Kozarich, *Annu. Rev. Biochem.*, 2008, **77**, 383-414.
66. W. Barlow, *Nature*, 1883, **29**, 186- 188.
67. M. Kolbe, H. Besir, L. O. Essen and D. Oesterhelt, *Science*, 2000, **288**, 1390-1396.
68. S. Hirose, *Epilepsy Res.*, 2006, **70**, S206-S217.

69. G. W. Abbott, *Curr. Pharm. Design*, 2006, **12**, 3631-3644.
70. A. M. Spiegel, *Annu. Rev. Physiol.*, 1996, **58**, 143-170.
71. B. A. Chromy, E. Arroyo, C. D. Blanchette, G. Bench, H. Benner, J. A. Cappuccio, M. A. Coleman, P. T. Henderson, A. K. Hinz, E. A. Kuhn, J. B. Pesavento, B. W. Segelke, T. A. Sulchek, T. Tarasow, V. L. Walsworth and P. D. Hoeprich, *J. Am. Chem. Soc.*, 2007, **129**, 14348-14354.
72. T. H. Bayburt, Y. V. Grinkova and S. G. Sligar, *Nano Lett.*, 2002, **2**, 853-856.
73. J. A. Cappuccio, C. D. Blanchette, T. A. Sulchek, E. S. Arroyo, J. M. Kralj, A. K. Hinz, E. A. Kuhn, B. A. Chromy, B. W. Segelke, K. J. Rothschild, J. E. Fletcher, F. Katzen, T. C. Peterson, W. A. Kudlicki, G. Bench, P. D. Hoeprich and M. A. Coleman, *Mol. Cell. Proteomics*, 2008, **7**, 2246-2253.
74. T. H. Bayburt, Y. V. Grinkova and S. G. Sligar, *Arch. Biochem. Biophys.*, 2006, **450**, 215-222.
75. C. Klammt, D. Schwarz, F. Lohr, B. Schneider, V. Dotsch and F. Bernhard, *Febs J.*, 2006, **273**, 4141-4153.
76. F. Katzen, J. E. Fletcher, J. P. Yang, D. Kang, T. C. Peterson, J. A. Cappuccio, C. D. Blanchette, T. Sulchek, B. A. Chromy, P. D. Hoeprich, M. A. Coleman and W. Kudlicki, *J. Proteome Res.*, 2008, **7**, 3535-3542.
77. D. Busso, R. Kim and S. H. Kim, *J. Biochem. Biophys. Methods*, 2003, **55**, 233-240.
78. D. Craig, M. T. Howell, C. L. Gibbs, T. Hunt and R. J. Jackson, *Nucleic Acids Res.*, 1992, **20**, 4987-4995.
79. Y. J. Chen, O. Pornillos, S. Lieu, C. Ma, A. P. Chen and G. Chang, *Proc. Natl. Acad. Sci. U. S. A.*, 2007, **104**, 18999-19004.
80. C. Klammt, D. Schwarz, K. Fendler, W. Haase, V. Dotsch and F. Bernhard, *Febs J.*, 2005, **272**, 6024-6038.
81. Y. Elbaz, S. Steiner-Mordoch, T. Danieli and S. Schuldiner, *Proc. Natl. Acad. Sci. U. S. A.*, 2004, **101**, 1519-1524.
82. K. Poole, *Cell. Mol. Life Sci.*, 2004, **61**, 2200-2223.
83. G. von Heijne, *J. Intern. Med.*, 2007, **261**, 543-557.
84. D. M. Livermore, *J. Antimicrob. Chemoth.*, 1998, **41**, 25-41.

85. G. Bou and J. Martinez-Beltran, *Antimicrob. Agents Ch.*, 2000, **44**, 428-432.
86. T. Palzkill and D. Botstein, *J. Bacteriol*, 1992, **174**, 5237-5243.
87. P. J. Wu, K. Shannon and I. Phillips, *Antimicrob. Agents Ch.*, 1994, **38**, 494-498.
88. K. Bush, *Clin. Microbiol. Rev.*, 1988, **1**, 14.
89. J. Chan, S. N. Khan, I. Harvey, W. Merrick and J. Pelletier, *RNA*, 2004, **10**, 528-543.
90. R. Jorgensen, A. R. Merrill, S. P. Yates, V. E. Marquez, A. L. Schwan, T. Boesen and G. R. Andersen, *Nature*, 2005, **436**, 979-984.
91. H. Morimoto and B. Bonavida, *J Immunol.*, 1992, **149**, 2089-2094.
92. R. D. Forrest, *J. Roy. Soc. Med.*, 1982, **75**, 198-205.
93. L. Falzon, M. Suzuki and M. Inouye, *Curr. Opin. Biotechnol.*, 2006, **17**, 347-352.
94. A. Rothe, R. N. Surjadi and B. E. Power, *Trends Biotechnol.*, 2006, **24**, 587-592.
95. K. Ozawa, N. E. Dixon and G. Otting, *IUBMB Life*, 2005, **57**, 615-622.
96. P. Angenendt, *Drug Discov. Today*, 2005, **10**, 503-511.
97. B. H. Chueh, D. Huh, C. R. Kyrtos, T. Houssin, N. Futai and S. Takayama, *Anal. Chem.*, 2007, **79**, 3504-3508.
98. Q. Mei, C. K. Fredrickson, W. Lian, S. G. Jin and Z. H. Fan, *Anal. Chem.*, 2006, **78**, 7659-7664.
99. K. A. Martemyanov, V. A. Shirokov, A. V. Kurnasov, A. T. Gudkov and A. S. Spirin, *Protein Expr. Purif.*, 2001, **21**, 456- 461.
100. J. G. Wijmans and R. W. Baker, *Journal of Membrane Science*, 1995, **107**, 1-21.
101. W. Y. Zhang, G. S. Ferguson and S. Tatic-Lucic, *MEMS 2004 Technical Digest*, 2004, 4.
102. K. Chang, C. W. Macosko and D. C. Morse, *Macromolecules*, 2007, **40**, 3819-3830.
103. P. Angenendt, L. Nyarsik, W. Szaflarski, J. Glokler, K. H. Nierhaus, H. Lehrach, D. J. Cahill and A. Lueking, *Anal. Chem.*, 2004, **76**, 1844-1849.

104. M. Aoki, T. Matsuda, Y. Tomo, Y. Miyata, M. Inoue, T. Kigawa and S. Yokoyama, *Protein Expr. Purif.*, 2009, **68**, 128-136.
105. R. A. Jefferson, S. M. Burgess and D. Hirsh, *Proc. Natl. Acad. Sci. U. S. A.*, 1986, **83**, 8447-8451.
106. J. Hofmann and M. Sernetz, *Anal. Biochem.*, 1983, **131**, 180-186.
107. B. Rotman, M. Edelstein and J. A. Zderic, *Proc. Natl. Acad. Sci. U. S. A.*, 1963, **50**, 1-6.
108. E. Koller and O. S. Wolfbeis, *Monatsh. Chem.*, 1985, **116**, 65-75.
109. M. Dryjanski and R. F. Pratt, *Biochemistry*, 1995, **34**, 3561-3568.
110. C. P. Govardhan and R. F. Pratt, *Biochemistry*, 1987, **26**, 3385-3395.
111. T. W. Kim, D. M. Kim and C. Y. Choi, *J. Biotechnol.*, 2006, **124**, 373-380.
112. K. A. Woodrow, I. O. Airen and J. R. Swartz, *J. Proteome Res.*, 2006, **5**, 3288-3300.
113. M. E. Bosch, A. J. R. Sanchez, F. S. Rojas and C. B. Ojeda, *Comb. Chem. High Throughput Screen*, 2007, **10**, 413-432.
114. A. E. Todd, C. A. Orengo and J. M. Thornton, *J. Mol. Biol.*, 2001, **307**, 1113-1143.
115. F. Katzen, T. C. Peterson and W. Kudlicki, *Trends Biotechnol.*, 2009, **27**, 455-460.
116. J. Drews, *Science*, 2000, **287**, 1960-1964.
117. N. R. Civjan, T. H. Bayburt, M. A. Schuler and S. G. Sligar, *Biotechniques*, 2003, **35**, 556-563.
118. A. Wlodawer, J. P. Segrest, B. H. Chung, R. Chiovetti and J. N. Weinstein, *FEBS Lett.*, 1979, **104**, 231-235.
119. J. H. Ahn, H. S. Chu, T. W. Kim, I. S. Oh, C. Y. Choi, G. H. Hahn, C. G. Park and D. M. Kim, *Biochem. Biophys. Res. Commun.*, 2005, **338**, 1346-1352.
120. C. Berrier, K. H. Park, S. Abes, A. Bibonne, J. M. Betton and A. Ghazi, *Biochemistry*, 2004, **43**, 12585-12591.

121. S. B. Vakulenko, B. Geryk, L. P. Kotra, S. Mobashery and S. A. Lerner, *Antimicrob. Agents Ch.*, 1998, **42**, 1542-1548.
122. D. J. Payne, R. Cramp, D. J. Winstanley and D. J. C. Knowles, *Antimicrob. Agents Ch.*, 1994, **38**, 767-772.
123. R. A. Bonomo, J. Z. Liu, Y. H. Chen, L. Ng, A. M. Hujer and V. E. Anderson, *Biochim. Biophys. Acta*, 2001, **1547**, 196-205.
124. J. R. Hesselberth, D. Miller, J. Robertus and A. D. Ellington, *J. Biol. Chem.*, 2000, **275**, 4937-4942.
125. A. A. Szewczak and P. B. Moore, *J. Mol. Biol.*, 1995, **247**, 81-98.
126. Q. Q. Tan, D. X. Dong, X. W. Yin, J. Sun, H. J. Ren and R. X. Li, *J. Biotechnol.*, 2009, **139**, 156-162.
127. P. Pfister, A. Risch, D. E. Brodersen and E. C. Bottger, *Antimicrob. Agents Ch.*, 2003, **47**, 1496-1502.
128. B. T. Porse, S. V. Kirillov, M. J. Awayez, H. C. J. Ottenheijm and R. A. Garrett, *Proc. Natl. Acad. Sci. U. S. A.*, 1999, **96**, 6.
129. N. Lee, K. Y. Yuen and C. R. Kumana, *Drugs*, 2003, **63**, 1511-1524.
130. H. P. Hofs, D. J. T. Wagener, D. Devos, H. C. J. Ottenheijm, H. J. Winkens, P. H. M. Bovee and W. J. Degrip, *Eur. J. Cancer*, 1995, **31A**, 1526-1530.
131. E. Berthier, J. Warrick, H. Yu and D. J. Beebe, *Lab Chip*, 2008, **8**, 852-859.

## BIOGRAPHICAL SKETCH

Ruba Khnouf was born in Amman, Jordan in 1982. She finished school in Amman and then left to the United States in 2000 where she earned her bachelor of science in Engineering and masters of science in engineering in biomedical engineering from the University of Michigan-Ann Arbor in 2004 and 2005. During her years in Ann Arbor she joined a couple of laboratories where she started learning and enjoying research.

In 2005, Ruba moved back to Jordan and worked as a lecturer in the Biomedical Engineering Department at the Hashemite University in Zarqa. During that year she realized that she also liked teaching and decided to pursue an academic career. To achieve that she started graduate school to earn her PhD from the University of Florida and joined the Microfluidics laboratory.